

**Predicting the effect of food on drug exposure through an understanding of the
impact of *in vitro* solubility and dissolution on the human *in vivo* absorption -
A research based on BCS Class II and IV compounds using PBPK modeling**

Dissertation

zur Erlangung des
Doktorgrades der Naturwissenschaften (Dr. rer. nat.)

der

Naturwissenschaftlichen Fakultät I

-Biowissenschaften-

der Martin-Luther-Universität

Halle-Wittenberg,

vorgelegt

von Frau Christina Fink

geb. am 03.06.1990 in Gießen

Gutachter:

1. Prof. Dr. Karsten Mäder
2. Prof. Dr. Sonja Keßler
3. Prof. Dr. Sebastian Wicha

Tag der öffentlichen Verteidigung: 07.07.2020 in Halle (Saale)

To my family and friends,
Arnold,
and Sheila.

Table of Contents

List of tables	III
List of figures	V
List of abbreviations	VII
1. Introduction	1
1.1. Oral absorption and food effect.....	1
1.2. Compound selection.....	2
1.3. Biopharmaceutic tools and classification frameworks.....	3
1.3.1. In vitro solubility and dissolution testing	4
1.3.2. In vivo PK analysis.....	6
1.3.3. In silico PBPK modeling.....	8
1.4. Research Objectives	9
2. Materials	11
2.1. Drug substances and drug products.....	11
2.2. Chemicals.....	11
2.3. Buffer and dissolution media	12
2.4. Instruments and software	13
2.5. Other materials	13
3. Methods.....	14
3.1. HPLC-methods for drug quantification.....	14
3.2. In vitro solubility testing.....	15
3.2.1. Thermodynamic solubility measurements.....	15
3.2.2. Dumping experiments	15
3.2.3. Solubility parameters for biopharmaceutical classification	16
3.3. In vitro dissolution.....	16
3.3.1. USP II dissolution tests	16
3.3.2. USP IV dissolution tests	17
3.3.3. Dissolution parameter fitting	18
3.4. Permeability assessment.....	19
3.4.1. Apparent permeability through a Caco-2 cell monolayer	19
3.4.2. Calculation of the effective intestinal permeability	20
3.5. Rat PK study.....	20
3.5.1. Preparation of the dosage forms	20
3.5.2. In vivo rat PK study	22
3.6. Analysis of clinical and preclinical pharmacokinetic data to identify solubility-limited absorption	23
3.6.1. Data collection.....	23
3.6.2. Gut bioavailability calculation	25
3.6.3. Top-down PBPK analysis.....	25

3.7.	Bottom-up food effect predictions using GastroPlus®	28
3.7.1.	Understanding the PK of the drug.....	29
3.7.2.	Obtaining clearance and volume of distribution from the IV PK profile.....	29
3.7.3.	Bottom-up oral PK prediction.....	30
3.7.4.	Model optimization and verification.....	31
3.7.5.	Food effect prediction strategy	33
4.	Results and Discussion	34
4.1.	Importance of in vitro solubility and dissolution data in food effect predictions.....	34
4.1.1.	In vitro solubility testing.....	34
4.1.2.	In vitro dissolution testing.....	41
4.1.3.	Summary of the relative fed/fasted differences in vitro and in vivo	47
4.1.4.	Permeability and solubility in BCS and DCS framework	50
4.2.	Predicting the food effect on exposure through understanding the mechanisms underlying absorption in human and rat	52
4.2.1.	Analysis of clinical PK data.....	52
4.2.2.	Analysis of preclinical PK data	59
4.2.3.	Solubility-limited absorption and food effect in human and rat.....	67
4.3.	Predicting the food effect on drug exposure using GastroPlus®	74
4.3.1.	Target fraction absorbed and input gut first pass for the model drugs.....	74
4.3.2.	Bottom-up oral PK prediction, model optimization and verification.....	75
4.3.3.	Predicting the effect of food on the model compounds' exposure	81
4.3.4.	Summary of the bottom-up PBPK food effect predictions.....	89
5.	Summary and Outlook	91
5.1.	Importance of in vitro solubility and dissolution data in food effect predictions.....	91
5.2.	Prediction of food effect on exposure through understanding the mechanisms underlying the absorption in human and rat	92
5.3.	Predicting the of food effect on exposure using GastroPlus®.....	93
5.4.	Conclusions.....	93
	References.....	94
	Acknowledgements	i
	Curriculum Vitae.....	iii
	Declaration under Oath/ Eidesstattliche Erklärung	v
	Appendix.....	vi

List of tables

Table 1: Drug substances and drug products used in this work.....	11
Table 2: Chemicals used in this work	11
Table 3: Buffer and dissolution media used in the solubility and release tests within this research ...	12
Table 4: Instruments and software used in this work.....	13
Table 5: Other materials used in this work	13
Table 6: HPLC methods for drug quantification	14
Table 7: Input parameters for calculation of the effective permeability of the ten model compounds	20
Table 8: Overview of the oral doses employed in the rat PK studies.....	21
Table 9: Clinical pharmacokinetic data analyzed to assess solubility-limited absorption	24
Table 10: Preclinical data to estimate the human clearance and volume of distribution of lapatinib and vemurafenib	26
Table 11: Clinical pharmacokinetic data used for building and validating the GastroPlus® models	30
Table 12: Parameters tested in the PSA to optimize the bottom-up PBPK predictions in the fasted state	32
Table 13: Increase in stomach pH after completion of a meal collected using the SmartPill® derived from mean values by Koziolk et al.....	33
Table 14: Parameters tested in the “Food PSA”	33
Table 15: Comparison of the model drugs’ FaSSIF and FaSSIF blank (without taurocholate and lecithin) solubility	39
Table 16: Observed supersaturation after dumping of drug solutions into FaSSIF	40
Table 17: Difference in pharmacokinetic parameters in the fed and fasted state versus the difference of in vitro measured parameters in fed state and fasted state simulated media	48
Table 18 : Summary of parameters in the biopharmaceutics classification frameworks	51
Table 19: Collection of human pharmacokinetic data used to identify solubility-limited absorption .	53

Table 20: Observed vs predicted human pharmacokinetic parameters at doses employed in their clinical food effect studies and simulation using hypothetical BCS class I-like solubility	54
Table 21: Results of the rat PK studies	60
Table 22: Observed vs predicted rat pharmacokinetic parameters and simulation using hypothetical BCS class I-like solubility	65
Table 23: Evaluation of the model compounds' dose proportionality of exposure in the rat available the FDA's Pharmacology Reviews	67
Table 24: Heatmap presenting the properties in the BCS and DCS frameworks along with properties/methods used in the analysis of human pharmacokinetic data	68
Table 25: Heatmap presenting the dose/solubility relationship in the rat along with properties/methods used in the analysis of rat pharmacokinetic data	68
Table 26: Target fraction absorbed and input gut first pass for the GastroPlus® models	75
Table 27: PBPK models with absorption related compound characteristics in the bottom-up oral PK prediction and their changes during model optimization.....	76
Table 28: Acceptance criteria in the verification simulations (fold of the observed value)	77
Table 29: Food effect prediction using the default Human-Physiological-Fed physiology and fed stomach physiology derived from Koziol et al.....	82
Table 30: Percentage deviation of AUC and C_{max} following the physiology related changes in the Food PSA for all compounds' optimized fasted state models.....	87

List of figures

Figure 1: Schematic illustration of the proposed methods to assess solubility-limited absorption behavior through a mechanistic analysis of pharmacokinetic data.....	7
Figure 2: Exemplary measured dissolution profile with exponential fit to illustrate the first-order model fitting	18
Figure 3: Schematic illustration of the Caco-2 permeability test setting.....	20
Figure 4: Optimizing the intrinsic microsomal clearance (CL_{int}) and K_p factor (multiplicative factor to scale all the tissue distribution coefficients at the same time), to best comply with the observed IV PK profiles.....	25
Figure 5: Schematic illustration of the top-down PBPK modeling approach	27
Figure 6: Schematic illustration of the developed bottom-up PBPK workflow to enhance food effect predictions.....	28
Figure 7: Measured pH dependent solubility (after 24 h) profiles of the model drugs (n=2).....	35
Figure 8: Measured solubility (n=2) of the model drugs (after 24 h) at pH 6.5 (FaSSIF blank) and pH 5.0 (FeSSIF blank) with different taurocholate and lecithin concentrations	38
Figure 9: FaSSIF and FeSSIF dissolution profiles of the selected model drugs erlotinib, gefitinib and M1 in the USP II apparatus with first order (exponential) fit	42
Figure 10: Votrient® 400 mg USP IV release profiles (cumulative and per fraction) with zero-order linear fit and expected release	45
Figure 11: Zelboraf® 240 mg USP IV release profiles (cumulative and per fraction) with zero-order linear fit and expected release	46
Figure 12: PBPK analysis of pazopanib pharmacokinetic profiles	56
Figure 13: PBPK analysis of erlotinib pharmacokinetic profiles	57
Figure 14: Mean (SD) plasma concentration-time profiles after IV and oral (capsules) administration in the rat.....	62
Figure 15: Dose proportionality of AUC and C_{max} in human single-dose PK studies confounded by high inter-subject variability	70
Figure 16: PSA of the fraction absorbed to optimize the bottom-up predicted pazopanib model in the fasted state.....	78

Figure 17: The impact of the physiological changes in the presence of food on the simulated AUC of the model Pazopanib Opt 1..... 85

Figure 18: The impact of the physiological changes in the presence of food on the simulated C_{\max} of the model Dabrafenib Opt 1..... 86

List of abbreviations

AAALAC	Association for Assessment and Accreditation of Laboratory Animal Care
ACAT	Advanced Compartmental and Transit
A_n	Absorption number
API	Active pharmaceutical ingredient
ARA	Acid-reducing agent
AUC	Area under the plasma concentration-time curve
AUC_{0-inf}	Area under the curve from 0 extrapolated to infinity
AUC_{0-last}	Area under the curve from 0 to the last measured time point
$AUC_{last-inf}$	Area under the curve from the last measured time point extrapolated to infinity
BCS	Biopharmaceutics classification system
Cl	Clearance
Cl_{int}	Intrinsic microsomal clearance
CLOGP	Calculated logP
C_{max}	Maximum plasma concentration
cP_{eff}	Calculated human effective permeability
CV%	Coefficient of variation
D_0	Dose number
DCS	Developability Classification System
DMPK	Drug metabolism and pharmacokinetics
DMSO	Dimethyl sulfoxide
EDTA	Ethylene diamine tetraacetic acid
F	Bioavailability
F_a	Fraction absorbed
$F_a * F_g$	Gut bioavailability (fraction of dose reaching the portal vein)
FaSSGF	Fasted state simulated gastric fluid
FaSSIF	Fasted state simulated intestinal fluid
FDA	U.S. Food and Drug Administration
FeSSIF	Fed state simulated intestinal fluid
F_g	Fraction of drug escaping the gut first-pass metabolism
F_h	Fraction of drug escaping the liver metabolism
GI	Gastrointestinal (tract)
HBD	Hydrogen Bound Donor Count
HCl	Hydrochloride/ Hydrochloric acid
HIF	Human intestinal fluid
HPLC	High performance liquid chromatography
HPMC	Hydroxypropyl methylcellulose
HPMC-AS	Hydroxypropyl methylcellulose acetate succinate
IV	Intravenous
IVIVC	In vitro in vivo correlation
k	First-order dissolution rate constant
k_0	Zero-order dissolution rate constant
k_e	Elimination rate constant

K_p factor	multiplicative factor to scale all tissue distribution coefficients in the generic MATLAB® PBPK model used in this work
M1	Development compound
NCE	New chemical entity
p.o.	per oral
P_{app}	Apparent permeability (through Caco-2 cell monolayer)
PBPK	Physiologically based pharmacokinetic
P_{eff}	Human effective permeability
PEG	Polyethylene glycol
P-gp	P-glycoprotein
Ph. Eur.	European Pharmacopoeia
PK	Pharmacokinetics
PSA	Parameter Sensitivity Analysis
rpm	Revolutions per minute
SD	Standard deviation
SDS	Sodium dodecyl sulfate
SGF	Simulated gastric fluid
SIF	Simulated intestinal fluid
SLAD	Solubility-limited absorbable dose
SR	Bile salt solubilization ratio in GastroPlus®
tBME	Tertiary-butyl methyl ether
TC	Sodium taurocholate
t_{max}	Time to reach the maximum plasma concentration
UPLC-MS/MS	Ultra-Performance Liquid Chromatography tandem mass spectrometer
USP	United States Pharmacopeia
V_{ss}	Volume of distribution at steady state
W_{max}	Maximum amount released
W_t	Amount released at time t

1. Introduction

1.1. Oral absorption and food effect

Oral drug delivery is often the preferred route of administration. It is convenient for the patient, and it is cost-effective. One of the major challenges in the development of orally administered drugs is the poor solubility of an increasing number of drug candidates (1, 2), especially for several kinase inhibitors in the oncology drug development pipeline (3). A compound with a low aqueous solubility, when being developed as an immediate-release solid oral dosage form, may exhibit a low and highly variable oral bioavailability due to solubility- or dissolution rate-limited absorption, that makes it susceptible to interactions with food or acid-reducing agents (ARA) (4). Delayed gastric emptying, altered pH levels along the gastrointestinal (GI) tract, increased bile flow and splanchnic blood flow are among the mechanisms that can impact the absorption of an orally administered drug when taken concomitantly with food (5). The interaction potential with ARAs is primarily based on the increase in gastric pH, which is a sub-aspect of the food effect and is therefore also considered in this work. To guide the clinical study design and provide labeling information, food and drug interaction studies with ARAs are requested by the health authorities during drug development (6, 7).

In the recent years, several research groups and initiatives (e.g. from the universities of Frankfurt/Main (Germany), Greifswald (Germany), Athens (Greece), or within large EU-funded projects like OrBiTo (8) or UNGAP (5)) have addressed methods to understand and predict food effects in human. Among them are in vitro based approaches using solubility and dissolution tests (9, 10) or biopharmaceutic classification (11, 12), in vivo preclinical testing, especially in the dog (13), and in silico approaches with physiologically based pharmacokinetic (PBPK) modeling (14). However, due to limited predictive power, it is not yet possible to replace clinical food effect studies. The goal of the thesis is to contribute to this desirable aim. In particular, the following goals were tackled:

- Evaluation of the performance of in vitro solubility and dissolution data in food effect predictions for poorly soluble compounds
- Improved prediction of food effects on drug exposure through understanding the mechanisms underlying the absorption/ exposure in human and rat
- Development of a workflow using the GastroPlus® PBPK model that addresses the current scientific challenges in food effect predictions

Therefore, previously proposed food effect prediction methods were taken up and applied to ten model drugs (with clinical food effect studies available) to evaluate their performance and suggest further improvements. The work included literature research and evaluation, in vitro solubility and

dissolution testing in combination with approaches to analyze and understand the in vivo pharmacokinetics (PK) and PBPK modeling.

1.2. Compound selection

Ten oral compounds in the therapeutic area of oncology have been selected as model drugs, as they can be especially susceptible to food effects due to their often low aqueous solubility and low to medium permeability (15) and as changes in the PK can have a significant impact on their safety profile (16). The compounds chosen for this research were selected from a review summarizing the effect of food and acid-reducing agents of oral targeted anticancer drugs by Willemsen et al. (17). The selection was based on the following criteria: Firstly, compounds with poor aqueous solubility (Biopharmaceutics classification system (BCS) class II and IV (18)) were chosen, as their absorption is expected to be more sensitive to changes in the GI environment in the presence of food compared to highly soluble drugs. The second criterion was the availability of intravenous (IV) pharmacokinetic data in humans, which is crucial for the identification of the oral bioavailability and the understanding of the PK through the quantification of the hepatic clearance. Moreover, drugs that did not require special handling following light sensitivity or occupational exposure level $< 1 \mu\text{g}/\text{m}^3$, were selected. Crizotinib, dabrafenib mesylate, erlotinib hydrochloride (HCl), gefitinib, imatinib mesylate, pazopanib HCl and trametinib 1:1 dimethyl sulfoxide (DMSO) co-solvate (in the following trametinib*DMSO) were selected as they met these criteria. M1 was included as a lead compound in drug development that meets the above criteria as well. Additionally, vemurafenib and lapatinib ditosylate were included despite the absence of intravenous pharmacokinetic data because the strong observed food effect makes them relevant.

The research was performed at the dose of their clinical food effect studies using the relevant salt form for each model compound, which is always referred to when the drug names are mentioned in this work unless stated otherwise.

Of particular note is the fact that the market formulations and formulations in the food effect studies contain crystalline active pharmaceutical ingredient (API), except for vemurafenib, which is co-precipitated with hydroxypropyl methylcellulose acetate succinate (HPMC-AS) as an amorphous solid dispersion in the Zelboraf® 240 mg film-coated tablets (19). Amorphous dispersions are of special interest in the pharmaceutical industry to improve the bioavailability of poorly soluble drugs (20). Therefore, the in vitro solubility and dissolution characterization of vemurafenib in this research is not only based on the crystalline API but also the amorphous form.

1.3. Biopharmaceutic tools and classification frameworks

The investigation of food and ARA effects on the absorption of orally administered drugs are topics within the biopharmaceutical research field. The term “biopharmaceutics” was introduced in the middle of the 20th century to entitle an upcoming research area on the relationship of the physicochemical drug properties and dosage forms, and the biological effects (21).

Biopharmaceutic classification frameworks have been proposed to evaluate drug properties that can determine the absorption and in vivo performance, such as the solubility, dose, and permeability, e.g. the BCS (18) or the Developability Classification System (DCS) (22). The BCS was introduced in the regulatory guidelines to investigate the bioequivalence of drug products and waive clinical bioequivalence studies for highly soluble and permeable drugs (23, 24). It has also been evaluated with respect to food effect predictions (11, 12), making it an interesting subject for discussion within this work. In the BCS (18), the solubility threshold for the high solubility classes (BCS I and III) is defined on the drug substance level using the highest dose strength that needs to be completely dissolved in 250 mL or less of an aqueous medium within the pH range of pH 1 - 6.8 at 37 °C. The high solubility drugs are classified as BCS I in case of high permeability and BCS III in case of low permeability, while the poorly soluble high permeability drugs are categorized as BCS class II and poorly soluble as well as poorly permeable drugs are assigned to BCS class IV (18). The BCS classification has been further modified with the DCS (22), in which a solubility boundary is introduced between IIa (dissolution rate-limited) and IIb (solubility-limited) for highly permeable drugs, defined by the threshold of solubility-limited absorbable dose (SLAD) that can be completely dissolved in 500 mL media. A drug with a SLAD lower than the clinical dose belongs to DCS class IIb. The DCS aims to guide the drug product development strategy for poorly soluble drugs. Complete absorption of class IIa drugs can be achieved by simpler means like particle size reduction, whereas class IIb drugs require more complex technologies, e.g. solid dispersions.

Permeability is the main driver controlling the absorption rate, besides the drug solubility. According to the guidelines, it can be evaluated in different in vitro or in vivo test systems, or indirectly through the fraction absorbed in humans (23, 24). In this research, the apparent permeability in Caco-2 cells and a calculated effective permeability in human intestines based on the structural properties (25) is considered to provide a certain range of permeability estimates of the model drugs.

Besides the in vitro solubility and permeability testing, in vivo preclinical testing and in silico PBPK modeling are important biopharmaceutic tools (8). Different biopharmaceutic tools are used in this work to characterize the selected model drugs and predict their food effect, which will be explained in the following sections.

1.3.1. In vitro solubility and dissolution testing

1.3.1.1. Media and buffer solutions

As the physiological pH levels are altered in the presence of food, the pH dependence of the model drugs' solubility in the physiological pH range of pH 1.2-7.4 (26) was tested. Food intake may especially impact (increase) the gastric pH, leading to reduced solubility of weakly basic drugs, representing a majority of the model drugs in this research.

To better estimate the drug solubilization in the fasted and fed state in vivo, biorelevant media have been proposed (27, 28), containing ingredients like bile salts and phospholipids, that are present in human intestinal fluids (HIF). In the meanwhile, the originally proposed compositions of the fasted state simulated intestinal fluid (FaSSIF) and fed state simulated intestinal fluid (FeSSIF) have been updated (29, 30). Unless indicated otherwise, the terms FaSSIF and FeSSIF in this work refer to the compositions shown in (31).

1.3.1.2. Solubility

The thermodynamic drug solubility is a material specific property which can solely be modified by chemical manipulation of the molecule itself (32). Solubility of drug candidates in aqueous media is one of the most important physicochemical properties that not only determine the hit/lead compounds for pre-clinical in vivo animal studies in drug discovery but also influence the formulation strategies and clinical study design in drug development (Table S 1). With the advent of combinatorial chemistry and high-throughput screening, it is technically feasible to screen for in vitro biological activities across a very large quantity of molecules which in turn generate a growing number of poorly water-soluble lead compounds (1, 2). Solubility is determined in vitro to evaluate the risk for poor absorption due to insufficient solubilization of the drug in the GI with increasing complexity while a compound is advancing in development. At the early discovery stage, high-throughput measurements of solubility aim to alert any solubility issues on pre-clinical in vivo testing and guide a rational drug design to improve solubility. Towards the late discovery stage, progressively more accurate and sensitive analytical methods are performed to measure the equilibrium solubility of hit/lead compounds to gain a better understanding of the overall drug developability (33). Poorly soluble drug candidates might require salt form approaches, solubility enabling formulations and more extensive clinical testing. Commonly, the pharmaceutical industry perceives poor solubility as a research/discovery rather than development issue because it is not cost-effective to modify the molecule or develop formulation strategies to overcome poor solubility at the development stage (4).

The solubility of the model drugs was measured, as food effects on exposure are often associated with low and pH dependent solubility. The solubility after 24 h in buffers of different pH with and without sodium taurocholate (TC) and lecithin was quantified via high performance liquid chromatography

(HPLC) analysis and assumed to represent the thermodynamic value. The pH range tested depended on the pK_a and solubility values itself. In case of very high (> BCS class I threshold) or very low (HPLC quantification not possible) solubility, the tests in pH levels at the lower or upper end of the selected range (pH 1.2 - 7.4) were omitted.

1.3.1.3. Dissolution

In contrast to the solubility, the dissolution kinetics, as extrinsic characteristic, are determined by various factors like the surface area- (particle size) and properties or solid state (32) in a drug formulation. Dissolution testing is described in the pharmacopeias (e.g. United States Pharmacopeia (USP) <711> or European Pharmacopeia (Ph. Eur.) 2.9.3) and recognized by the health authorities as a tool to assess the batch to batch consistency of a drug product, in formulation development and in the assessment of bioequivalence for high solubility and permeability drugs (24, 34, 35).

Biorelevant dissolution testing with the intention to predict the in vivo performance of a dosage form requires specific media, physiologically relevant volumes, and can also be done in non-pharmacopeial setups (36). Biorelevant dissolution tests have been performed in fasted and fed state simulating media to predict food effects on exposure, also in combination with PBPK modeling (37-40). In biorelevant dissolution tests in pharmacopeial USP II setup, usually 500 mL volume of intestinal simulated media and 250 mL for simulation the fasted stomach are used with a paddle speed of 50 revolutions per minute (rpm) (37, 38), 75 rpm (39-41), or 100 rpm (42). In this research, dissolution tests in FaSSIF and FeSSIF are applied to a subset of the selected model anticancer drugs, to examine their suitability as a standard screening tool for food effect predictions. The compound selection of the subset for dissolution tests in 500 mL and 250 mL USP II setup was based on the drug solubility and the observed food effect in clinical studies. Tarceva® (erlotinib) 100 mg film-coated tablets, Iressa® (gefitinib) 250 mg film-coated tablets, and M1 30 mg film-coated tablets were chosen. Their solubility in FaSSIF and FeSSIF is sufficient to ensure the release of at least 5 % of the dose but still not too high, so that differences between the release profiles in 500 mL or 250 mL FaSSIF and FeSSIF might be seen. As neither of those three drugs showed a significant food effect in their clinical studies (43, 44), Votrient® (pazopanib) 400 mg film-coated tablets and Zelboraf® (vemurafenib) 240 mg film-coated tablets with considerable (possibly dissolution-related) food effect in human (45, 46), were additionally selected. Due to the low solubility of pazopanib (0.0012 mg/mL in FaSSIF) and vemurafenib (0.0054 mg/mL in FaSSIF, as HPMC-AS coprecipitate) in those media, the tests were performed in the USP IV dissolution apparatus.

The comparison of the measured dissolution profiles is facilitated by fitting a mathematical function to describe the release curve and obtain profile specific dissolution parameters. Nicolaidis et al. (47) evaluated the usefulness of different mathematical models, where the first order model was found to

be one of the most generally applicable. Therefore, it was selected also for this research. A linear zero-order model was fitted to the cumulative USP IV dissolution profiles with incomplete release.

Following the increasing number of poorly soluble drug candidates, their ability to form supersaturated solutions to increase absorption has gained more and more interest (36). Besides the transfer model developed by Kostewicz et al. (10), different setups have been presented (48). A simplified procedure, the so called “dumping” method (49), where a drug solution is dumped into FaSSIF, was applied to measure the precipitation kinetics of the model drugs in this research.

1.3.2. In vivo PK analysis

Before candidate drugs enter the first in man study and clinical testing, their PK, safety, and efficacy is tested in preclinical species. Also in the later phase, specific (e.g. biopharmaceutical) issues can be investigated in animals, as the studies are facilitated regarding ethical justification and costs compared to human studies, and subsequently confirmed in humans (50).

The collected preclinical and clinical in vivo data can provide information on the mechanisms underlying the PK of a drug, e.g. if poor solubility measured in vitro limits drug absorption in vivo (51). Evidence suggest that the oral bioavailability may not always depend on the thermodynamic solubility of drug substances that were determined to be poorly water-soluble. First, adequate oral absorption has been reported for several BCS II/IV drugs including non-steroidal anti-inflammatory drugs (e.g. naproxen and ketoprofen) (52, 53) and other therapeutics such as phenytoin, diazepam, warfarin, lamotrigine, glipizide and sulfamethoxazole having an absolute bioavailability (F) greater than approximately 90 % (54). Secondly, although poorly water-soluble, lipophilic compounds are generally expected to show better solubilization in GI fluids with food and thus a better oral absorption in the fed state (12), poorly water-soluble anticancer drugs such as imatinib, sunitinib, trametinib, and vandetanib have a limited food effect (17). Moreover, enabling formulations improving the apparent or kinetic solubility of poorly water-soluble active ingredients do not always enhance oral bioavailability (55), indicating that solubilization is not the key factor limiting the systemic exposure. Lastly, poor oral bioavailability may be caused by other mechanisms such as first-pass gut and hepatic metabolism, and transporter-mediated intestinal efflux. To identify these, additional confirmatory studies are required, such as metabolite quantification studies comparing the PK profiles between oral and intravenous administrations (56, 57) and quantification of fecal drug.

Figure 1 shows the workflow applied in this research to identify the model drugs with solubility-limited absorption based on early human or preclinical PK data. A potential loss of drug in the gut can be identified by calculating the gut bioavailability from single dose IV and oral PK studies. The gut bioavailability or gastro intestinal availability ($F_a \cdot F_g$) represents the fraction of the administered dose reaching the portal vein and was calculated using the oral bioavailability and systemic clearance. The

oral bioavailability (F) of a drug represents the fraction of the administered dose that becomes available in the systemic circulation. It consists of the fraction absorbed into the enterocytes (F_a), the fraction that escapes any potential metabolism in the gut (F_g) and the fraction that escapes the first pass metabolism (F_h).

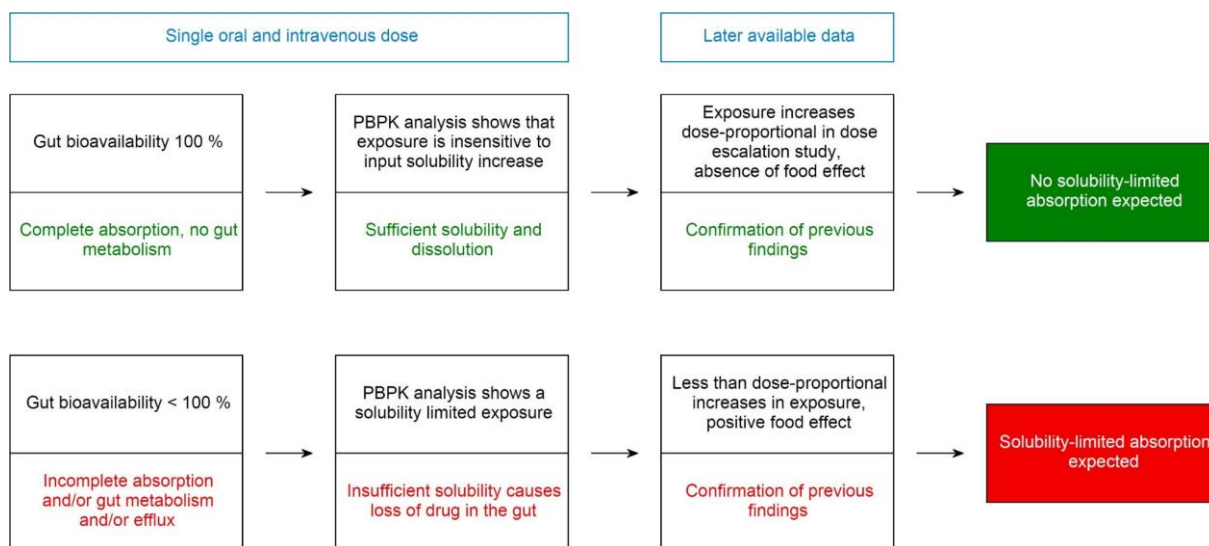


Figure 1: Schematic illustration of the proposed methods to assess solubility-limited absorption behavior through a mechanistic analysis of pharmacokinetic data (51)

A gut bioavailability of 100 % indicates limited drug metabolism in the gut and a complete oral absorption due to adequate solubility and intestinal permeability. The subsequent PBPK analysis can clarify, whether a potentially reduced gut bioavailability is caused by insufficient solubilization or pre-systemic metabolism. Later available clinical data such as ascending oral dose PK or food effect study can confirm the outcomes of the PBPK modeling approach. Exposure increasing in a less-than dose proportional manner can indicate limited absorption at higher doses due to insufficient solubilization. Increased exposure of a poorly soluble drug in the fed state compared to the fasted state can also indicate solubility-limited absorption in the fasted state. As solubility-limited absorption and food effect are often associated (4), they can help to indicate one another.

The PK analysis was based on human PK data from the literature and rat PK data. One goal was to investigate, whether or not the rat is a good model to predict solubility-limited absorption in human. Appropriate rat PK data at the required dose (human food effect dose scaled by body weight) were not available in the literature and the different formulations/ unknown particle sizes used by the investigators can affect the results. Therefore, a dedicated rat PK study was performed for the purposes of this work.

1.3.3. In silico PBPK modeling

PBPK models are powerful *in silico* tools that describe drug absorption, disposition, metabolism, and elimination through the integration of PK mechanisms, compound data, anatomy and physiology (58). PBPK models for absorption modeling often consist of a complex gut compartment and one or more systemic compartments that determine the decrease in drug concentrations after dosing, following its distribution and elimination properties that can be obtained from IV PK characterization of the drug. The advanced compartmental and transit (ACAT) model (59) is a comprehensive gut model, that consists of nine luminal gut compartments with different physiological properties, nine associated enterocyte compartments and provides different states of the drug, e.g. dissolved and undissolved, to simulate the absorption.

PBPK models can be primarily built based on observed PK data, e.g. to analyze covariates, in a top-down setting or based on *in vitro* data to extrapolate clinically untested scenarios in a so-called bottom-up prediction (60).

The PBPK modeling approach used for the analysis of clinical and rat PK data in this work was a top-down modeling approach to find out about the mechanisms responsible for the observed PK. A lineshape analysis as described by Peters (61) was performed using a generic PBPK model built in MATLAB®. The identification of solubility-limited absorption using this model is straight forward, as the absorption relies on the input solubility at a certain pH and the input permeability. If the simulated exposure is insensitive to changes in permeability, potential absorption problems can be attributed to the solubility.

PBPK modeling is not yet recognized by the health authorities to waive food effect studies, but it has been used to predict and explain food effects on the exposure of several drugs. Recently, Li et al. reviewed the performance of PBPK modeling in published food effect predictions (14). 50 % of the reported food effects were found to be predicted within 1.25-fold and 75 % within 2-fold of the observed value. Gaps in knowledge on the drug product, API and physiology were identified that currently hinder better prospective predictions by PBPK. Mostly, the food effects simulations were performed retrospectively, and the models were case-specifically adjusted to fit the observed fed state PK profile and gut first pass metabolism is often unconsidered (62-65). The need for a standardized procedure for food effect predictions with PBPK modeling, including proper validation of the model with clinical PK data, has been recognized and recently a workflow for food effect predictions has been suggested by Tistaert et al. (62).

Following up on this, bottom-up food effect predictions with PBPK were also part of this research. The goal was to develop and evaluate a workflow for prospective food effect predictions that does not require compound specific solutions to fit the observed food effect. To cover the knowledge gaps in

compound-specific input parameters and the physiological variability, the approach proposed in this work includes several simulations using different parameter settings. Therefore, the commercially available software GastroPlus® was used, which provides a very detailed ACAT model with the flexibility to adjust the relevant parameters. It offers different dissolution models, for example the default Johnson Model based on the modified Nernst-Brunner equation (66) and in vitro solubility, or the Z-Factor model based on Takano et al. (67), that enables the use of in vitro dissolution data as input.

1.4. Research Objectives

Concomitant food intake can alter the absorption and PK of a drug through various mechanisms. Therefore, food-drug interactions represent a challenge in the development of orally administered drugs. The objective of this work is to evaluate and improve the current food effect prediction strategies based on ten oral anticancer model drugs. To this aim, in vitro solubility and dissolution testing, mechanistic analysis of human and rat PK data using top-down PBPK modeling and food effect simulations by bottom-up PBPK modeling are in the focus of this research. Based on these selected tools, the research objectives can be divided into three parts:

1. Evaluation of the performance of in vitro solubility and dissolution data in food effect predictions for poorly soluble compounds (BCS II and IV)

- Investigation whether there is a connection between pH dependent solubility in vitro and observed food effect in vivo
- Comparison of the relative difference between FaSSIF and FeSSIF solubility and the observed food effect in clinical studies
- Comparison of the relative difference between dissolution parameters from FaSSIF and FeSSIF release profiles with the effect of food on the PK of the model drugs in the clinical studies
- Examination whether common biorelevant dissolution conditions provide good food effect predictions for the model drugs and can be recommended as a screening method

2. Improved prediction of food effects on drug exposure through understanding the mechanisms underlying the absorption/ exposure in human and rat

- Analyzing early clinical pharmacokinetic data in combination with top-down PBPK analysis to identify drugs whose absorption is truly limited by solubility in vivo and therefore expected to exhibit food effect
- Assessment of the relevance of in vitro solubility for in vivo absorption using PBPK top-down analysis

- Examination of the rat as a model for solubility-limited absorption in human

3. Development of a workflow in GastroPlus® for food effect predictions that addresses current scientific challenges

- Development of a workflow for improved food effect prediction using in GastroPlus®, that meets the following requirements
 - does not require fitting the model to the observed fed state PK profile
 - includes considerations on gut first pass metabolism
 - deals with the uncertainty of compound-related input parameters
 - accounts for the highly variable physiological conditions in the GI
- Evaluation of the developed procedure based on the ten model drugs of this research

2. Materials

2.1. Drug substances and drug products

Table 1: Drug substances and drug products used in this work

Material	Manufacturer
Crizotinib	Merck KGaA, Darmstadt, Germany (internal batch)
Dabrafenib mesylate	Chem Shuttle, Hayward, CA, USA
Erlotinib hydrochloride	Activate Scientific, Prien-Chiemsee, Germany
Gefitinib	Merck KGaA, Darmstadt, Germany (internal batch)
Imatinib mesylate	abcr GmbH, Karlsruhe, Germany
Lapatinib ditosylate monohydrate	Ark Pharm, Arlington Heights, IL, USA
M1	Merck KGaA, Darmstadt, Germany (internal batch)
Pazopanib hydrochloride	Ark Pharm, Libertyville, IL, USA
Trametinib*DMSO (1:1)	Asta Tech, Bristol, PA, USA
Vemurafenib (crystalline)	Chem Shuttle, Hayward, CA, USA
Iressa® 250 mg film-coated tablets	AstraZeneca GmbH, Wedel, Germany
M1 30 mg film-coated tablets	Merck KGaA, Darmstadt, Germany (internal batch)
Tarceva® 100 mg film-coated tablets	Roche Pharma AG, Grenzach-Wyhlen, Germany
Votrient® 400 mg film-coated tablets	Novartis Pharma GmbH, Nürnberg, Germany
Zelboraf® 240 mg film-coated tablets	Roche Pharma AG, Grenzach-Wyhlen, Germany

2.2. Chemicals

Table 2: Chemicals used in this work

Material	Manufacturer
1 N Hydrochloric acid	Merck KGaA, Darmstadt, Germany
1 N Sodium hydroxide (NaOH)	Merck KGaA, Darmstadt, Germany
10 % sodium dodecyl sulfate (SDS) solution	Merck KGaA, Darmstadt, Germany
Acetonitrile	Merck KGaA, Darmstadt, Germany
FaSSIF/FeSSIF/FaSSGF (“SIF Powder”)	Biorelevant.com Ltd, London, UK
Formic acid	Merck KGaA, Darmstadt, Germany
Glacial acetic acid	Merck KGaA, Darmstadt, Germany
Kleptose®	Roquette, Lestrem, France
Lactochem® Fine Powder	DTFE Pharma, Goch, Germany
Methanol	Merck KGaA, Darmstadt, Germany
NaOH pellets	Merck KGaA, Darmstadt, Germany
Potassium dihydrogen phosphate (KH ₂ PO ₄)	Merck KGaA, Darmstadt, Germany
Sodium acetate trihydrate	Merck KGaA, Darmstadt, Germany
Sodium chloride (NaCl)	Merck KGaA, Darmstadt, Germany
Sodium dihydrogen phosphate monohydrate (NaH ₂ PO ₄ *H ₂ O)	Merck KGaA, Darmstadt, Germany
Sodium formate	Merck KGaA, Darmstadt, Germany
Trifluoroacetic acid	Merck KGaA, Darmstadt, Germany

2.3. Buffer and dissolution media

Table 3: Buffer and dissolution media used in the solubility and release tests within this research

Simulated Gastric Fluid (SGF) pH 1.2	
NaCl	2.0 g
1 N Hydrochloric acid	80 mL
Purified water	ad 1 L
Fasted state simulated gastric fluid without SIF Powder (FaSSGF blank) pH 1.6	
NaCl	2.0 g
0.025 N Hydrochloric acid pH 1.6	ad 1 L
FaSSGF pH 1.6	
SIF Powder	0.06 g
FaSSGF blank pH 1.6	ad 1 L
Formate buffer pH 3.0	
Sodium formate	0.54 g
Formic acid	1.58 mL
Purified water	ad 1 L
Acetate buffer pH 4.0	
Solution A (822 mg sodium acetate trihydrate in 100 mL purified water)	approx. 20 mL
Solution B (1.44 mL glacial acetic acid in 250 mL purified water)	approx. 100 mL
FeSSIF blank pH 5.0	
NaOH	4.04 g
Glacial acetic acid	8.65 g
NaCl	11.87 g
Purified water	ad 1 L
FeSSIF pH 5.0	
SIF Powder	11.2 g
FeSSIF blank pH 5.0	ad 1 L
FaSSIF blank pH 6.5	
NaOH	0.42 g
NaH ₂ PO ₄ *H ₂ O	3.95 g
NaCl	6.19 g
Purified water	ad 1 L
FaSSIF pH 6.5	
SIF Powder	2.24 g
FaSSIF blank pH 6.5	ad 1 L
Phosphate buffer pH 7.4	
0.2 N KH ₂ PO ₄	250.0 mL
0.1 N NaOH	394.4 mL

2.4. Instruments and software

Table 4: Instruments and software used in this work

Instrument/ Software	Manufacturer
780 pH Meter	Metrohm GmbH & Co. KG, Herisau, Switzerland
Analytical balance Mettler Toledo XP205	Mettler Toledo, Giessen, Germany
Eppendorf Centrifuge 5804 R	Eppendorf AG, Hamburg, Germany
Erweka DT 80 dissolution tester with 400 mL mini vessel and mini paddle	Erweka, Heusenstamm, Germany
Excel® for Office 365 MSO	Microsoft Corporation, Redmond, WA, USA
Fraction collector C 615	Sotax, Aesch, Switzerland
GastroPlus® v 9.5	Simulations Plus, Lancaster, CA, USA
Hitachi LaChrom Elite® HPLC System	Hitachi High-Technologies Co., Tokyo, Japan
Magnetic stirrer RCT basic	IKA®-Werke GmbH & CO. KG, Staufen, Germany
MATLAB® software version R2017a	The MathWorks, Inc., Natick, MA, USA
Micro balance XP6U Comparator	Mettler Toledo, Giessen, Germany
Milli-Q water purification system	Merck KGaA, Darmstadt, Germany
Multipette® Xstream	Eppendorf AG, Hamburg, Germany
OpenLab® chromatography data system	Agilent Technologies, Santa Clara, CA, USA
Piston Pump CP 7-35	Sotax, Aesch, Switzerland
Precision balance Sartorius MSE3203S-1CE-DR	Sartorius, Lab Instruments, GmbH & Co.KG, Goettingen, Germany
Shaking water bath 1083	GFL, Burgwedel, Germany
USP II dissolution tester AT 7 smart	Sotax, Aesch, Switzerland
USP IV dissolution tester CE 7 smart	Sotax, Aesch, Switzerland
WinSOTAX® plus - Dissolution Software	Sotax, Aesch, Switzerland

2.5. Other materials

Table 5: Other materials used in this work

Material	Manufacturer
Acrodisc CR 0.45 µm PTFE syringe filters (25 mm)	Pall Life Sciences, East Hills, NJ, USA
Capsugel® PCcaps®	Capsugel, Lonza, Bornem, Belgium
Chromolith® High resolution RP-18e 100x4.6 mm HPLC column	Merck KGaA, Darmstadt, Germany
Chromolith® Performance RP-18e 100 x 3 mm HPLC column	Merck KGaA, Darmstadt, Germany
Eppendorf Tubes® 1.5 mL	Eppendorf AG, Hamburg, Germany
Glass beads 1mm	Sotax, Aesch, Switzerland
Whatman® glass microfiber filters GF/D	Whatman, Dassel, Germany
Whatman® glass microfiber filters GF/F	Whatman, Dassel, Germany

3. Methods

3.1. HPLC-methods for drug quantification

The dissolved amount of drug in the solubility and dissolution assays was quantified by HPLC analysis in reference to a 0.1 mg/mL (or further diluted) standard solution. If possible, a largely universally applicable and economic HPLC method, further referred to as HPLC method 1, was employed. For crizotinib, gefitinib and M1 quantification an alternative method, further referred to as HPLC method 2, was used to ensure reliable quantification. Details are given in Table 6 and the appendix (Table S 2, Table S 3, Table S 4). Compound specific changes to optimize the presented basic HPLC methods are shown in Table S 5. The data was processed using the OpenLab® chromatography data system.

Table 6: HPLC methods for drug quantification

Parameter	HPLC Method 1	HPLC Method 2
Equipment	Hitachi LaChrom Elite® HPLC System	
Detector	UV detector	
Wavelength	see Table S 2	
Injection System	Autosampler	
Injection volume	see Table S 2	
Column	Chromolith Performance; RP-18e, 100 x 3 mm	Chromolith High Resolution; RP-18e, 100 x 4.6 mm
Eluent A	Purified water + 0.1 % Formic acid	950 mL Purified water 50 mL Acetonitrile 1 mL Trifluoroacetic acid
Eluent B	Acetonitrile + 0.1 % Formic acid	950 mL Acetonitrile 50 mL Purified water 1 mL Trifluoroacetic acid
Gradient	see Table S 3	see Table S 4
Column Temperature	37 °C	35 °C
Autosampler Temperature	25 °C	25 °C
Applied for compounds	dabrafenib, erlotinib, imatinib, lapatinib, pazopanib, trametinib, vemurafenib	crizotinib, gefitinib, M1

3.2. *In vitro* solubility testing

3.2.1. Thermodynamic solubility measurements

The solubility of the model compounds was measured in duplicate in buffers from pH 1.2 to pH 7.4 as appropriate. Additionally, solubility was measured in biorelevant buffers containing different amounts of “SIF Powder” (commercially available TC/ lecithin-mixture in the molar proportion of 5:1 for the preparation of FaSSIF and FeSSIF) at pH 5.0 (based FeSSIF blank) and pH 6.5 (based on FaSSIF blank) to obtain concentrations of 0/ 3/ 15 mM TC and 0/ 0.75/ 3.75 mM lecithin. The buffer compositions are presented in Table 3. Drug substances in the marketed salt form were used and in case of vemurafenib ground market product, Zelboraf® 240 mg film-coated tablets (containing amorphous vemurafenib coprecipitate). API was weighed into an Erlenmeyer flask in excess with 10 mL of the media. The flask was incubated at 37 °C in a shaking water bath with 250 movements per minute. After 1 h, 2 h and 24 h, samples were taken and centrifuged at 14,000 rpm and 37 °C for 5 minutes to remove the remaining solid drug. Additionally, the pH of the solution was measured. The supernatant was analyzed by HPLC after dilution with an appropriate organic solvent to prevent re-precipitation.

3.2.2. Dumping experiments

Two-stage solubility tests were performed to explore the precipitation kinetics of the model drugs in solution dumped into 37 °C FaSSIF. The dose of the clinical food effect study as well as the intestinal volume of 500 mL was scaled-down by a factor of 25 to reduce the required API amount. 20 mL FaSSIF in an Erlenmeyer flask were preheated in a shaking water bath at 37 °C. 1/25 of the food effect study dose (as API in the clinically relevant salt form) completely dissolved in 0.6 mL simulated gastric fluid (SGF) pH 1.2 if possible, or otherwise DMSO (resulting in max. 3 % DMSO in the final mixture) was added under gentle shaking (approx. 120 movements per minute) and afterward incubated with 250 movements per minute. Samples were drawn after 15, 30 and 120 min, centrifuged and diluted prior to the HPLC analysis as described in 3.2.1. The dumping tests were performed in duplicate. To identify supersaturation, the concentrations at 15 min, 30 min and 120 min after dumping of the drug solutions were compared to the thermodynamic solubility after 24 h in pure FaSSIF. The potential bias that the supersaturation is attributed to the presence of DMSO can be excluded when the concentration after 15 min is higher than 120 min after dumping the solution. If this was not the case, a shake-flask solubility test of the drug in FaSSIF + 3 % DMSO was performed, to identify the thermodynamic solubility in FaSSIF + 3 % DMSO and confirm the supersaturated state in the dumping experiment.

3.2.3. Solubility parameters for biopharmaceutical classification

The BCS classification of the model compounds was taken from literature (17). Additionally, the dose number (D_0) was calculated for the dose applied in the clinical food effect studies (M_0) according to Amidon et al. (18) with Equation 1 using the measured thermodynamic solubility in FaSSIF (C_s) and volume (V_0) of 250 mL.

$$\text{Equation 1: } D_0 = \frac{M_0/V_0}{C_s}$$

Furthermore, the SLAD was calculated according to Butler et al. (22) to classify the model compounds based on the DCS classification system using Equation 2 with the thermodynamic solubility in FaSSIF (S_{si}) and volume (V) of 500 mL. The permeability-dependent multiplier (M_p) equals the absorption number (A_n) for high permeability compounds (in this work, all model drugs with calculated $P_{eff} \geq 1 \times 10^{-4}$ cm/s), and is kept at unity for others (here only pazopanib). A_n was calculated according to Equation 3 (18) using the calculated human effective permeability (cP_{eff}) according to (25), a tube radius (R) of 1 cm (18) and residence time (t_{res}) of 3.32 h (22). In the case of pazopanib, the cP_{eff} was quite low (< 1) and M_p was kept at unity.

$$\text{Equation 2: } SLAD = S_{si} * V * M_p$$

$$\text{Equation 3: } A_n = \frac{cP_{eff}}{R} * t_{res}$$

To discuss the relationship of dose and solubility with regard to the rat GI, the required volume of FaSSIF to dissolve the oral doses used in the rat PK study designed for this research was calculated. To this aim, the dose (for a rat of 0.25 kg body weight) was divided by the measured thermodynamic FaSSIF solubility of the drug.

3.3. In vitro dissolution

3.3.1. USP II dissolution tests

Dissolution tests of Tarceva® 100 mg film-coated tablets (containing 109.28 mg erlotinib HCl), Iressa® 250 mg film-coated tablets (containing 250 mg gefitinib free base) and M1 30 mg film-coated tablets were performed in 500 mL medium in the USP II paddle apparatus described in USP <711> and Ph. Eur. 2.9.3. The tests were conducted with $n=3$ tablets and sampling after 5, 10, 15, 20, 30, 45, 60, 90, 120, 180 and 240 min. A paddle speed of 75 rpm was used unless coning and adhesion to the vessel wall required an increase to 100 rpm. Moreover, mini-dissolution tests in 250 mL FaSSIF and FeSSIF were performed in a mini paddle apparatus, scaled down by 1/3 of the USP II apparatus, with comparable hydrodynamics (68). After filtration with 0.45 μm PTFE filters and appropriate dilution, the dissolved drug was analyzed by amount HPLC analysis.

The sample volume was not replaced, so the released amount of drug at the first sampling time was calculated according to Equation 4 and for the subsequent timepoints according to Equation 5.

$$\text{Equation 4: } w = \frac{A_S}{A_{Std}} * V_D * \frac{m_{Std} * P_{Std} * f}{V_{Std} * D}$$

$$\text{Equation 5: } w = \left[\left(\frac{A_S}{A_{Std}} * (V_S - V_{S,tot}) \right) + \left(\left(\sum_{t=1}^{n-1} \frac{A_S}{A_{Std}} \right) * V_P \right) \right] * \frac{m_{Std} * P_{Std} * f}{V_{Std} * D}$$

w	% of dose released
A _S	Area sample
A _{Std}	Area standard solution
V _D	Dissolution volume [mL]
m _{Std}	drug weight for standard solution [mg]
P _{Std}	purity of standard substance [%]
f	dilution factor of the sample solution prior to HPLC analysis
V _{Std}	Volume for the preparation of the standard solution [mL]
D	dose [mg]
V _S	sample volume [mL]
V _{S,tot}	total volume of the samples taken up to the current time point [mL]

3.3.2. USP IV dissolution tests

Dissolution tests of Votrient® 400 mg film-coated tablets (containing 433.33 mg pazopanib HCl) and Zelboraf® 240 mg film-coated tablets (containing 240 mg vemurafenib in form of HPMC-AS coprecipitate) were performed in the USP IV (flow-through cell) apparatus described in USP <711> and Ph. Eur. 2.9.3 using 22.6 mm cells and open circuit. The cells were filled with 6 g of 1 mm glass beads to ensure laminar flow and the tablets were placed in the described holder. A 2.7 µm Whatman GF/D glass fiber filter was used to retain the coarse particles followed by a 0.7 µm Whatman GF/F glass fiber filter to retain the undissolved fine material. 30 mL of the eluted buffer after 2, 4, 6, 8, 10, 15, 20, 25, 30, 35, 45, 55, 65, 75 and 85 min each, were automatically sampled in the fraction collector, representing 93.75 % of the eluted buffer in the fractions of 2 min duration (between 0-10 min of the release test), 37.5 % of the eluted buffer in the fractions over 5 min (between 10-35 min of the test), and 18.75 % of the 10 min-fractions (between 35-85 min of the test), adequately splitted by the WinSOTAX®plus dissolution software. To prevent precipitation in the fraction collector a previously evaluated buffer was filled into the vials in the fraction collector prior to the dissolution test. The release from the dosage forms was tested in FaSSiF and FeSSiF with a flow-rate of 16 mL/min and n=3 tablets each.

The released amount of drug in each sampling interval was calculated according to Equation 6 and summed up to obtain the cumulative release versus time profile.

$$\text{Equation 6: } \% \text{released}_{\text{per fraction}} = \frac{A_S * C_{Std} * V_{tot}}{A_{Std} * D} * 100\% * f$$

A_S Area sample

A_{Std} Area standard solution

C_{Std} Concentration of the standard solution [mg/mL]

V_{tot} total volume containing the released amount of drug in the regarding time span including the discarded sample volume during splitting and the sample dilution [mL]

D dose [mg]

F dilution factor of the sample from the fraction collector prior to HPLC analysis

3.3.3. Dissolution parameter fitting

3.3.3.1. First-order and zero-order model fit

To compare the USP II dissolution profiles in FaSSIF and FeSSIF, a first-order exponential function (Equation 7) was fitted to the measured data as illustrated in Figure 2, with W_t as the amount dissolved at time t , W_{max} the maximum amount dissolved and k the first order dissolution constant (47) using the Solver Add-in in Excel® for Office 365 MSO.

$$\text{Equation 7: } W_t = W_{max} (1 - e^{-kt})$$

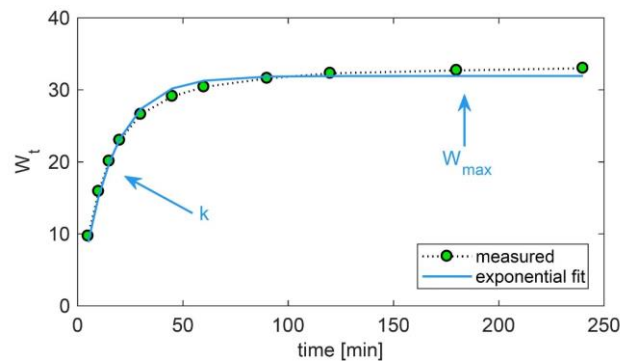


Figure 2: Exemplary measured dissolution profile with exponential fit to illustrate the first-order model fitting

For USP IV dissolution profiles from open circuit that do not show in complete release during the time of the test, fitting an exponential function is not appropriate (as the maximum amount is not yet reached). Therefore, a zero-order model (Equation 8) with W_t as the amount dissolved at time t and k_0 the zero-order dissolution constant, was fitted to the initial linear part of the cumulative dissolution profiles, observed between 0-6 min for Votrient® 400 mg tablets and 0-15 min for Zelboraf® 240 mg tablets by linear regression in Excel® for Office 365 MSO®.

$$\text{Equation 8: } W_t = k_0 * t$$

The coefficient of determination (R^2) was calculated according to Equation 9.

$$\text{Equation 9: } R^2 = 1 - \frac{\sum_{i=1}^n (\%released_{observed} - \%released_{fitted})^2}{\sum_{i=1}^n (\%released_{observed} - \overline{\%released_{observed}})^2}$$

3.3.3.2. Z-Factor fit

The z-factor (z) for the use in GastroPlus® was fitted according to Equation 10 in the built-in module in the software to the USP II dissolution profiles and to the USP IV dissolution profiles using the Solver Add-in in Excel® for Office 365 MSO® assuming that the luminal concentration (C_l) equals 0, as the release tests were performed under sink conditions.

$$\text{Equation 10: } \frac{dM_D}{dt} = z M_{u,0} \left(\frac{M_{u,t}}{M_{u,0}} \right)^{\frac{2}{3}} (C_s - C_l)$$

M_D amount dissolved

$M_{u,0}/M_{u,t}$ amount undissolved at the time 0 or t

C_s solubility in the medium

3.4. Permeability assessment

3.4.1. Apparent permeability through a Caco-2 cell monolayer

Permeability data of the model compounds across a TC7 Caco-2 monolayer on a microporous polycarbonate membrane filter (Figure 3) was provided by the In Vitro DMPK Design 1 lab at Merck Healthcare KGaA (Darmstadt, Germany). The apparent permeability (P_{app}) was measured bidirectionally, from apical (A) to basolateral (B) and B to A, in a 24-well plate and up to five compounds per well. The passive apparent permeability was calculated as the geometric mean of P_{app} A to B and P_{app} B to A. The assay was performed using Hank's balanced salt solution (pH 7.4) as apical and basolateral matrices and in the presence of cyclosporine A that inhibits the transporter P-glycoprotein (P-gp). The compounds were added in form of DMSO stock solutions to obtain a final drug concentration of 1 μ M, with a final DMSO concentration of ≤ 1 %. Before the reaction over 2 h at 37 °C, 5 % CO₂ and saturated humidity, the transepithelial resistance was measured to ensure the monolayer integrity ($\geq 250 \Omega$). The reference compounds including propranolol (high permeability reference), pindolol (medium permeability reference), atenolol (low permeability reference), melagatran (impermeable), indinavir (reference substrate for P-gp efflux) were used. HPLC analytic was used to quantify the drug concentrations after the reaction in the apical and basolateral matrix.

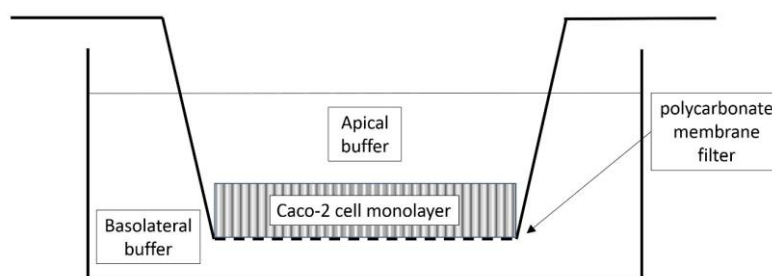


Figure 3: Schematic illustration of the Caco-2 permeability test setting

3.4.2. Calculation of the effective intestinal permeability

The effective human intestinal permeability was calculated, based on log P (CLOGP), the polar surface area and the number of hydrogen bond donors (HBD) according to Equation 11 (25). The input values used for the calculation are shown in Table 7.

$$\text{Equation 11: } \log P_{eff} = -3.061 + 0.190 \text{ CLOGP} - 0.010 \text{ PolarSurfaceArea} - 0.246 \text{ HBD}$$

Table 7: Input parameters for calculation of the effective permeability of the ten model compounds

	Polar Surface Area* [\AA^2]	CLOGP*	HBD*
Crizotinib	77.99	3.57	2
Dabrafenib	110.86	5.46	2
Erlotinib	74.73	3.2	1
Gefitinib	68.74	3.75	1
Imatinib	86.28	4.38	2
Lapatinib	106.35	4.64	2
M1	94.71	4.21	0
Pazopanib	119.03	3.55	2
Trametinib	102.06	3.18	2
Vemurafenib	91.92	4.62	2

* sourced from drug bank (<https://www.drugbank.ca/>), except for M1

3.5. Rat PK study

3.5.1. Preparation of the dosage forms

IV PK studies (cassette) at 0.2 mg/kg were performed in 40 % Polyethylene glycol (PEG) 200/ 60 % water+0.3 % DMSO per compound (from DMSO stock solutions) with up to 4 compounds per cassette plus a reference drug to ensure the PK is appropriate. For the IV PK studies at a higher dose of crizotinib (4.9 mg/kg) and erlotinib (3.0 mg/kg), a vehicle screening was performed. Aqueous buffers of pH 3.0 - 5.5 (due to the better crizotinib and erlotinib solubility in acidic media) were tested with different adjuvants to ensure complete solubilization of the required dose within 1 h, stability for at

least 24 h (confirmed with HPLC analysis) and a final pH between pH 3 and pH 5.0 mm acetate buffer pH 4.0 was found suitable for a bolus injection of 1 mL/kg of crizotinib (4.9 mg/kg) and 2 % DMSO/20 % Kleptose® (beta-cyclodextrin) in 50 mm acetate buffer pH 4.0 for erlotinib (3.0 mg/kg), with a final pH of 4.6 and 4.0, respectively.

The doses for the oral PK studies were derived from the doses at the human food effect studies and were body weight-scaled (Table 8). The drugs were administered as pure API in the form of the clinically relevant salt in Capsugel® PCcaps® (length 7.18 mm, internal diameter 2.06 mm) of gelatin. In case the dose did not fit into one capsule, it was evenly divided into two capsules. The market formulation of lapatinib, that undergoes a positive food effect in human as well, could not be tested as the sample amount exceeded the capacity of two capsules. M1 rat PK at 0.5 mg/mL was already available in an internal database at the desired dose from oral suspension in DMSO/PEG 400/water (20:40:40, V/V/V) and was used for the PK analysis to identify solubility-limited absorption.

Table 8: Overview of the oral doses employed in the rat PK studies

	Dose (free base) human 70 kg [mg]	Dose (free base) [mg/kg]	Dose (free base) rat 250 g [mg]	Dose (salt form) 250g rat [mg]	Amount of ground tablet 250g rat [mg]
Crizotinib	250	3.6	0.89	0.89	-
Dabrafenib	150	2.1	0.54	0.63	-
Erlotinib	150	2.1	0.54	0.59	-
Gefitinib	250	3.6	0.89	0.89	-
Imatinib	400	5.7	1.43	1.71	-
Lapatinib	1500	34.8	5.36	8.70*	-
M1	27	0.39	0.10	0.11	-
Trametinib	2	0.03	0.007	0.008	-
Pazopanib	800	11.4	2.86	3.10	4.71
Vemurafenib	960	13.7	3.43	3.43	12.43*

* 2 capsules were used to deliver the high dose

Prior to the capsule preparation, the particle size of all APIs and the ground market products were homogenized using mortar and pestle until most of the particles were < 10 µm in diameter. The particle size was controlled by light microscopy. In the case of the ground Zelboraf® film-coated tablet, many particles remained > 100 µm. This could not be improved by ball-milling (Fritsch Pulverisette 23, Fritsch, Idar-Oberstein, Germany) with different milling times, speed and grinding balls. However, it is not considered relevant as the API is already solidly dispersed within the formulation so that there are no actual API crystals whose particle size could influence the dissolution.

The capsules were filled with the funnel and stand provided by the capsule manufacturer. Due to the low dose of 0.008 mg, trametinib was diluted with lactose (Lactochem® Fine Powder) by 1:100 prior to

the capsule filling using mortar and pestle. The drug content and content uniformity of the blend were tested with HPLC analysis and 0.008 mg trametinib could be dosed with an average content of 103.8 % and relative standard deviation of 1.67 % (n=10).

3.5.2. In vivo rat PK study

3.5.2.1. Contribution statement and ethical declaration

The rat PK studies were conducted at Nuvisan GmbH (Grafing, Germany) according to established practice and operation procedures, in cooperation with the NCE Discovery DMPK department at Merck Healthcare KGaA, Darmstadt, Germany. The oral PK studies were performed with capsules prepared by myself. The vehicles for the IV PK testing of 3 mg/kg erlotinib and 4 mg/kg crizotinib were prepared according to the instructions, resulted from my vehicle screening. The results were reported to me in form of the measured plasma concentration time profiles, the percentage amount of parent drug recovered in the feces and calculated PK parameters.

All animal experiments were approved by the District Government of Upper Bavaria and conducted in compliance with German and European Animal Welfare Laws and Regulations in an Association for Assessment and Accreditation of Laboratory Animal Care (AAALAC) accredited facility.

3.5.2.2. IV PK testing in the rat

Female Han Wistar Rats (n=3) received a single tail vein intravenous bolus injection of the model drugs at 0.2 mg/kg in cassette or alone (in case of 3.0 mg/kg erlotinib and 4.9 mg/kg crizotinib IV) in the formulations described in 3.5.1. Consecutive blood samples were taken sub-lingually under isoflurane anesthesia, after 0.1, 0.5, 1, 2, 4, 6 and 24 h and were further processed to obtain plasma. The animals were housed in individual metabolism cages allowing the collection of feces for a period of 24 h or 48 h. Samples were stored at -20 ± 5 °C until the bioanalytical quantification.

3.5.2.3. Oral PK testing with capsules in the rat

The rats were deprived of food for 6 h prior to administration of the capsules. Water was offered ad libitum. Female Han Wistar rats (n=3) received a single oral administration of the model drugs in capsules by gavage, at the dose levels listed in Table 8. Blood samples (40 µL per sampling point; sublingual) were taken after 0.25, 0.5, 1, 2, 4, 6, and 24 h using ethylene diamine tetraacetic acid (EDTA)-coated capillaries. Plasma samples were obtained after centrifugation (10,000 g; 4 °C; 5 min) and stored at -20 °C until UPLC-MS/MS analysis. The animals were housed in individual metabolism cages allowing the collection of feces for a period of 24 h or 48 h. Samples were stored at -20 ± 5 °C until the bioanalytical quantification.

3.5.2.4. Quantification of the drug concentrations in the plasma and feces samples

The concentrations of the model drugs in the plasma were quantified using an UPLC method with tandem mass spectrometric detection (UPLC-MS/MS) previously developed at Nuvisan GmbH. The

UPLC-MS system consisted of a Waters Acquity UPLC coupled to an AB Sciex mass spectrometer API 5500 Q-trap. The UPLC separation was carried out on a reversed phase column (HSS T3, 1.8 μ M, 2.1 x 50 mm) using a mobile phase gradient with 0.1% formic acid and acetonitrile as eluents. The plasma samples were spiked with internal standard and the analyte was extracted from the matrix using tertiary-butyl methyl ether (tBME). The organic phase was evaporated to dryness under a stream of nitrogen and the residue was dissolved in acetonitrile/water (1:1, v/v) for LC-MS/MS analysis.

The feces samples were extracted with 4 times the volume of ethanol/water (4:1, v/v) and further diluted with blank fecal extract. Aliquots of the diluted aqueous-ethanolic extracts were then spiked with internal standard and diluted in acetonitrile/water (1:1, v/v) for UPLC-MS/MS analysis.

3.5.2.5. Pharmacokinetic Evaluation

The pharmacokinetic parameters maximum plasma concentration (C_{max}) and time to reach the maximum plasma concentration (t_{max}) were taken from the observed data. The area under the plasma concentration-time curve (AUC), clearance (Cl), volume of distribution at steady state (V_{ss}), and half-life ($t_{1/2}$) were calculated using the custom-made software 'DDS-TOX'. DDS-TOX' was previously evaluated for several compounds and found to generate results comparable to the validated software WinNonlin® (Princeton, New Jersey, USA). The AUC values were calculated by non-compartmental analysis using the linear up/log down method. The oral bioavailability is derived from oral and IV AUCs from time 0 extrapolated to infinity (AUC_{0-inf}) and the percentage of extrapolated AUC is given related to the measured AUC from time 0 to the last sampling time (AUC_{0-last}).

3.6. Analysis of clinical and preclinical pharmacokinetic data to identify solubility-limited absorption

3.6.1. Data collection

The different steps in the identification of solubility-limited absorption are presented in Figure 1. The human clinical PK data from the literature used for the analysis is presented in Table 9. For the calculation of the human gut bioavailability, the IV PK profiles and absolute bioavailability studies were used. To verify and optimize the PBPK absorption models, the IV and oral fasted PK profiles from the food effect study were used. The reported PK after orally administered ascending doses were reviewed with respect to the dose-proportionality of exposure. For erlotinib HCl and imatinib mesylate, some of the required PK data were not available. The absolute bioavailability of erlotinib was determined in healthy volunteers after administering an oral dose of 150 mg and an IV dose of 25 mg (69), but the resulting plasma clearance is not given in the publication. Instead, the IV PK profiles and renal clearance of erlotinib in patients were used. The clearance decreases from 8.41 L/h to 3.12 L/h with an increasing dose from 25 mg to 100 mg (70).

Table 9: Clinical pharmacokinetic data analyzed to assess solubility-limited absorption. The numbers in brackets represent the reference numbers

	<u>Single dose Pharmacokinetics</u>				<u>Food effect study</u>	<u>Oral dose escalation</u>
	<u>Oral dose [mg]</u>	<u>Intravenous dose [mg]</u>	<u>Clearance [L/h]</u>	<u>Absolute bioavailability</u>	<u>Dose (mg)</u>	<u>Dose range [mg]</u>
Crizotinib	250 (71)	50 (71)	46.8 (71)	43 % (71)	250 (71) Figure 3	50-300 (72)
Dabrafenib	150 (73)	0.05 (73, 74)	12 (73)	94.5 % (73)	150 (75) Table 11.2	12-300 (76)
Erlotinib	150 (70)	100 (69)	3.12 (69)	59 % (70)	150 (43) Figure 2a	3-1000 (77)
Gefitinib	250 (44)	50 (44)	41.6 (44)	57 % (44)	250 (44) Figure 3	50-700 (78)
Imatinib	400 (79)	100 (79)	10 (79)	98 % (79)	400 (79, 80) Figure 2 (79) (capsule)	25-1000 (81)
Lapatinib	not available	not available	not available	not available	1,500 (82) Figure 1	approx. 600-1800 (83)
M1	500	0.0156	12.8	72 %	30	30-1400
Pazopanib	800 (84)	5(84)	0.246 (84, 85)	21 % (84)	800 (86) Table 11.11	50-2000 (87)
Trametinib	2 (88)	0.005 (88)	3.21 (88)	72 % (88)	2 (89) Table 11.1	0.125-10 (90)
Vemurafenib	not available	not available	not available	not available	960 (46) Figure 1	240-960 (19)

Considering that the range of renal clearance of erlotinib is quite small compared to a liver blood flow of 90 L/h, the lowest value of renal clearance (i.e., 3.12 L/h following 100 mg IV) was used to obtain the lowest “worst-case”-gut bioavailability. In the erlotinib PBPK top-down analysis, the 75 mg IV PK profile (69), was used as the plasma concentrations are the closest to the oral profile. For imatinib mesylate, the oral PK profiles of the 400 mg capsule formulation in the absolute bioavailability study (79) were used to substitute the plasma-concentration time profiles of the food study that are not available.

For the assessment of solubility-limited absorption in the rat, the results of the rat PK study presented in 4.2.2.1 were used. Information on dose-proportionality in the rat was collected from the literature. Due to its size, the rat is not a common model to test the effect of food on the oral dosage forms of drugs (12) and limited data for the model compounds is available. Therefore, food effect studies in the rat are not covered by this work.

3.6.2. Gut bioavailability calculation

The gut bioavailability or gastro intestinal availability ($F_a \cdot F_g$) was derived from the absolute bioavailability F according to Equation 12 (91), with the fraction that escapes the first pass metabolism (F_h) calculated using a liver blood flow (Q) of 90 L/h in human (92) and 72 mL/min/kg in the rat (93). In this case, the hepatic clearance is assumed to be equal to the systemic clearance (Cl).

$$\text{Equation 12: } F = F_a \times F_g \times F_h = F_a \times F_g \times \left(1 - \frac{Cl}{Q}\right)$$

3.6.3. Top-down PBPK analysis

A PBPK top-down lineshape analysis of observed plasma concentration-time profiles as described by Peters (61) was performed using a generic PBPK Model built in MATLAB® (61). Before the oral simulations, the clearance and distribution parameters were fitted by optimizing the intrinsic microsomal clearance (Cl_{int}) and K_p factor, a multiplicative factor to scale all the tissue distribution coefficients at the same time, to best comply with the observed IV PK profiles (Figure 4, taken from Peters et al. (94)). The entire workflow is illustrated in Figure 5.

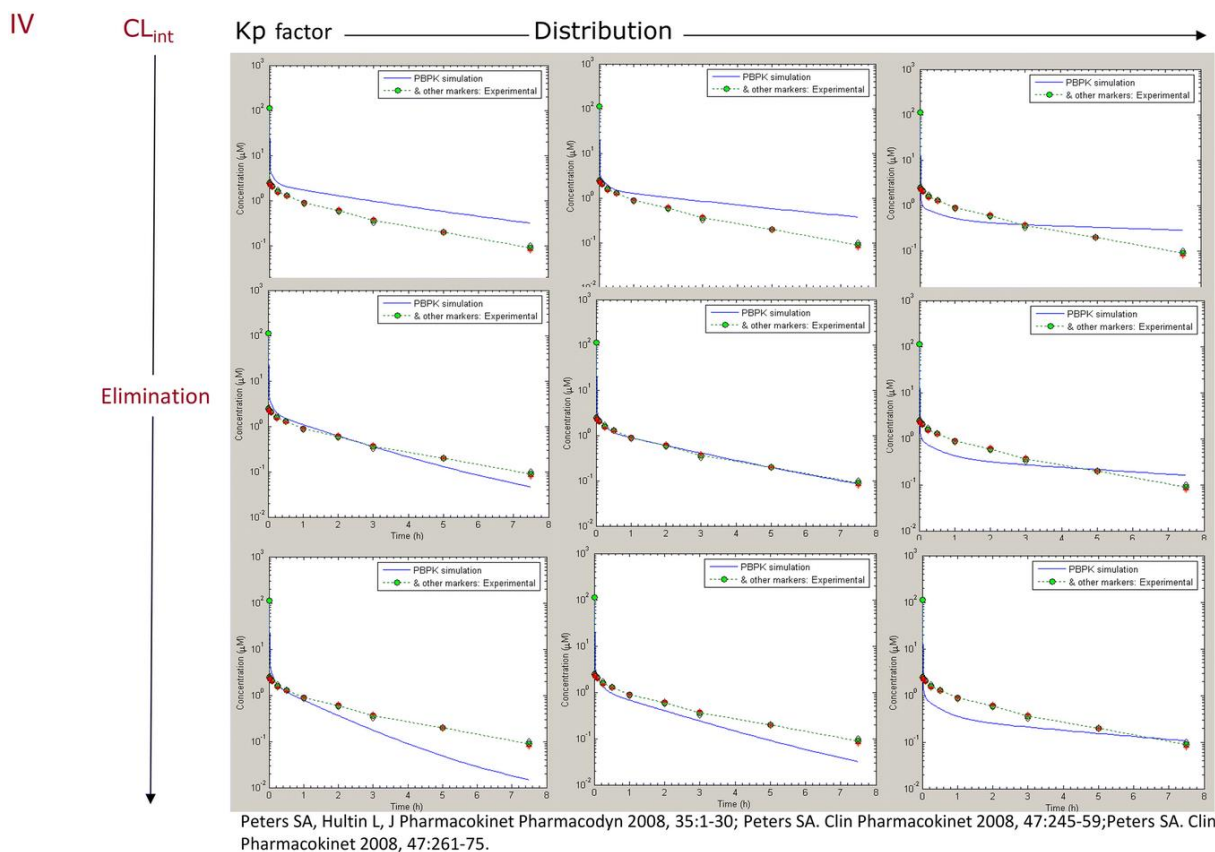


Figure 4: Optimizing the intrinsic microsomal clearance (Cl_{int}) and K_p factor (multiplicative factor to scale all the tissue distribution coefficients at the same time), to best comply with the observed IV PK profiles. Increasing the Cl_{int} shifts down the profile, while the K_p factor changes to shape of the predicted profile (94).

For vemurafenib and lapatinib, whose pharmacokinetic data after an intravenous administration in humans are not available, Cl_{int} and K_p factor were derived from the plasma concentration-time profiles

following a single dose of oral administration. The clearance was derived from the elimination-slope of the oral PK profiles in logarithmic scale, whose elimination rate constant (k_e) depends on the clearance (Cl) and unbound volume of distribution ($V_{ss,u}$) (Equation 13) at time points well beyond the absorption phase (usually after 24 h for immediate-release dosage forms). The volume of distribution was estimated according to the $V_{ss,u}$ equivalency approach presented in (95). The mean value of the volume of distribution per kilogram body weight in mouse, rat, and (in case of lapatinib) dog was used based on the assumption plasma protein binding, is the same across different species, as shown in Table 10.

$$\text{Equation 13: } k_e = Cl/V_{ss,u}$$

Table 10: Preclinical data to estimate the human clearance and volume of distribution of lapatinib and vemurafenib. The numbers in brackets represent the reference numbers.

	Lapatinib Volume of distribution [L/kg]	Vemurafenib Volume of distribution [L/kg]	Lapatinib plasma protein binding [%]	Vemurafenib plasma protein binding [%]
mouse	8.55 (96)	0.263 (97) ^{a, b}	≥ 99.0 (96)	99.81 (98)
rat	6.15 (96)	0.211 ^b	≥ 99.0 (96)	99.85 (98)
dog	5.70 (96)	not available	≥ 99.0 (96)	99.79 (98)
human	not available	not available	≥ 99.0 (96)	99.86 (98)
average	6.80	0.237	-	-

^a Volume of distribution in mice reported to be 7.9 mL for mice of an average body weight 30 g (97)

^b Volume of distribution after single intravenous dose (steady state data not available, but the plasma protein binding is high and very similar across the different species)

Besides the CL_{int} and K_p factors, the oral PBPK simulations at the dose of the food effect study were based on FaSSIF solubility and effective permeability. The PBPK input parameters are shown in Table S 6 for the human simulations and Table S 7 for the simulations of rat PK.

The mismatch between observed and predicted AUC or profile shape can deliver an understanding of the mechanisms underlying exposure, which can be used to optimize the models (61) (Figure 5, left case). When a simulated profile cannot match the steep upswing of the observed profile and is characterized by a poor sensitivity to permeability increase, solubility in vivo might be greater than the measured FaSSIF solubility. In the models underpredicting the observed PK, the input solubility was increased to the minimum value that best captures the observed profile (75-125% of the observed AUC), in the following called “in vivo solubility”. The true solubility in vivo could be even higher. However, a good fit to the observed profile of low (BCS class III/ IV) or borderline permeability drugs may also be achieved by increasing the input permeability. To investigate the permeability sensitivity, the oral simulations were performed with effective permeability derived from apparent permeability

in Caco-2 cells (scaled to the effective human intestinal permeability by a factor of 25) as well as effective permeability calculated from structural properties.

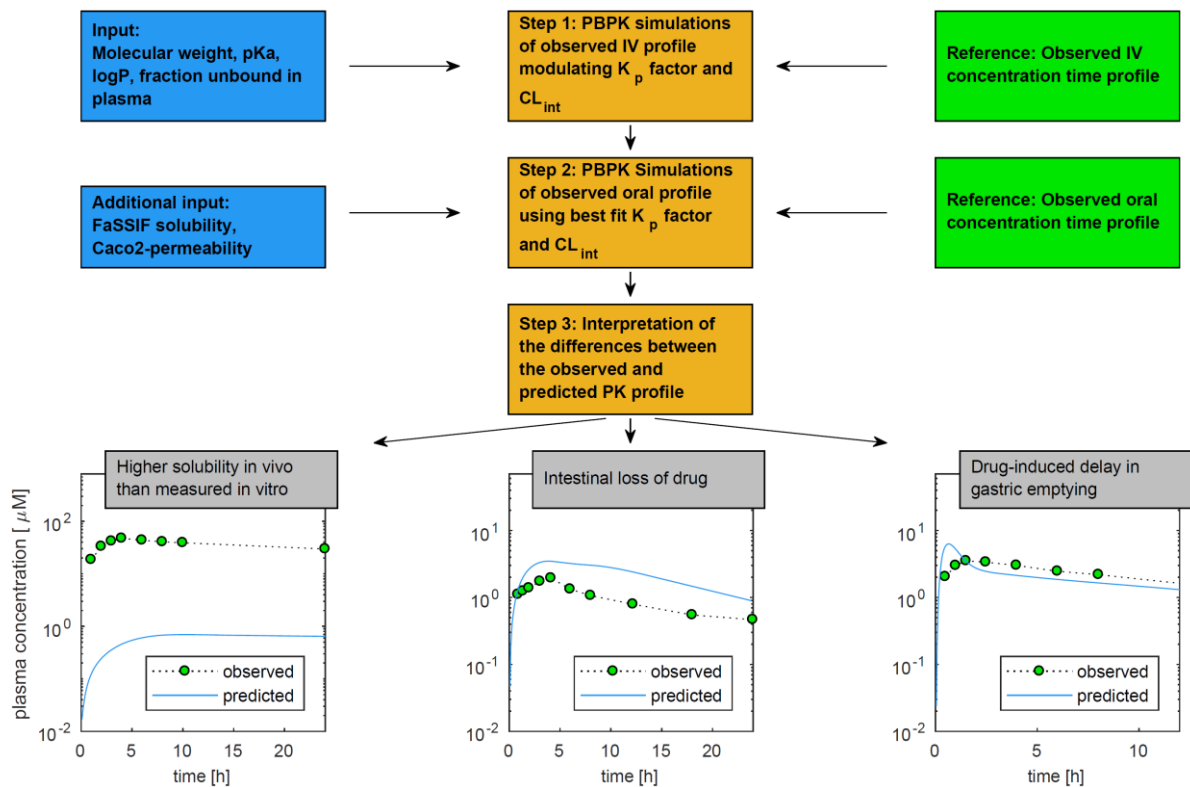


Figure 5: Schematic illustration of the top-down PBPK modeling approach (51)

If a loss of drug in the intestine in vivo is caused through gut metabolism or efflux, the predicted profiles show significantly higher plasma concentrations and AUC than the observed profile (Figure 5, middle case). In these cases, the intestinal loss was introduced to the PBPK by reducing the regional absorption in the intestinal compartments.

To match the observed profile, the gastric emptying rate was reduced in the models of the drugs that might delay the gastric emptying (Figure 5, right case). Data on drug-induced gastric emptying are not always published, but the model has been validated for the identification of delayed gastric emptying in the rat (99).

To identify solubility-limited exposure, the PBPK simulations were repeated with a hypothetically high solubility. Analog to the BCS class I solubility criterion, a solubility value of dose/250 mL was used, and 1 mg/mL for low-dose (< 250 mg) drugs. AUC or C_{max} ratios of the PBPK simulations using hypothetical BCS class I-like solubility to the best fit simulations that are significantly higher than 1 indicate solubility-limited exposure. A ratio of 1 or close to 1, identifies non-solubility-limited absorption.

3.7. Bottom-up food effect predictions using GastroPlus®

A workflow (Figure 6) to improve prospective food effect predictions was developed, that does not require model fitting to the observed fed state PK profile, considers the potential bias through gut first pass metabolism, incorporates the uncertainty in compound related input parameters as well as the highly variable physiological conditions.

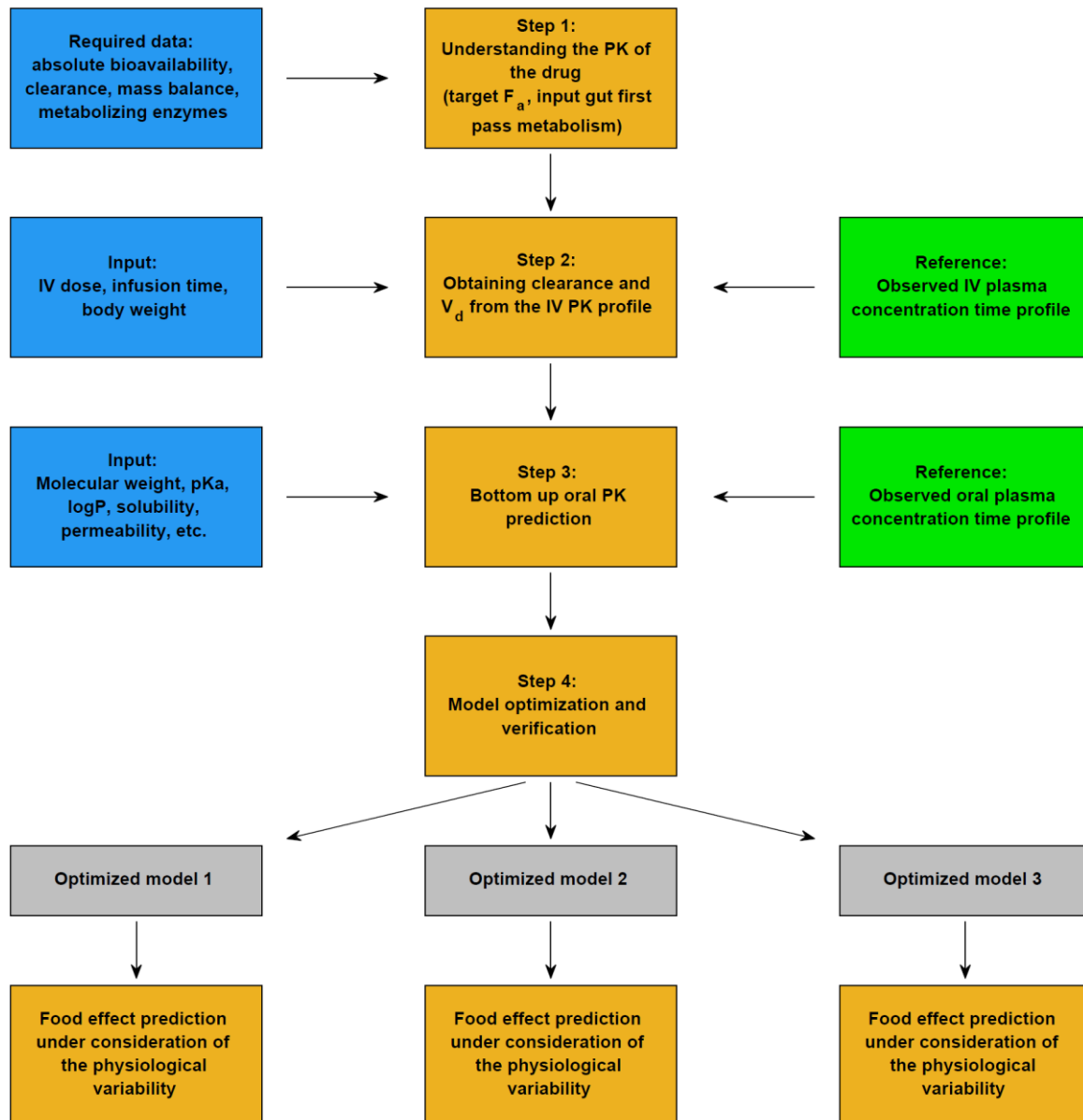


Figure 6: Schematic illustration of the developed bottom-up PBPK workflow to enhance food effect predictions. In case in Step 4 a similarly good models can be obtained using different parameter settings, one model with each possible setting is built (Optimized model 1 - n), as the input parameters cannot be validated only based on the plasma profile.

3.7.1. Understanding the PK of the drug

The first step in Figure 6 provides an understanding of two important mechanisms in the gut contributing to the PK - absorption and gut first pass metabolism. To estimate the fraction absorbed, the gut bioavailability was calculated as described in 3.6.2 as it provides information on a potential loss of drug in the gut. Moreover, information on the amount of parent drug excreted in the feces, for example in radiolabeled mass balance studies (ideally at the same dose as the food effect study), was collected as it contributes to the estimation of the fraction absorbed by delivering information on the amount of unabsorbed drug. For drugs that are reported to undergo biliary excretion, differentiation from unabsorbed and biliary excreted drug was enabled through the time window of excretion (unabsorbed drug from immediate release formulations is usually excreted after 24-48 h (100, 101)). The differentiation between unabsorbed drug and gut metabolism was supported by the analysis of available clinical PK data described in 3.6 including top-down PBPK modeling and analysis of dose-exposure proportionality. To further assess the amount of gut first pass metabolism, information in the literature on gut metabolism of the model compounds was collected and relevant metabolism via CYP3A4, as the most prominent gut metabolizing enzyme (102). Moreover, the systemic clearance was consulted, as a significant gut first pass is rather unlikely if the systemic clearance is low. Intestinal loss due to efflux transporters has been neglected, as the most prominent intestinal efflux transporter, p-glycoprotein is easily saturable and is only clinically relevant for a very limited number of drugs (103). For the model drugs with good gut bioavailability and non-solubility-limited absorption, a fraction absorbed of 1 (complete absorption) was assumed. For solubility-limited drugs with low systemic clearance or limited CYP3A metabolism, the calculated gut bioavailability was used as the target fraction absorbed. In the absence of IV PK data, the fraction absorbed can only be roughly estimated based on the amount of excreted parent drug in the feces. In this research, it was further refined based on the assumption that the observed food effect is solubility-driven, for example, if the exposure increased by 5-fold in the fed state, the fasted state fraction absorbed was estimated $\leq 20\%$.

3.7.2. Obtaining clearance and volume of distribution from the IV PK profile

The parameters for compartmental PK models (1-3 compartments) were fitted to the mean observed intravenous PK profiles based on the IV dose, infusion time, and body weight using the PKPlus module in GastroPlus®. The IV PK data used is shown in Table 11.

Table 11: Clinical pharmacokinetic data used for building and validating the GastroPlus® models. The numbers in brackets represent the reference numbers.

	<u>Observed IV PK profile</u>	<u>Observed p.o. profile (fasted)</u>	<u>Observed p.o. profile (fed)</u>	<u>AUC and C_{max} under different conditions for verification ^a</u>	
	Dose [mg]	Dose [mg]	Dose [mg]	Lower and higher dose [mg]	With/ without ARA at dose [mg]
Crizotinib	50 (71) Figure 1	250 (71) Figure 3	250 (71) Figure 3	50/ 300 (72)	250 (104)
Dabrafenib	0.05 (74) Table 11.3	150 (75) Table 11.2	150 (75) Table 11.2	75 (105) ^b 95 (oral suspension) (106)	not available
Erlotinib	75 (69) Figure 2	150 (43) Figure 2a	150 (43) Figure 2a	50/ 200 (107)	150 (108)
Gefitinib	100 (44) Figure 1	250 (44) Figure 3	250 (44) Figure 3	50/ 500 (78)	250 (109)
Imatinib	100 (79) Figure 1	400 (79) Figure 2 (capsule)	not available	25/ 750 (110)	400 (111)
Lapatinib	not available	1,500 (82) Figure 1	1,500 (82) Figure 1	175/ 1800 (112)	1250 (113)
M1	0.0156	30	30	30/ 1400	not available
Pazopanib	5 (85) Figure 11.8	800 (86) Table 11.11	800 (86) Table 11.11	50/ 2000 (114)	800 (115)
Trametinib	0.005 (116) Table 11.3	2 (89) Table 11.1	2 (89) Table 11.1	0.5/ 10 (90)	not available
Vemurafenib	not available	960 (46) Figure 1	960 (46) Figure 1	240/ 720 (117) ^c	not available

^a Assumption: AUC and C_{max} given as free base

^b dose higher than 150 mg in HPMC capsule are not available

^c higher dose not available

3.7.3. Bottom-up oral PK prediction

The oral bottom-up PBPK simulations at the doses of the food effect studies were based on the fitted compartmental PK parameters as well as logP, pK_a, molecular weight of the relevant salt form, fraction unbound in plasma, blood to plasma ratio from literature and measured pH dependent and biorelevant (FaSSIF and FeSSIF) solubility of the relevant salt form after 24 h (4.1.1.1 and 4.1.1.2), as well as Caco-2 permeability (4.1.4). For erlotinib and M1, whose solubility depends on the chloride concentration of the buffer, the pH dependent solubility profile in the presence of 130 mM NaCl was used, as it is assumed to be more physiologically relevant. As reference solubility, the lowest measured value was used, because it is the most critical. The solubility in phosphate buffer pH 7.4 was used as reference solubility value with the following exceptions: Dabrafenib and vemurafenib with acidic pK_a close to 7 have increased solubility at pH 7.4. Pazopanib and lapatinib aqueous solubility at pH 7.4 was too low

for HPLC quantification using the generic quantification method. The pK_a and pH dependent solubility profile, as well as the bile salt solubilization ratio (SR), were fitted to the measured data, as recommended in GastroPlus®. The bile salt solubilization ratio is a model parameter that can be derived from the solubility differences in buffer with (FaSSiF, FeSSiF) and without (FaSSiF blank, FeSSiF blank) bile salts to establish the compound solubility depending on the intestinal bile salt concentrations in the model (Equation 14) (118). For capsules, the recommended shorter stomach transit time of 0.1 h was used, as the released capsule content might be emptied faster from the stomach than API from dosage forms that depend stronger on prior disintegration. The Caco-2 permeability was converted to the human effective permeability based on the reference compounds propranolol and atenolol in the assay using the built-in tool in GastroPlus®. The input parameters are presented in Table S 8. If evident from clinical PK data, gut first-pass metabolism was implemented according to 3.7.1. In case, a certain gut first pass input value could not be defined, it was covered during model optimization.

$$\text{Equation 14: } C_{sx} = C_{so} + SC_{bs} * SR * MW * [TC]$$

C_{sx} solubility in the presence of sodium taurocholate

C_{so} solubility in the absence of sodium taurocholate

SC_{bs} solubilization capacity of the bile salt for the drug

SR bile salt solubilization ratio

MW molecular weight

[TC] sodium taurocholate concentration

3.7.4. Model optimization and verification

3.7.4.1. Model optimization

The models were optimized to meet the predefined target fraction absorbed (3.7.1) and observed plasma concentration-time profiles (Table 11).

The following parameters were optimized, as they are uncertain to some degree. The in vivo relevant precipitation time cannot be measured, the particle size of the drug products used in the clinical studies is not published and the composition of the intestinal fluids is highly variable, which affects the bile salt solubilization ratio (30, 119). The reference solubility in a defined aqueous buffer is a parameter that is adequately measurable in vitro and is therefore only adapted as the last choice. A parameter sensitivity analysis (PSA) for these parameters was conducted according to Table 12. The default minimum and maximum values in GastroPlus® were used except for the maximum border of the precipitation time, where the maximum possible value that GastroPlus® allows of 1,000,000 s was used and the maximum border of the bile salt solubilization ratio. The maximum possible bile salt

solubilization ratio for each compound was evaluated by using a hypothetically 10-fold different FaSSIF and FeSSIF solubility for the fitting and is presented in Table S 9.

In case a similarly good fit to the observed fasted state profile and target fraction absorbed could be obtained using different parameter settings, a model with each possible setting was built. This covers for the parameter non-identifiability, as the input parameters cannot be validated only based on the plasma profile.

Table 12: Parameters tested in the PSA to optimize the bottom-up PBPK predictions in the fasted state

	Minimum	Baseline value	Maximum
Particle radius [μm]	baseline value/10	25*	baseline value*10
Precipitation time [s]	baseline value/10	900*	1,000,000
Bile salt solubilization ratio	baseline value/10	fitted to in vitro data (Table S 8)	fitted to hypothetically different in vitro data (Table S 9)
Reference Solubility	baseline value/10	individual in vitro value (Table S 8)	baseline value*10

*GastroPlus® default value

3.7.4.2. Determination of a verification procedure

Besides the AUC and C_{max} in the fasted state of the food effect study, AUC and C_{max} of the lowest and highest dose available and after ARA intake (Table 11) were simulated to verify the PBPK absorption models. The PK under acid reduced conditions were simulated by changing the stomach pH from pH 1.3 to pH 4.5 (120).

To define the acceptance limits, the coefficient of variation (CV%) in the food effect study was consulted and calculated from the standard deviation (SD) if necessary. In case the CV% was < 50 %, an acceptance limit for the simulated AUC or C_{max} at the dose of the food effect study of 1.5-fold (lower or higher) of the observed values was used. When the CV% was 50 %-100 %, maximum 2-fold deviation from observed values were accepted and following a CV% > 100 % in the food effect study maximum 3-fold of the observed. The limits for the lower and higher dose as well as acid reduced condition simulations were based either on the CV% (like for the food effect dose) or the fold-difference in AUC at the food effect dose between the respective study and the food effect study, to account for the inter-study variability. The higher value was used. In the cases where single-dose ARA studies were not available for verification, the models were verified using the AUC or C_{max} ratios without ARA to with ARA. In these cases, the model passed the verification when the predicted ratio was within the AUC or C_{max} without ARA/ with ARA-ratios' 90 % confidence interval reported in the literature.

When there are different models that adequately simulate the observed fasted exposure at the food effect dose of one drug, the verification exercise may reveal differences in the performance of these models, when simulating different scenarios.

3.7.5. Food effect prediction strategy

Food effect predictions for each model drug were performed using the default Human-Physiological-Fed physiology (Table S 10), with a stomach transit time of 1 h and a constant stomach pH of pH 4.9, as well as a customized more detailed fed stomach physiology regarding the re-acidification derived from Koziolok et al. (100) (Table 13), implemented in a mixed-multiple dose file.

Table 13: Increase in stomach pH after completion of a meal collected using the SmartPill® derived from mean values by Koziolok et al. (100). The data was collected locally using the SmartPill® and was highly variable between time points within one subject. The fed stomach content is heterogenic and exhibits pH gradients. pH values between pH 1 and pH 7 might coexist at the same time (100).

Time [min]	Stomach pH
0-5	4.6
5-30	3.8
30-45	3.3
45-60	3.2
60-90	3.0
90-108	2.7
108-138	2.4
138-148	2.2
148-158	2.0
158-208	1.7
208-224	1.3
224-270	1.0

To distinguish the impact of the different factors that change at the same time during the fed state simulation, a PSA of the absorption relevant physiological parameters that change in the presence of food was performed - in the following called "Food-PSA". The parameters tested are shown in Table 14 along with the minimum and maximum limits. The bile salt solubilization ratio was used in the PSA as a surrogate for the intestinal bile salt concentrations that actually change in the presence of food. Additionally, simulations were performed with increased bile salt concentrations of:

- the mean value between the Human-Physiological-Fasted and Human-Physiological-Fed physiology (Table S 10),
- the concentrations of the Human-Physiological-Fed physiology,
- and double concentrations of the Human-Physiological-Fed physiology.

Table 14: Parameters tested in the "Food PSA"

	Minimum	Baseline value	Maximum
Stomach pH	0.5	1.3	5.0
Stomach Transit Time [h]	Baseline value/2	0.25 (tablet) 0.1 (capsule)	6 h
Bile salt solubilization ratio	Baseline value/10	Model specific (Table 27)	Baseline value*10

4. Results and Discussion

4.1. Importance of in vitro solubility and dissolution data in food effect predictions

4.1.1. In vitro solubility testing

4.1.1.1. pH dependent solubility

The solubility of the model drugs after 24 h in buffers of physiologically relevant pH 1.2 - pH 7.4 (26) is presented in Figure 7, along with the pK_a values reported in the U.S. Food and Drug Administration's (FDA) Clinical Pharmacology and Biopharmaceutics Reviews or (80, 113). The solubility of crystalline vemurafenib (19) (Table S 11) and trametinib*DMSO (90) (Table S 12) is not displayed. It is extremely low (< 0.26 µg/mL and < 0.6 µg/mL, respectively), which complicates an exact quantification, and not pH-dependent across the entire pH range. Therefore, the reported data in the literature for crystalline vemurafenib and trametinib*DMSO (19, 90) (Table S 11, Table S 12) were used for the purposes of this work. The solubility of the amorphous vemurafenib obtained from ground Zelboraf® 240 mg film-coated tablets shown in Figure 7 was measured according to the procedure described in 3.2.1. Crizotinib, gefitinib and imatinib mesylate are highly soluble in acidic media (78, 80, 121). The amounts of drug substance (equivalent to 10 mg/mL solubility for crizotinib and gefitinib/ 5 mg/mL for imatinib) weighed in for the solubility tests were completely dissolved at the lowest pH shown in Figure 7. The actual solubility could be even higher, but as it already complies with the BCS class I solubility criterion of ≥ dose/ 250 mL (18), it is not expected to make a difference for the purposes of this work.

As expected based on the weakly basic nature of all compounds excluding vemurafenib, their solubility declines when the increasing pH approaches their basic pK_a values (Figure 7). This is because the amount of ionized species decreases, whose solubilization is usually facilitated. Dabrafenib and vemurafenib have an acidic pK_a value within or close to the measured range (19, 76) and therefore show increased solubility when approaching pH 6.6 and pH 7.9, respectively. Moreover, vemurafenib is co-precipitated with the acid-insoluble HPMC-AS (19) in the tested ground market formulation, preventing dissolution at low pH and facilitating solubilization at higher pH. The solubility of both, crystalline and non-crystalline vemurafenib, were found to be low (< 0.26 µg/mL) up to pH 4.5 (19) (Table S 11).

The measured solubility profiles of erlotinib HCl and M1 are characterized by lower solubility at pH 1.2 and pH 1.6 than at pH 3 or pH 4, as well as better solubility at pH 6.5 (FaSSIF blank) compared to pH 7.4, and do not comply with their pK_a values. This is because the solubility of these drugs depends on the chloride concentration in the buffer (common-ion effect). In the solubility profiles of erlotinib HCl and M1 in buffers of the same chloride concentration (130 mM) (Figure 7 in blue), the pH dependent solubility is overruled between pH 1.2 and pH 4 in case of erlotinib, and completely set off for M1. The

solubility profile at 130 mM chloride is assumed to be the more physiologically relevant, as 130 mM chloride is a common concentration in the human GI (122-124).

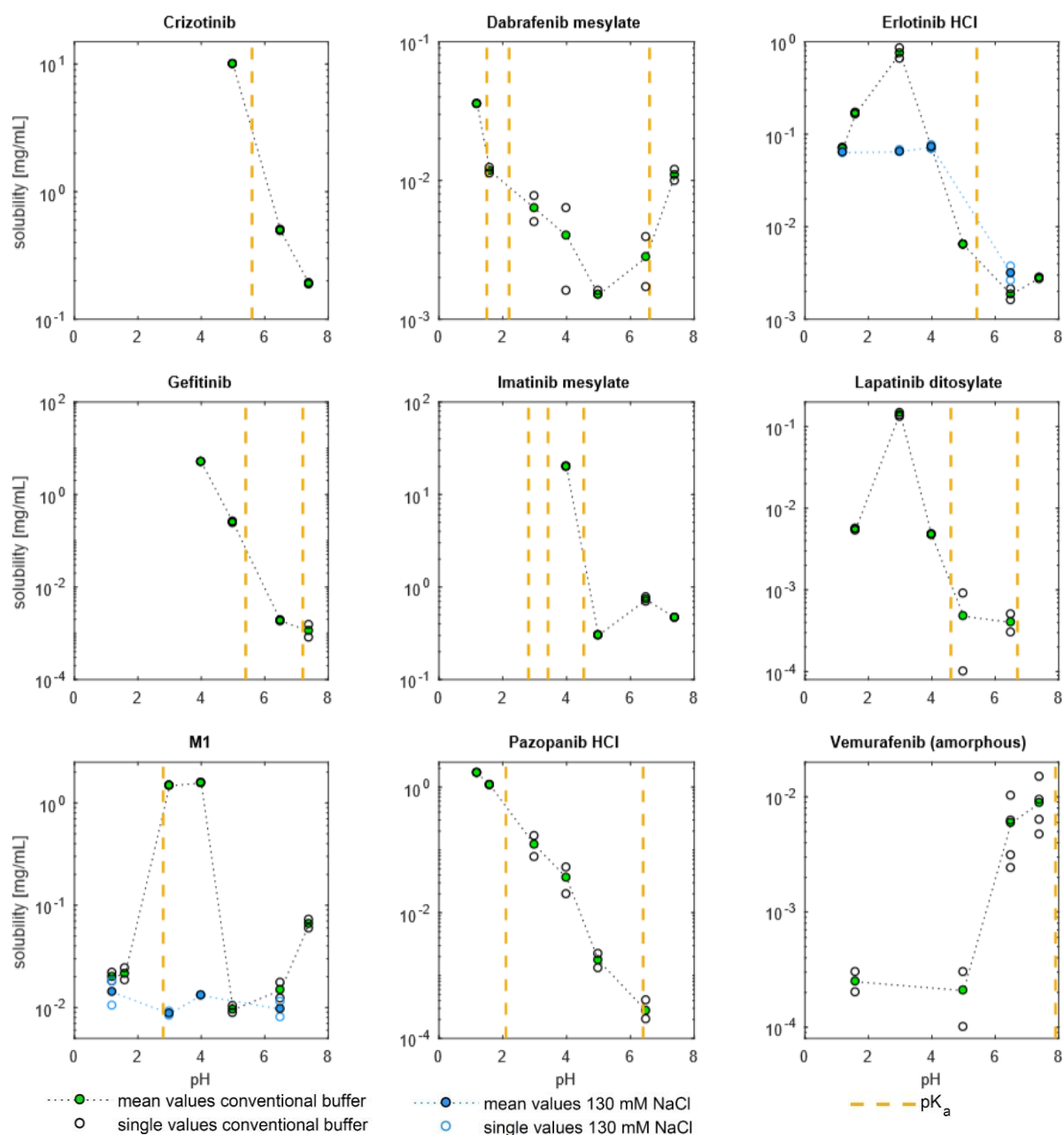


Figure 7: Measured pH dependent solubility (after 24 h) profiles of the model drugs (n=2)

Overall, the measured solubility is well in line with the values reported in the literature (for example in the FDA's Clinical Pharmacology and Biopharmaceutics Reviews) and their pKa values. Only a few values differ significantly from the expectations. Of particular note is the unexpectedly high lapatinib ditosylate solubility in formate buffer pH 3.0 with approx. 0.1 mg/mL after 1 h, 2 h and 24 h. The solubility reports of this compound in the literature are conflicting, with 0.001 mg/L in 0.1 N hydrochloric acid (HCl) (83) vs. 0.001 mg/mL in 0.1 N HCl acid (at 25 °C) (125), and the pH dependence is not thoroughly discussed (a 1000-fold decrease in solubility from pH 4 to pH 7 was reported in (113)). However, the measured value at pH 3 is not in line with these observations, neither with its pKa values.

Therefore, it is not considered in the further course of this work. Maybe, the thermodynamic solubility was not yet reached in the in-house experiment, or factors other than the pH, e.g. the buffer species or osmolarity have a huge impact on the solubility. Besides the lapatinib solubility at pH 3, there were only small deviations from the literature. For example, the measured pazopanib solubility in SGF pH 1.2 (1.68 mg/mL) and erlotinib in formate buffer pH 3.0 (0.75 mg/mL) are 2-3-fold higher than the greatest reported pazopanib solubility (0.65 mg/mL at pH 1.1 (121)) and erlotinib solubility (approximately 0.4 mg/mL at approximately pH 2 (77)). These differences can be batch-related, and no further data were excluded from the use in this work.

For some of the drugs, supersaturation after 1 h and 2 h compared to the 24 h solubility was observed, due to their salt form. For example, the solubilities of erlotinib HCl, imatinib mesylate, lapatinib ditosylate after 1 h were up to 3-fold, \geq 18-fold, 46-fold higher in FaSSIF blank pH 5.0 (erlotinib and imatinib), acetate buffer pH 4 (lapatinib) than after 24 h, respectively.

Salt form approaches for ionizable drug candidates can speed up their dissolution and increase the rate and extent of absorption (4, 126). Upon dissolution, the acid/ base nature of the counter ions or the drug itself can alter the pH of the solution, especially in the case of salts with medium-strong acids or bases like mesylate or tosylate. The pH of the solution was measured after the 2 h and 24 h sampling to make sure the final pH is still as desired. The deviations from the initial pH were less than 0.2 pH-units with the following exceptions: The pH of the imatinib mesylate solution decreased during the solubility test in pH 7.4 to pH 6.5 after 2 h and further to pH 6.0 after 24 h. This explains why the pH 7.4-solubility seems to be higher than in FaSSIF blank (pH 6.5), where the pH was stable. During the crizotinib pH 5 and the gefitinib pH 4 solubility test, the pH increased by 0.4 units, due to the basic nature of these drugs. It shows that even at the resulting higher pH, the solubility is BCS class I like. A change in pH was especially observed for the model drugs with high solubility and large amounts of drug substance used in the test. Small changes in pH and solubility are less critical to absorption when solubility is high. In vivo, there might also be gastrointestinal pH fluctuations due to a limited buffer capacity (26), but the pH shift can be less pronounced than in vitro when the dose is lower and the volume is higher.

The generated pH dependent solubility data can be used for the purposes of this work. This includes the discussion of the relative differences in the fasted versus fed state, the use as gastric input solubility in the generic PBPK model built in MATLAB® (pH 1.6 for human, pH 4 for the rat) and input for the GastroPlus® absorption models. The measured solubility data are adequately in line with the values reported in the literature and their pK_a profile. For the different exercises within this work, the 24 h solubility (assumed equilibrium) was used, as it is well established in later stages of drug development (4), better reproducible than kinetic phenomena (127) and therefore more comparable between the

different model drugs. However, the solubility differences between fasted and fed state pH can be different at time points earlier than 24 h. The GI transit time might not always be long enough to reach the thermodynamic solubility in vivo.

4.1.1.2. Biorelevant solubility

The solubility after 24 h in the presence of 0/ 3/ 15 mM sodium taurocholate and 0/ 0.75/ 3.17 mM lecithin (fixed combinations) in pH 6.5 (FaSSIF blank) and pH 5.0 (FeSSIF blank) is presented in Figure 8. The concentrations were selected according to the first published FaSSIF and FeSSIF versions (27), which are available as instant “SIF-Powder” since 2008 (128), and have become widely used in the academia and industry (129). The combination of 3 mM TC/ 0.75 mM lecithin is derived from FaSSIF and 15 mM TC/ 3.75 mM is used in FeSSIF. To distinguish the bile salt vs. pH effect on solubility, the FaSSIF-TC/lecithin concentrations were also tested in the FeSSIF blank buffer and the other way around.

As expected based on their amphiphilic nature and ability to act as surfactants (118), the solubility in buffers containing greater amounts of TC/ lecithin is higher than in the buffers without or with lower TC/lecithin concentrations. And as expected based on the pH dependent solubility, the solubility at pH 6.5 is generally lower than at pH 5.0 at the same TC/ lecithin concentration. It is not the case for dabrafenib with an acidic pK_a of 6.6 and M1, where the higher chloride concentration in the FeSSIF blank buffer pH 5.0 prevents better solubility compared to the buffer FaSSIF blank pH 6.5. The low solubility of the vemurafenib-HPMC-AS coprecipitate at pH 5.0 is increased by the presence of 3 mM TC/ 0.75 mM lecithin to the level of FaSSIF blank (pH 6.5) + 3 mM TC/ 0.75 mM lecithin and with 15 mM TC/ 3.75 mM lecithin even higher than in the analog pH 6.5 buffer. Substantially higher concentrations have been observed after 1 h for vemurafenib (amorphous) and lapatinib with up to 17-fold and 3.6-fold of the 24 h-solubility. Supersaturation with < 2-fold of the 24 h-solubility has been observed for erlotinib, gefitinib, and pazopanib after 1 h.

The TC/ lecithin dependence of crizotinib, imatinib mesylate and trametinib*DMSO solubility is not shown in Figure 8. The solubility of crizotinib in FeSSIF blank pH 5.0 is already very high (≥ 10 mg/mL), and a potential further solubility increase by TC/ lecithin is not considered relevant for absorption. The interaction of imatinib with the micelles leading to a gel formation (130), hindered the solubility determination in the supernatant with 15 mM TC/ 3.75 mM lecithin. For the above explained analytical reasons, the reported trametinib*DMSO solubility in (90) (Table S 12) was used in this work. Trametinib FaSSIF pH 6.3 and FeSSIF pH 4.9 solubility were found to be 0.8 $\mu\text{g/mL}$ and 3.9 $\mu\text{g/mL}$ after 24 h, respectively. The differences in FaSSIF and FaSSIF blank solubility (pH 6.5) are shown in Table 15.

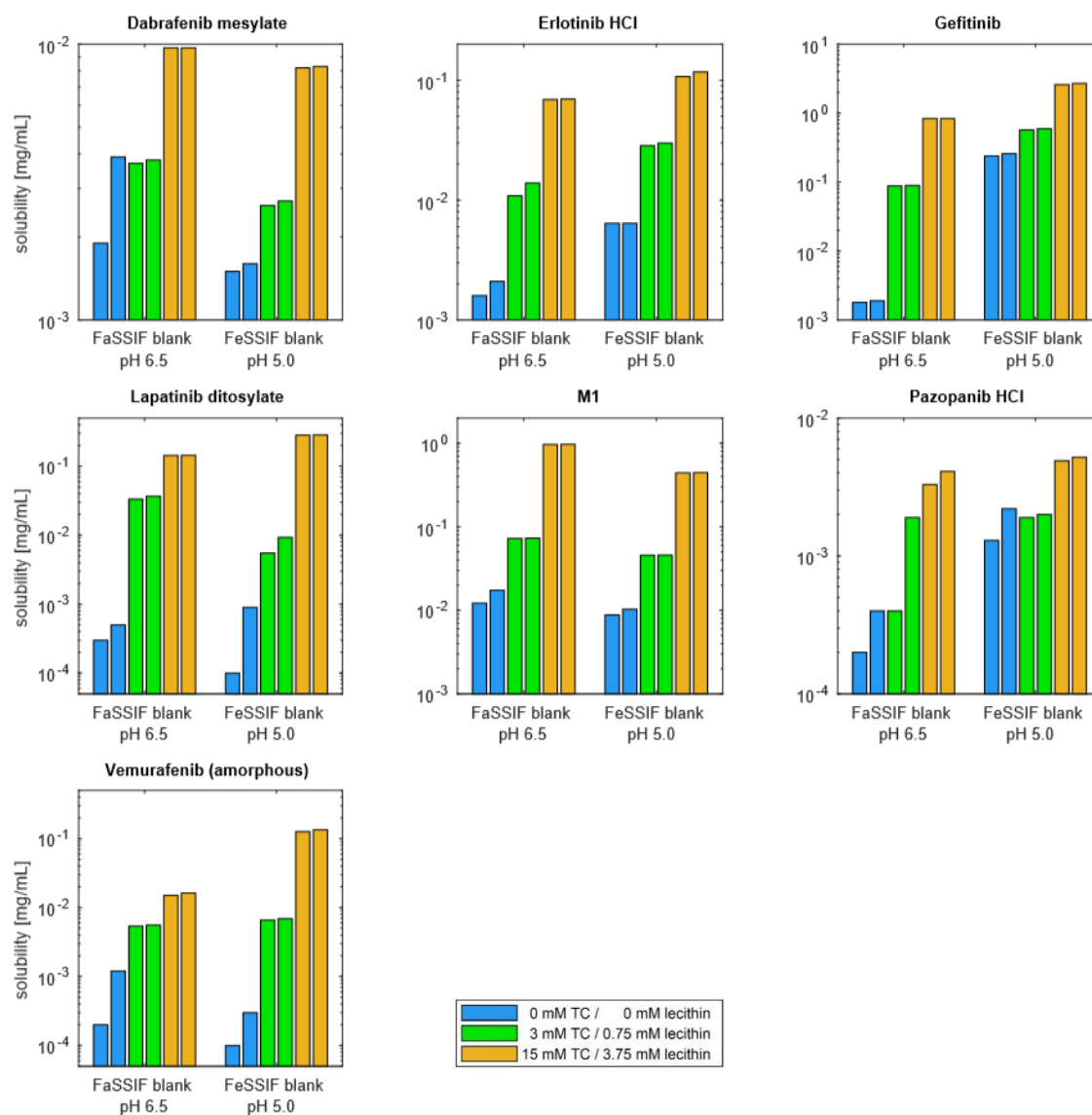


Figure 8: Measured solubility (n=2) of the model drugs (after 24 h) at pH 6.5 (FaSSIF blank) and pH 5.0 (FeSSIF blank) with different taurocholate and lecithin concentrations

To better quantify the bile salt sensitivity of the solubility, the ratios of FaSSIF (3 mM TC/ 0.75 mM lecithin) solubility to FaSSIF blank (without TC/ lecithin) solubility were calculated (Table 15). Lapatinib is the compound with the most sensitive solubility to 3 mM TC/ 0.75 mM lecithin addition to the buffer FaSSIF blank (pH 6.5), with 87-fold solubility increase. The solubility of the gefitinib and amorphous vemurafenib is also very sensitive to 3 mM TC addition with 48 and 26-fold increase, respectively, while the solubility of the other model drugs increases < 10-fold. The ratios of FeSSIF (15 mM TC/ 3.75 mM lecithin) solubility to FeSSIF blank solubility were also calculated for comparison (data not shown), and confirmed that lapatinib is most sensitive drug to the presence of bile salts, followed by vemurafenib (gefitinib was not outstanding).

Table 15: Comparison of the model drugs' FaSSIF and FaSSIF blank (without taurocholate and lecithin) solubility. The numbers in brackets represent the reference numbers.

	FaSSIF solubility [mg/mL]	FaSSIF blank solubility [mg/mL]	FaSSIF solubility/ FaSSIF blank solubility
Crizotinib	0.7430	0.4964	1.5
Dabrafenib mesilate	0.0037	0.0028	1.3
Erlotinib HCl	0.0124	0.0019	6.7
Gefitinib	0.0887	0.0018	48.0
Imatinib mesilate	≥ 5	0.7314	≥ 6.8
Lapatinib ditosylate	0.0350	0.0004	87.4
M1	0.0728	0.0148	4.9
Pazopanib HCl	0.0012	0.0003	4.4
Trametinib*DMSO	0.0008 (90)	0.0003* (90)	2.7
Vemurafenib (amorphous)	0.0054	0.0002	26.0

* unspecified buffer pH 6

The data shown in Figure 8 and Table 15 indicates a risk of a positive food effect for all drugs. Solubility enhancement via the increased bile salt concentration as well as a potential intestinal pH decrease through the chyme enhance the solubility of erlotinib, gefitinib, lapatinib, pazopanib, and vemurafenib. Dabrafenib and M1 solubility is enhanced by the bile salts in the buffer compositions tested. This topic is further elucidated in 4.1.3, together with the results of the dissolution tests.

The presented solubility data in the presence of bile salts and lecithin for the discussion on the performance of the in vitro solubility and dissolution data in to food effect predictions. Moreover, it is used in this work as (intestinal) input solubility in the generic PBPK model built in MATLAB® (FaSSIF solubility) and in GastroPlus® for bottom-up PK predictions (FaSSIF and FeSSIF solubility). The dose number, SLAD and required volume of FaSSIF to dissolve the dose for the rat were calculated based on the FaSSIF solubility.

4.1.1.3. Dumping experiments

The goal of the dumping tests was to investigate, whether the model drugs are capable of generating and maintaining supersaturated concentrations upon the transfer of a solution into a medium where the solubility is lower. This is relevant for the MATLAB® PBPK modeling part of this work. The need for increasing the input solubility of a drug is supported if it can generate supersaturation (caused by the stomach pH or a solubility enhancing formulation), that might then enhance absorption. The results are shown in Table 16. The red color code highlights the drugs and time points, where the measured concentrations after dumping the drug solutions are higher than the thermodynamic (24 h) solubility in FaSSIF.

Table 16: Observed supersaturation after dumping of drug solutions into FaSSIF. Legend: Red = the measured concentrations at the given sampling time are higher than the thermodynamic (24 h) solubility in FaSSIF; green = the measured concentrations at the given sampling time are below the thermodynamic (24 h) solubility in FaSSIF; yellow = slight supersaturation. If there was a difference between the n=2 samples, the fold-difference in solubility for both is given in the table.

	Supersaturation after 15 min compared to 24 h solubility in FaSSIF	Supersaturation after 30 min compared to 24 h solubility in FaSSIF	Supersaturation after 120 min compared to 24 h solubility in FaSSIF
Crizotinib	no	no	no
Dabrafenib	yes (43-fold)	1.4-fold/ 1.5-fold	no
Erlotinib	no	no	no
Gefitinib	yes (6-fold)	yes (6-fold)	no
Imatinib	no	no	no
Lapatinib	yes (2-fold)	yes (3-fold)	yes (4-fold)
M1	no	no	no
Pazopanib	yes (3-fold)	yes (2-fold/ 3-fold)	no
Trametinib	yes (6-fold)	yes (6-fold)	yes (6-fold)
Vemurafenib*	yes (118-fold/ 128-fold)	yes (7-fold/ 50-fold)	yes (3-fold/ 5-fold)

*crystalline

Dabrafenib shows supersaturation up to 15-30 min, gefitinib and pazopanib up to 30-120 min, and lapatinib, trametinib, and crystalline vemurafenib for at least 120 min. The solubility of the vemurafenib batch in FaSSIF of 0.7 µg/mL after 24 h was measured for comparison, which is slightly higher than in aqueous buffers (19) (Table S 11) and therefore plausible.

All 5 compounds that required a solubility increase in the MATLAB® PBPK model (dabrafenib, lapatinib, pazopanib, trametinib, vemurafenib) showed higher concentrations in the dumping experiment than measured via shake flask method after 24 h. Dabrafenib, pazopanib, vemurafenib showed higher concentrations after 15 min than after 120 min, so that the supersaturation could be directly confirmed. In the cases of lapatinib and trametinib, the supersaturated state 2 h after dumping was confirmed through a comparison with the concentrations after 2 h and 24 h of a shake flask solubility test in FaSSIF + 3 % DMSO using solid API. Gefitinib shows supersaturation in the dumping test as well, but there was no need to adjust solubility in the model, as the thermodynamic value is high enough to enable the simulation of the observed PK. For imatinib, crizotinib and M1, the assay was not expected to generate supersaturation, as the solubility of these drugs in FaSSIF is sufficient to dissolve the weighed amount. Precipitation of the erlotinib dose was quick, and the thermodynamic value was reached already after 15 min, but there was no need to adjust the solubility in the model. To summarize, increasing the input solubility of dabrafenib, lapatinib, pazopanib, trametinib, and vemurafenib can be justified, as the compounds can generate supersaturated solutions for at least 15 min.

4.1.2. In vitro dissolution testing

The common biorelevant USP II dissolution setup uses 500 mL FaSSIF or FeSSIF (39-41). This was not useful for all model drugs, as the expected release in most buffers of the food effect dose was < 5 % according to the previously presented low solubility, e.g. for dabrafenib, pazopanib and vemurafenib. When only low amounts of drug are released, it is difficult to interpret the differences in performance between the different test conditions. Moreover, the low solubility might be the main factor shaping the release profile in these experiments, not the dissolution kinetics. For the USP II dissolution tests, erlotinib (Tarceva® 100 mg film-coated tablets), gefitinib (Iressa® 250 mg film-coated tablets), and M1 30 mg film-coated tablets were selected. The medium paddle speed of 75 rpm, that is often used in the biorelevant release tests (39-41), could not be applied in all release tests of the selected drug products, as the release rate was in some instances strongly affected by assay related influencing factors, e.g. coning behavior. Among the USP II dissolution tests in 500 mL FaSSIF and FeSSIF, there was strong coning or tablets sticking to the vessel wall in at least one of the buffers at 75 rpm, so that the paddle speed was increased to 100 rpm in both media. For the M1 formulation, this might not even be sufficient, as discussed below. To summarize, a “one-fits-all” biorelevant dissolution test procedure in FaSSIF and FeSSIF could not be identified. The test conditions are given along with the results.

The human exposure of erlotinib, gefitinib and M1, selected for the USP II dissolution tests, is not substantially altered in the presence of food (Table 9). Therefore, pazopanib (Votrient® 400 mg film-coated tablets) and vemurafenib (Zelboraf® 240 mg film-coated tablets) with a huge positive food effect in human were also included - but in the USP IV (flow-through cell) open system to enable more drug release than in an USP II vessel, where saturation is easily reached.

4.1.2.1. Dissolution testing of the selected model drugs in the USP apparatus II

Prior to the release tests in biorelevant media, the dissolution of the drug products in buffers that enable complete release was tested. For erlotinib the QC medium (available at the FDA Dissolution Database (131) by the time the experiment was performed) 0.1 N HCl + 1 % sodium dodecyl sulfate (SDS)) was used, and FaSSGF pH 1.6 for gefitinib and M1. In all cases, complete release could be achieved and the full dose was recovered. This indicates that the tablets and filters are suitable for the following experiments.

The release profiles in 500 mL FaSSIF and FeSSIF of the selected model drugs erlotinib, gefitinib and M1 in the USP II apparatus with first order (exponential) fit are shown in Figure 9. The mean profiles of the Tarceva® 100 mg release tests met the maximum amount released expected based on the thermodynamic drug solubility. While the variability in FaSSIF was low, the three tablets in FeSSIF behaved differently, as two of them showed supersaturated concentrations while the third tablet

approached the solubility limit only slowly. A good first-order model fit to the mean profile could be obtained for both, FaSSIF and FeSSIF, with higher W_{\max} and k in FeSSIF.

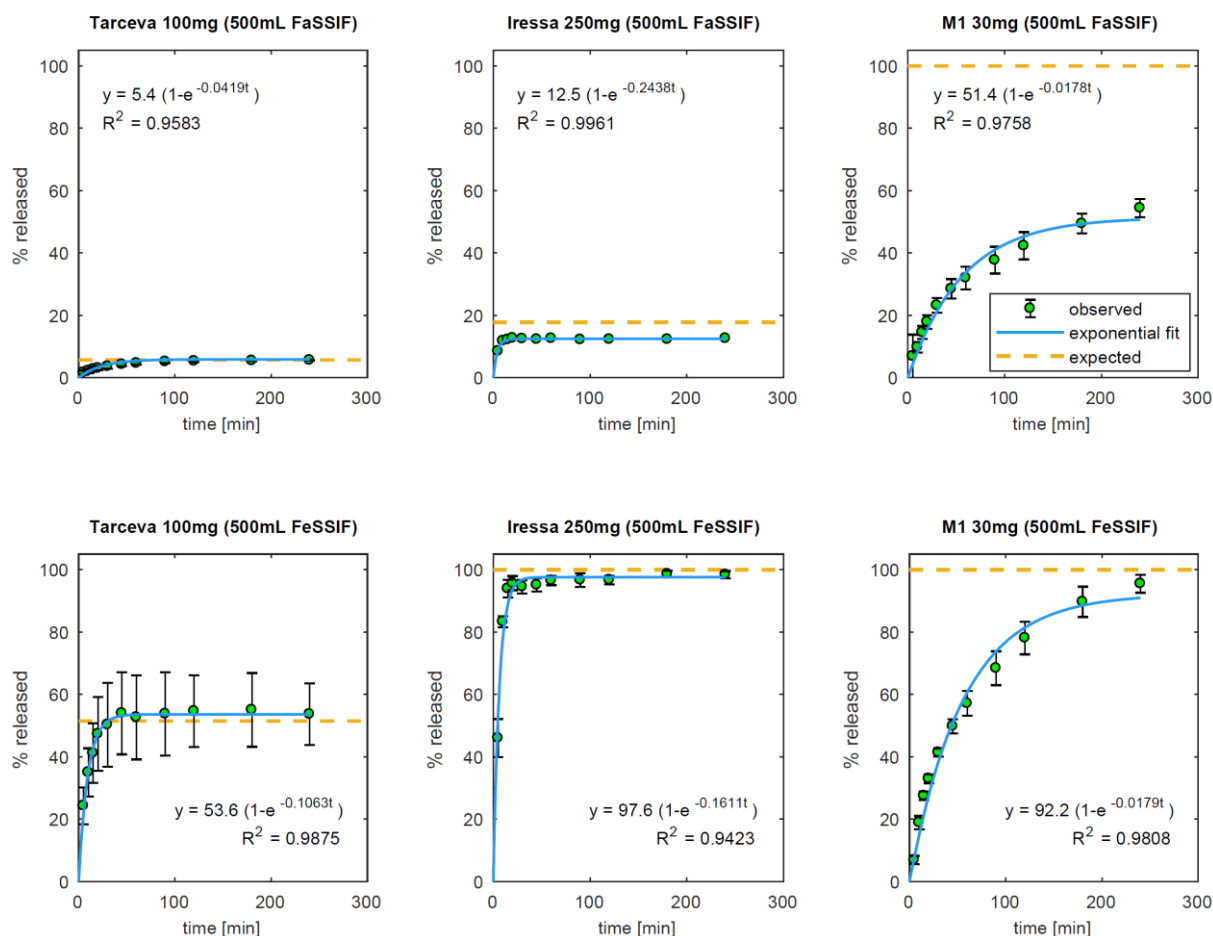


Figure 9: FaSSIF and FeSSIF dissolution profiles of the selected model drugs erlotinib, gefitinib and M1 in the USP II apparatus with first order (exponential) fit. The tested drug products Tarceva® 100 mg film-coated tablets and Iressa® 250 mg film-coated tablets contain 109.28 mg erlotinib HCl and 250 mg gefitinib free base, respectively. The tested M1 tablets contain 30 mg M1. The dissolution tests were performed with $n=3$ dosage units at 37 °C and 100 rpm paddle speed. The expected release was calculated based on the thermodynamic solubility in the shake-flask test and a first-order model was fitted to the dissolution profile.

During the release tests of Iressa® 250 mg film-coated tablets, the maximum amount released was reached very rapidly (approximately after 15 min) in FaSSIF as well as in FeSSIF, with very low variability in both media. The standard deviation is not shown in the Iressa® FaSSIF dissolution profile, as only two vessels were evaluated, because the paddle in the third vessel was not properly fixed. The released amount of drug in the remaining two vessels did not differ by more than $\pm 1\%$ at any time-point, so the experiment was not repeated. The expected maximum amount released in FaSSIF of 18% based on the gefitinib solubility of about 0.09 mg/mL, was not achieved, suggesting that the tablet batch has lower solubility after 240 min (0.06 mg/mL) than the tested API batch after 24 h. In FeSSIF, complete gefitinib release was observed as expected. Good first-order model fits to the mean Iressa® release profiles in FaSSIF and FeSSIF could be obtained. W_{\max} was higher in FeSSIF than in FaSSIF, while k was

lower in FeSSIF than in FaSSIF. This observation can be explained by the fact that the film of the Iressa® 250 mg tablets adhered to the vessel wall in the FeSSIF but not in the FaSSIF dissolution tests.

As mentioned earlier, there was massive coning in the M1 dissolution tests, even with 100 rpm paddle speed, preventing proper mixing and drug release from inside the cone. This is visible in the release profiles in Figure 9 as the expected complete release of 30 mg M1 in 500 ml FaSSIF and FeSSIF is not yet achieved after 240 min. The exponential fit to the release profiles is possible, but might be misleading, when the actual W_{\max} is not covered by the profile or the low k is an artifact caused by strong coning in the vessel.

Recently, intestinal volumes lower than 500 mL have been reported (132, 133). To investigate the influence of the volume, the release tests of Tarceva® 100 mg, Iressa® 250 mg and M1 30 mg film-coated tablets were also performed in 250 mL in a mini-dissolution apparatus. As the dimensions are scaled down by 1/3 of the USP II apparatus, a first-order dissolution rate k similar to the 500 mL profile is expected, but a lower W_{\max} , when the solubility is not sufficient for complete dissolution of the dose in 250 mL of the buffers. Overall, the dissolution profiles in 250 mL met these expectations. The release tests in 250 mL in the mini-dissolution apparatus confirm the previously reported findings that the release behavior can be similar to the regular USP II apparatus, but does not always match (68), for example when supersaturated concentrations occur like in the Tarceva® 100 mg release tests or in case of serious coning as observed for M1.

The FeSSIF/FaSSIF k and W_{\max} -ratios in the 500 mL release tests are shown in Table 17 and discussed in 4.1.3, together with the relative differences in FaSSIF and FeSSIF solubility with regard to the observed food effects in the clinical studies.

4.1.2.2. Dissolution testing of the selected model drugs in the USP apparatus IV

The release from the selected drug products Votrient® 400 mg film-coated tablets (containing 433.33 mg pazopanib HCl) and Zelboraf® 240 mg film-coated tablets (containing 240 mg vemurafenib in form of HPMC-AS coprecipitate) was tested in FaSSIF and FeSSIF at 37 °C with a flow rate of 16 mL/min over 85 min. The maximum flow rate of the pump (16 mL/min) was chosen to speed up the dissolution tests of these very low solubility drugs to achieve the maximum performance. The run time was limited, by the maximum volume of 10 L buffer that is allowed in the associated lab. As the equipment supplies seven cells in parallel, each tablet was released in 1360 mL of buffer.

Figure 10 and Figure 11 present the cumulative profiles (upper plots, a and b) of the USP IV release tests in FaSSIF and FeSSIF with linear fit and expected release of drug according to the solubility after 1 h in the shake-flask test. In the lower plots (c and d), the percentage of dose released in the individual sampling intervals over 2 min (in the sampling intervals from 0-10 min after the start of the release

tests), 5 min (between 10-35 min of the release test) and 10 min (between 35-85 min of the test), is shown. The amount released per sampled fraction is expected to increase with the sampling duration, as illustrated by the dashed line in the plots c and d. The solubility after 1 h in the shake-flask test was chosen as a reference to calculate the expected release as it delivered the better fit to the measured profiles than the thermodynamic solubility after 24 h.

The release profiles of pazopanib in both, FaSSIF and FeSSIF (Figure 10) are characterized by a rapid initial dissolution rate, followed by a very slow dissolution rate after 15 min. The solubility-wise expected total amount released during the duration of the test was exceeded in both, FaSSIF and FeSSIF dissolution tests, during the first minutes of rapid release. This could be explained by the presence of excipients in high concentrations in the cell upon disintegration and dissolution before they are washed out. The film coating contains polysorbate 80 (134), which is commonly known as a solubilizing agent, and the contained Povidone K30 can inhibit the precipitation of dissolved pazopanib (135). Once these soluble excipients are washed out from the cell, the dissolution rate of pazopanib decreases massively, although sink conditions are permanently assured. The dissolution rate beyond 15 min matches quite well with the expectations based on the shake flask-solubility after 1 h (Figure 10c and d). It was excluded that this phenomenon is an artifact due to precipitation in the fraction collector, as the resulting concentrations were lower than the thermodynamic solubility in the buffer mixture in the fraction collector at room temperature. The sample stability for at least 24 h was also tested and confirmed. The oral bioavailability of 800 mg pazopanib is 21 % in the fasted state (84). In the selected experimental setting, the release of the absorbed amount *in vivo* appears impossible within 3-4 h, a typical small intestinal transit time (136). This indicates that the absorption of the weakly basic pazopanib *in vivo* might depend on the solubilization in the stomach at lower pH than in FaSSIF and FeSSIF. A zero-order model was fitted to the initial part of the cumulative dissolution profile that was linear up to 6 min after the start of the test. The zero-order dissolution rate constant k_0 is higher in FeSSIF than in FaSSIF, in accordance with the better solubility in this medium (Figure 8).

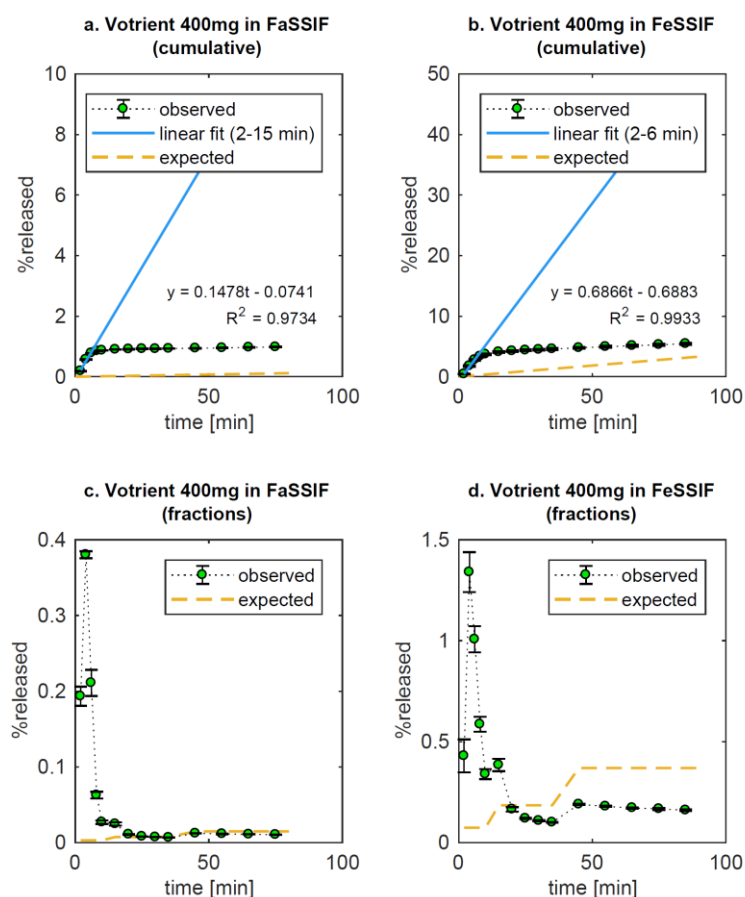


Figure 10: Votrient® 400 mg USP IV release profiles (cumulative and per fraction) with zero-order linear fit and expected release. Votrient® 400 mg film-coated tablets contain 433.33 mg pazopanib HCl. The dissolution tests were performed using a flow rate of 16 mL/min at 37 °C. The plots a and b represent the cumulative dissolution profiles, while the plots c and d show the released drug amount in the individual collected fractions. The zero-order model was fitted to the initial part of the cumulative dissolution profile that was linear up to 6 min after the start of the test. The expected release was calculated based on the API solubility after 1 h in the shake-flask test.

The release profiles of Zelboraf® 240 mg in FaSSIF and FeSSIF (Figure 11) were linear up to 15 min, followed by a continuous decrease in dissolution rate. Usually, the release rate is only expected to decrease when the amount of undissolved drug is depleted. However, this phenomenon can also be observed in the USP IV dissolution data reported by other groups (137, 138), and was attributed to the hydrodynamics in (137). The profile in FaSSIF could only be recorded up to 20 minutes, as the cell became clogged. The issue could not be fixed by using different filters. However, the linear part of the profile was adequately captured to fit the zero-order dissolution rate constant k_0 . It was fitted to the linear part from 0-15 min of the FaSSIF and FeSSIF release profiles and is similar in both media (even slightly higher in FaSSIF), which was unexpected given the 24-fold higher thermodynamic FeSSIF solubility (Figure 8). However, the solubility after 1 h is only 1.6-fold higher in FeSSIF than in FaSSIF, where massive supersaturation was observed, probably through the better solubility of the HPMC-AS matrix at the higher pH 6.5. The supersaturation in FaSSIF after 15 min can be even higher than after

1 h (Figure 11c), enabling higher drug release than in FeSSIF, which explains the slightly higher k_0 , derived from the initial part of the profile.

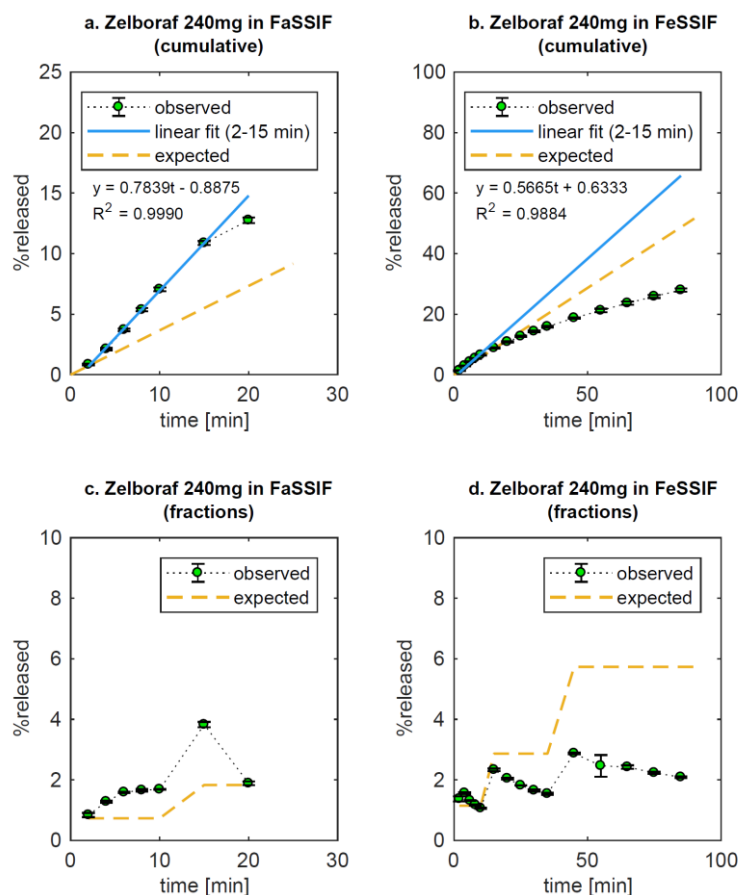


Figure 11: Zelboraf® 240 mg USP IV release profiles (cumulative and per fraction) with zero-order linear fit and expected release. Zelboraf® 240 mg film-coated tablets contain 240 mg vemurafenib in form of HPMC-AS coprecipitate. The dissolution tests were performed using a flow rate of 16 mL/min at 37 °C. The plots a and b represent the cumulative dissolution profiles, while the plots c and d show the released amount in the individual collected fractions. The zero-order model was fitted to the initial part of the cumulative dissolution profile that was linear up to 15 min after the start of the test. The expected release was calculated based on the vemurafenib solubility from ground Zelboraf® 240 mg film-coated tablets after 1 h in the shake-flask test.

The release profiles of Votrient® 400 mg (pazopanib) and Zelboraf® 240 mg (vemurafenib) in the flow-through cell apparatus, differ in the extent of the release and profile shape due to the different solubility in the tested media, as well as the nature of the formulations. Votrient® 400 mg contains crystalline pazopanib HCl and shows (after an initial boost through the excipients) a release rate that complies with the solubility of the crystalline drug. In contrast, Zelboraf® 240 mg contains amorphous vemurafenib, creating high drug concentrations in solution, when the polymer dissolves. The enabled vemurafenib release is permanently higher than expected based on the crystalline solubility (0.7 µg/mL in FaSSIF and 1.9 µg/mL FeSSIF after 24 h), which would be for example 0.1 % of the dose after 20 min in FaSSIF and 1 % of the dose after 85 min in FeSSIF (data not shown in Figure 11). Of note,

the clinical doses of both, pazopanib and vemurafenib, require the intake of more than one tablet. In the USP IV dissolution apparatus, only one tablet per cell can be tested, but as sink conditions are permanently assured, the dissolution rate might not be different if higher doses are tested. The maximum flow rate (16 mL/min) of the pump was chosen to speed up the dissolution tests of these very low solubility drugs to achieve the maximum performance. In the literature, different lower flow rates in biorelevant dissolution experiments in the USP IV flow-through cell apparatus have been investigated (64, 137-139). However, this would not help to overcome the discussed in vitro-in vivo misfit of the pazopanib release. In the absence of vemurafenib oral bioavailability in human, no conclusions about the correlation of the amount of drug released in vitro and absorbed in vivo can be drawn. To discuss the food effect, the FeSSIF/FaSSIF k_0 and W_{\max} -ratios are shown in Table 17.

4.1.3. Summary of the relative fed/fasted differences in vitro and in vivo

The performance of in vitro solubility and dissolution tests in food effect predictions is evaluated through a comparison of the relative differences of in vitro measured parameters in fed state and fasted state simulated media (solubility, dissolution rate k , and total amount released W_{\max}) with the relative difference in the pharmacokinetic parameters (AUC and C_{\max}) in the fed and fasted state (Table 17).

The clinical data show a strong (> 2-fold) positive food effect for lapatinib, pazopanib, and vemurafenib. The ratios of FeSSIF/FaSSIF solubility after 24 h, indicate better solubility in the fed state of these three drugs, but also for all other model drugs, whose exposure is not increased by concomitant food intake in the clinical trials. The extent of observed food effect does not correlate with the 24 h FaSSIF/FeSSIF solubility ratio and is generally overpredicted. Calculating the FaSSIF/FeSSIF solubility ratio using the 1 h or 2 h concentrations in the shake flask solubility test results in an even higher value for most model drugs, because the supersaturation (if any) in the shake-flask solubility tests after 1 h and 2 h compared to 24 h was higher in FeSSIF than in FaSSIF, except for vemurafenib. Therefore, it is concluded that the general mismatch of the solubility-ratio and the AUC and C_{\max} fed/fasted ratios, is not caused by the use of the 24 h solubility. It could be promoted by the fact, that the volume in the gut is not infinite and differences in fasted and fed state solubility may be leveled out. When fasted and fed state solubility are both high enough, the dose can be completely dissolved, independent of the food state. Moreover, the concomitant absorption process removes dissolved drug from the lumen, allowing further solubilization of the remaining solid in vivo. It is worth noting, that a food effect is only observed for the three model drugs with dose number $D_0 \geq 277.78$ (Table 18), suggesting that for the other 7 model drugs with $D_0 \leq 193.55$, solubility is already sufficient in the fasted state.

Table 17: Difference in pharmacokinetic parameters in the fed and fasted state versus the difference of in vitro measured parameters in fed state and fasted state simulated media. The C_{max} and AUC fed/fasted ratios are taken from the clinical food effect studies of the model drugs, referenced in this table. The FeSSIF/ FaSSIF 24 h-solubility ratios were calculated from the measured data presented in 4.1.1. The FeSSIF/ FaSSIF W_{max} and k ratios were fitted to the presented dissolution profiles the USP II apparatus in 500 mL FaSSIF and FeSSIF (4.1.2). The FeSSIF/ FaSSIF k_0 ratios were fitted to the presented dissolution profiles in FaSSIF and FeSSIF in the USP IV apparatus (4.1.2). The numbers in brackets represent the reference numbers.

	C_{max} fed/ fasted ratio	AUC fed/ fasted ratio	FeSSIF/ FaSSIF 24 h-solubility ratio	FeSSIF/ FaSSIF W_{max} ratio (500 mL)	FeSSIF/ FaSSIF k or k_0 ratio (500 mL)
Crizotinib	0.86 (71)	0.86 (71)	≥ 14	not tested	not tested
Dabrafenib	0.49 (140)	0.70 (140)	2	not tested	not tested
Erlotinib	1.56 (43)	1.66 (43)	9	9.9	2.5
Gefitinib	1.32 (44)	1.37 (44)	29	7.8	0.7
Imatinib	0.89 (80)	0.92 (80)	n.a.*	not tested	not tested
Lapatinib	3.03 (82)	4.25 (82)	8	not tested	not tested
M1	1.29	1.17	6	1.8	1.0
Pazopanib	2.08 (45)	2.34 (45)	4	n.a.	4.0
Trametinib	0.301 (141)	0.897 (141)	5	not tested	not tested
Vemurafenib	2.5 (46)	4.7 (46)	26	n.a.	0.7

* interaction of imatinib with the micelles leading to a gel formation (130), hinders solubility determination in the supernatant

The pH dependent solubility does not seem connected with a negative food effect. Almost all compounds are weak bases showing decreased solubility at higher pH levels (Figure 7), but only dabrafenib and trametinib show a negative effect of food on exposure (Table 17), whereby trametinib is a neutral compound with pH independent solubility (90) (Table S 12). It seems to be overruled by other factors like the better bile-salt mediated solubilization in the fed state. Moreover, the intensity of the pH independent solubility (pH 1.6/ pH 5.0 solubility ratio) does not correlate with the appearance of a negative effect of ARA on the exposure for the six model drugs where ARA studies are available (Table S 13). A negative ARA effect is already observed at lower D_0 (Table 18) for drugs that do not show positive food effect (e.g. erlotinib and gefitinib), indicating that pH dependent loss in gastric solubility can be compensated by other factors.

Testing the release from oral dosage forms can provide additional information to drug substance solubility tests, as the physiological relevance can be enhanced when the clinical dose is released in an appropriate gastrointestinal volume, and the dissolution kinetics are captured. A drug can have better solubility in FeSSIF than in FaSSIF but still show the same USP II dissolution profile in both media, when the solubility is equally sufficient. Imatinib, for example shows similar release profiles in aqueous buffers of pH 1, pH 4.5 and pH 6.8 (81), and therefore most probably also in FaSSIF (pH 6.5) and FeSSIF

(pH 5.0), which would indicate the absence of a solubility mediated food effect. The erlotinib, gefitinib, and M1 W_{\max} FeSSIF/FaSSIF ratios of > 1 (Table 17), however, indicate a risk for a positive food effect, just like the FeSSIF/FaSSIF solubility ratios. For erlotinib and gefitinib, this consistency is because the W_{\max} values are determined by the low solubility. The food effect prediction by release tests in 250 mL volume can be even more misleading, for example in the case of gefitinib, when the low FaSSIF solubility only allows a 50 % lower W_{\max} than in 500 mL, but still complete release in FeSSIF. The first-order dissolution rate constant k FeSSIF/FaSSIF ratios of erlotinib, gefitinib and M1 released in 500 mL (Table 17) or 250 mL (data not shown) do not show a correlation with the observed food effect. Factors like coning (especially for M1), and tablet adherence to the vessel wall (especially Iressa® 250 mg in FeSSIF) lead to a strong dependency of the amount released to paddle speed and hydrodynamics, that are different from the physiological situation and therefore do not simulate the actual in vivo release. The zero order k_0 FeSSIF/FaSSIF ratio from pazopanib USP IV release tests (Table 17), indicates a faster dissolution onset in the first 6 minutes of the FeSSIF release test, which is in line with the FeSSIF/FaSSIF solubility ratio and the observed positive food effect in the clinical study (45). However, extrapolating the total amount of released drug in this setting to an intestinal transit time of 3-4 h zero-order k_0 , is similar in FaSSIF and FeSSIF and does not indicate a risk for the observed positive food effect in the clinical study (46). As vemurafenib is a low permeability drug (19), its absorption may not depend strongly on the initial dissolution rate, but more on the total dissolved amount during the entire GI passage, which is likely higher in the fed state than in the fasted state as shown by the FeSSIF/FaSSIF solubility ratio, and can explain the food effect.

In both dissolution apparatuses, USP II and USP IV, in vitro in vivo correlations (IVIVC) have been obtained by other research groups after testing different dissolution media and agitation speed/ flow rates, e.g. in (64, 142). However, the common biorelevant dissolution setup, used in this research, may not always be able to achieve this. Currently many working groups focus on enhancing the understanding of the physiology and the optimization of the in vitro assays, for example for 2-stage or even multi-compartmental dissolution testing to better mimic and predict the in vivo behavior of oral dosage forms (48).

In vitro in vivo correlations and comparisons rely on the assumption that the appearance of the drug in blood following oral administration is only limited by formulation-related factors such as release and dissolution. This assumption is invalid when intestinal loss by efflux or drug metabolism become relevant for a drug. In this research, solutions are provided to identify the mechanisms contributing to an intestinal loss based on clinical pharmacokinetic data. In the section 4.2, the identification of compounds with solubility-limited absorption in the fasted state is described, for which enhanced solubility in fed state simulated media in vitro is also meaningful in vivo.

4.1.4. Permeability and solubility in BCS and DCS framework

The solubility-relevant parameters in BCS (D_0) and DCS (SLAD) framework determined for the model compounds are presented along with the results of the permeability assessment in Table 18. The dose number of > 1 calculated from the FaSSIF solubility matches the BCS classification as low soluble drugs (i.e. BCS class II or IV) reported in the literature for all compounds except for imatinib. The dose number calculated for imatinib of 0.38 indicates that the full dose can be dissolved in 250 mL of FaSSIF. This might differ from the BCS classification for regulatory purposes, as aqueous (not biorelevant media) are employed in the solubility tests when evaluating a biowaiver. A low solubility of 50 $\mu\text{g/mL}$ at pH 7.4 was reported for imatinib (80). However, solubility in biorelevant media is considered more in vivo relevant (28). The DCS classification is more liberal, as it is based on a volume of 500 mL FaSSIF and the possibility for high permeability to compensate the effect of poor solubility or dissolution on the absorption (22). Therefore, crizotinib, gefitinib, and M1 were identified next to imatinib as drugs that may not have solubility-limited absorption at the doses employed in the food effect studies (DCS class IIa), based on their SLAD greater than that dose. As biopharmaceutics classification systems are not available for the rat, required volume of FaSSIF to dissolve the dose/0.25 kg for the rat was calculated to discuss the relationship of dose and solubility with regard to the rat GI. The apparent permeability through a Caco-2 cell monolayer is relatively high for all model compounds (considering the P_{app} of the high permeability marker propranolol ($31.89 \cdot 10^{-06}$ cm/s) and low permeability marker atenolol ($0.13 \cdot 10^{-06}$ cm/s) in the assay), except for vemurafenib and lapatinib. This is in line with the reported BCS classifications (Table 18), except for crizotinib that appears to have moderate rather than low permeability in the current assessment. The calculated P_{eff} was provided to obtain a certain range of possible permeability estimates for the use in the generic PBPK model in MATLAB®.

The presented biopharmaceutics parameters are discussed later with regard to the predictivity of solubility-limited absorption and food effects compared to the proposed analysis of clinical and preclinical PK data.

Table 18 : Summary of parameters in the biopharmaceutics classification frameworks. The numbers in brackets represent the reference numbers.

Parameters	Crizotinib	Dabrafenib	Erlotinib	Gefitinib	Imatinib	Lapatinib	M1	Pazopanib	Trametinib	Vemurafenib
Measured solubility in FaSSIF pH 6.5 [mg/mL]	0.7430	0.0037	0.0124	0.0887	≥ 5	0.0350	0.0728	0.0012	not measured	0.0054
Clinical dose in food effect study [mg] ^a	250	150	150	250	400	1500	clinical dose is yet to be established	800	2	960
Dose number	1.35	193.55	53.10	11.27	0.38	277.78	> 1	2909.09	11.43	711.11
BCS classification	IV (72)	II (76)	II (77)	II (78)	II (17)	IV (83)	likely IV	II (87)	II (90)	IV (19)
SLAD [mg] ^a	985.72	4.41	24.18	227.43	6527.96	23.75	> dose in food effect study	0.55	0.45 ^b	8.20
DCS classification	IV	IIb	IIb	IIa	IIa	IV	likely IV	IIb	IIb	IV
required volume of FaSSIF to dissolve the rat dose/0.25 kg [mL]	1.5	234.5	59.9	11.6	0.3	248.5	1.7	2698	13.8	555.6
Measured Caco-2 P _{app} passive [10 ⁻⁶ cm/s]	15.35	12.45	40.43	10.41	25.90	0.21	14.70	28.46	15.44	0.11
Calculated human P _{eff} [10 ⁻⁴ cm/s]	2.22	2.38	3.58	5.23	2.61	1.84	6.19	0.85	1.07	2.54

^a dose given as parent drug

^b calculated using literature solubility from FDA Clinical Pharmacology and Biopharmaceutics Review (90)

4.2. Predicting the food effect on exposure through understanding the mechanisms underlying absorption in human and rat

4.2.1. Analysis of clinical PK data

4.2.1.1. Gut bioavailability in human

All compounds except for pazopanib (0.21) and erlotinib (0.61) demonstrated good gut bioavailability > 0.75 (Table 19) in the absolute bioavailability study, which was tested at the same dose as food effect, with the exception of M1, where the absolute bioavailability was determined at 500 mg and the food effect at 30 mg. It can be assumed, that the gut bioavailability at 30 mg is equal or even higher. The gut bioavailability suggests sufficient solubility for adequate absorption of crizotinib, dabrafenib, gefitinib, imatinib, M1, and trametinib at the doses employed in their food effect studies. It cannot be calculated in the absence of IV PK of vemurafenib and lapatinib.

4.2.1.2. Human top-down PBPK analysis

The CL_{int} and K_p factors were obtained from IV PBPK simulations and for vemurafenib and lapatinib, in the absence of IV PK data, the CL_{int} could be derived from the oral PK profile after the volume of distribution was estimated (Table 10). The data is presented along with the input parameters in Table S 6. The oral PBPK simulations of all compounds at the doses of their food effect studies captured the observed PK adequately, (Table 20, Figure S 1) except for erlotinib and M1. The exposures of erlotinib and M1 were over-predicted using the in vitro solubility data and either of the permeability estimates (derived from Caco-2 P_{app} or calculated P_{eff}) due to an intestinal loss or in case of M1 retention of the drug. Crizotinib, gefitinib, and imatinib were identified as drugs that might delay gastric emptying so that the gastric emptying rate was decreased in their models. To allow the observed t_{max} with a subsequent decrease in plasma concentrations, the colonic absorption of vemurafenib and pazopanib was decreased in the models. To simulate the observed exposure of the extremely poorly soluble dabrafenib, lapatinib, trametinib, and vemurafenib (with solubility in FaSSIF or FaSSGF blank pH 1.6 < 0.01 mg/mL), the input solubilities were increased. This suggests that the in vitro solubility measurement of the drug substance in a defined solvent may underestimate the true solubility in vivo. Weak bases such as dabrafenib and lapatinib are expected to generate supersaturated solutions in vivo after the transit from the acidic stomach to a neutral environment of the intestinal tract. Moreover, the highly variable buffer capacity, pH and bile salt concentrations in the GI fluids may not be accurately characterized under the in vitro conditions (44). Like in the case of vemurafenib, the API may be released from enabling formulations, containing amorphous drug, improving the apparent solubility and absorption (143).

Table 19: Collection of human pharmacokinetic data used to identify solubility-limited absorption. The numbers in brackets represent the reference numbers.

	<u>Gut Bioavailability</u>	<u>Dose-proportionality of exposure</u>			<u>Observed clinical food effect on AUC and C_{max}</u>		
	Calculated F _a *F _g	Dose range tested [mg]	Dosing schedule	Increase in exposure	Food effect study dose [mg]	AUC fed/fasted ratio	C _{max} fed/fasted ratio
Crizotinib	0.90	50-300 50-200 200-300	single dose steady state steady state	less than proportional more than proportional more than proportional (72)	250	0.86 (71)	0.86 (71)
Dabrafenib	1.09	12-300	single dose steady state	dose proportional less than proportional (76)	150	0.70 (140)	0.49 (140)
Erlotinib	0.61	100-1,000	not available	dose proportional (77)	150	1.97/0.93 (43)	1.57/1.15 (43)
Gefitinib	1.06	50-500 50-400 50-700	single dose (HV) steady state (pat.) steady state (pat.)	dose proportional dose proportional more than proportional (78)	250	1.37 (44)	1.32 (44)
Imatinib	1.16	25-1,000	not available.	dose proportional (81)	400	0.92 (144)	0.89 (144)
Lapatinib	n.a.	approx. 600-1,800	steady state	dose proportional (83)	1,500	4.25 (82)	3.03 (82)
M1	0.86	30-1,400	steady state	less than proportional (food effect dose is within the linear region)	30	1.17	1.29
Pazopanib	0.21	50-2,000	single dose steady state	less than proportional less than proportional (87)	800	2.34 (45)	2.08 (45)
Trametinib	0.75	0.125-10	single dose	more than proportional (C _{max} proportional) (90)	2	0.897 (141)	0.301 (141)
Vemurafenib	n.a.	240-960	single dose steady state	dose proportional dose proportional (19)	960	4.7 (46)	2.5 (46)

Table 20: Observed vs predicted human pharmacokinetic parameters at doses employed in their clinical food effect studies and simulation using hypothetical BCS class I-like solubility

	Observed PK parameters			PK Parameters from best fit PBPK Simulations using Caco-2 Permeability				PK Parameters from best fit PBPK Simulations using calculated P _{eff}				AUC and C _{max} ratios using hypothetical BCS class I-like solubility to best fit			
	AUC _{0-24 h} [h*μM]	C _{max} [μM]	t _{max} [h]	AUC _{0-24 h} [h*μM]	C _{max} [μM]	t _{max} [h]	Solubility increase [mg/mL]	AUC _{0-24 h} [h*μM]	C _{max} [μM]	t _{max} [h]	Solubility increase [mg/mL]	Caco-2 permeability		Calculated P _{eff}	
												AUC _{0-24 h} ratio	C _{max} ratio	AUC _{0-24 h} ratio	C _{max} ratio
Crizotinib	3.635	0.311	5.05	3.36	0.261	3.6	none	3.34	0.257	4	none	1.0	1.0	1.0	1.0
Dabrafenib	25.38	3.99	2	18.6	3.89	2.48	0.0037 → 0.0616	18.4	3.52	2.72	0.0037 → 0.0616	1.0	1.3	1.0	1.3
Erlotinib	21.3	1.94	4.13	53.9	4.03	3.67	none	35.6	1.98	4.71	none	1.1	2.1	1.6	3.4
Gefitinib	2.549	0.161	3.72	2.24	0.142	3.82	none	2.27	0.145	3.42	none	1.0	1.0	1.0	1.0
Imatinib	28.91	3.51	1.51	36.4	2.78	1.6	none	36	2.65	2.24	none	1.0	1.0	1.0	1.0
Lapatinib	18.07	1.46	3.96	15.3	1.18	2.88	0.0350 → 6.6044	22.7	1.4	3.92	0.0350 → 0.0943	1.0	1.0	4.6	11.0
M1	1.073	0.0621	8	1.75	0.312	0.96	none	1.76	0.352	0.8	none	1.0	1.0	1.0	1.0
Pazopanib	843.6	47.3	4	889	50.7	5.44	0.0012 → 0.0237	978	55.7	5.12	0.0012 → 0.2370	3.9	4.0	2.7	2.7
Trametinib	0.1162	0.0136	1.5	0.0912	0.0052	2.16	0.0008 → 0.0069	0.0896	0.0054	1.76	0.0008 → 0.0416	1.1	1.7	1.0	1.0
Vemurafenib	94.71	6.41	4.08	109	5.91	4.7	0.0054 → 0.6124	133	7.3	6.14	none	2.6	2.6	54.1	53.8

Moreover, hydroxypropyl methylcellulose (HPMC) presented in the shell of dabrafenib capsules may inhibit precipitation of supersaturated dabrafenib solution over an extended period of time (41), or the presence of SDS in trametinib (27) tablets may increase the apparent solubility in vivo through enhanced solubilization. By dumping an API solution into FaSSIF (described in 3.2.2), it was shown, that dabrafenib, lapatinib, trametinib, and vemurafenib, whose solubility was increased in the model, are capable of generating supersaturation for at least 15 min in vitro (Table 16).

The effect of solubility on the oral absorption was investigated by simulating the PK metrics with a hypothetical BCS class I-like solubility in the established PBPK models. The ratios of C_{max} and AUC between increased hypothetical BCS class I-like solubility input to the best-fit “in vivo solubility” are summarized in Table 20. The PBPK models identify crizotinib, dabrafenib, gefitinib, imatinib, M1, and trametinib as insensitive to an increase in the input solubility parameters with an AUC or C_{max} ratio close to 1. The exposure in the models of pazopanib and vemurafenib is increased with the BCS class I input solubility, using either the Caco-2 permeability or the calculated P_{eff} by 2.6 - 54.1-fold, and is therefore likely to be limited by solubility.

The PBPK modeling example of pazopanib is illustrated in Figure 12. First, the CL_{int} and K_p factor were obtained from PBPK simulation of observed IV PK data (Figure 12a). The PBPK simulation of oral PK profiles using in vitro FaSSIF solubility and Caco-2 permeability data under-predict the observed PK profile (Figure 12b). A 20-fold increase in the input solubility was required to capture the observed absorption rate, (Figure 12c) and a reduced colonic absorption was required for the elimination to overtake after the t_{max} (Figure 12d). By increasing the solubility to a hypothetical BCS class I-like non-absorption limiting value, simulated C_{max} and AUC are 4-fold higher than the observed C_{max} and AUC (Figure 12e). This suggests that the absorption of pazopanib is limited by poor solubility. In contrast, sensitivity to a hypothetically high permeability increase is low (Figure 12f), as expected for a BCS class II drug.

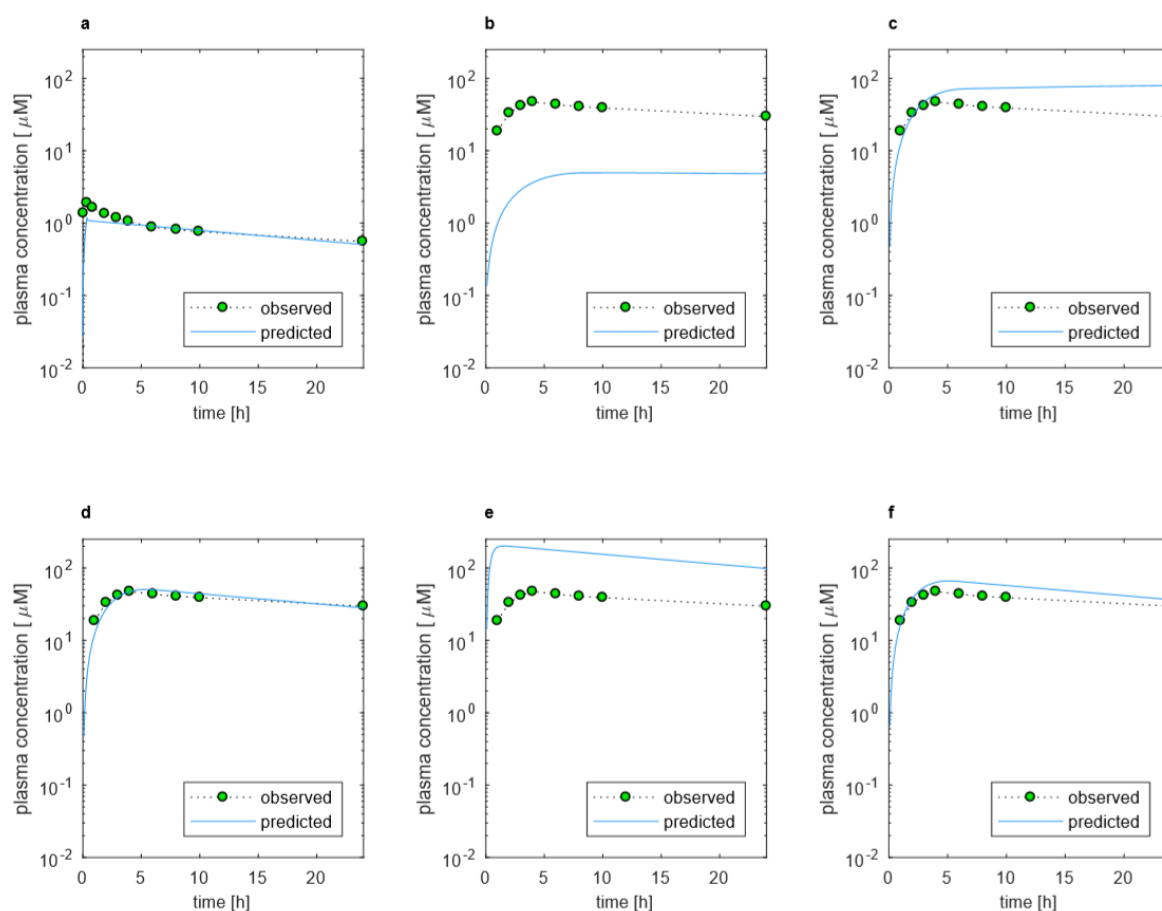


Figure 12: PBPK analysis of pazopanib pharmacokinetic profiles (51); a) PBPK simulation of intravenous infusion of 5 mg pazopanib over 5 minutes to obtain the intrinsic clearance and K_p factor, for simultaneously scaling all tissue distribution coefficients; b) Pazopanib 800 mg oral administration simulated with in vitro FaSSIF solubility and Caco-2 permeability; c) Pazopanib 800 mg oral administration simulated with Caco-2 permeability and an input solubility that is 20-fold higher than FaSSIF solubility; d) Pazopanib 800 mg oral administration simulated with Caco-2 permeability, an input solubility that is 20-fold higher than FaSSIF solubility and reduced colonic absorption; e) Pharmacokinetic profile using hypothetical BCS class I-like solubility in the pazopanib PBPK model with good fit in d); f) Pharmacokinetic profile using hypothetically high permeability of $10 \cdot 10^{-4} \text{ cm/s}$ in the pazopanib PBPK model with good fit in d)

The PBPK simulations of erlotinib are shown in Figure 13. The in vitro FaSSIF solubility was sufficient to explain the observed erlotinib PK profile. Erlotinib C_{max} was stronger increased using the hypothetical BCS class I-like solubility in the PBPK model than the AUC (Figure 13c), indicating that its rate of absorption depends on dissolution, rather than solubility. Moreover, the PBPK simulations indicate that erlotinib undergoes an intestinal drug loss of drug that could be related to gut metabolism or efflux. Erlotinib is a CYP3A substrate and gut metabolism has been previously reported (145). With only 1% of the dose as parent drug in the feces after oral administration (145), the contribution of transporter-mediated intestinal efflux to the loss of drug is unlikely. As shown in 4.3.1, CYP3A is metabolizing other model compounds as well, but the good gut bioavailability of > 0.75 of most of

these compounds and the PBPK analysis do not indicate a contribution to an intestinal loss. Gut first pass metabolism of lapatinib is mentioned in (146). However, lapatinib is an example of a compound where it might be difficult to distinguish gut metabolism from poor absorption in the PBPK, as the very low solubility is probably contributing in addition to its poor exposure in human. Since there is no IV PK data for the compound, the gut bioavailability cannot be calculated. To really quantify the gut first pass, the appearance of metabolites in radiolabeled IV and per oral (p.o.) studies could be compared.

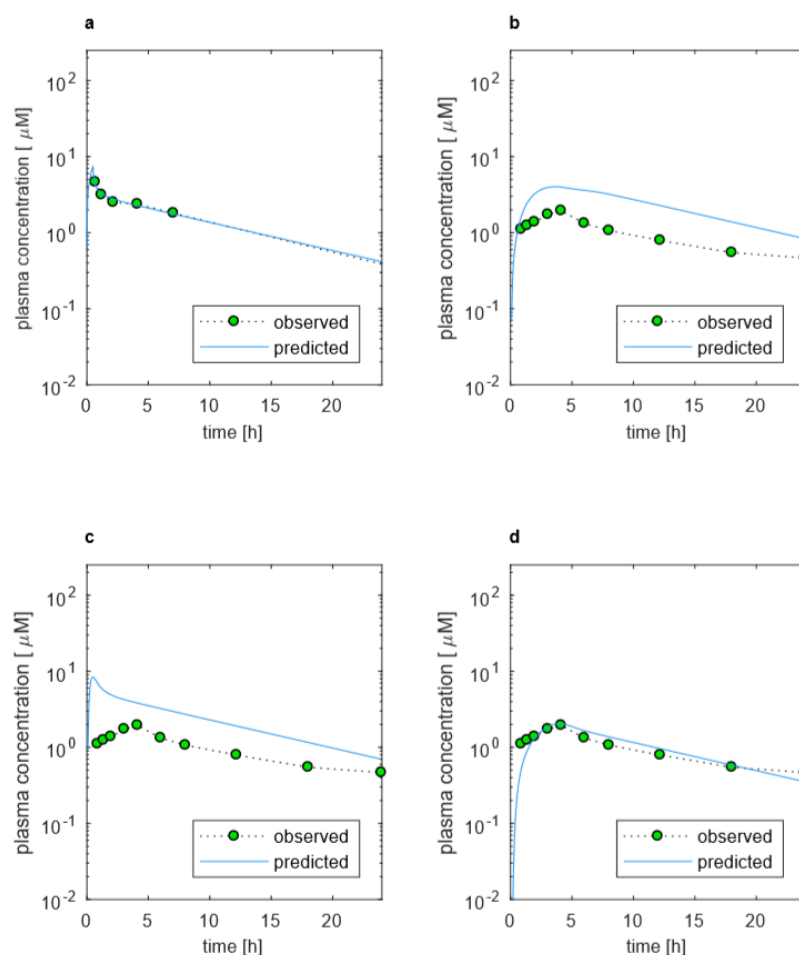


Figure 13: PBPK analysis of erlotinib pharmacokinetic profiles (51); a) PBPK simulation of intravenous administration of 75 mg erlotinib to obtain the intrinsic clearance and multiplicative K_p factor, for simultaneously scaling all tissue distribution coefficients; b) Erlotinib 150 mg oral administration simulated with in vitro fasted FaSSIF solubility and Caco-2 permeability. The discrepancy in exposure between predicted and observed may be attributed to intestinal loss mediated by metabolism or efflux rather than due to an in vitro to in vivo disconnect in solubility. In vitro measurements of solubility tend to be much lower than observed, as the dynamics of dissolution cannot be adequately captured in the assays. c) Erlotinib 150 mg oral administration simulated with hypothetical BCS class I-like solubility and Caco-2 permeability enables a higher C_{max} while AUC remains similar to simulated profile in c, indicating a slow in vivo dissolution and an absorption not limited by solubility; d) Erlotinib 150 mg oral administration simulated with in vitro FaSSIF solubility and Caco-2 permeability, using reduced intestinal absorption scaling factors to simulate the intestinal loss, probably mediated by efflux or gut metabolism

For most compounds, there is only a minor difference between the simulations using the two different permeability values (Table 20). After scaling the Caco-2 permeability by a factor of 25 for the use in the PBPK model, the difference in calculated and Caco-2 derived human P_{eff} is 2-fold or more, except for dabrafenib and M1 with < 2-fold. However, changing the permeability of dabrafenib and M1 by more than 2-fold, has no effect on the simulated C_{max} and AUC. In the cases of the poorly permeable vemurafenib and lapatinib, in contrast, changing from the low measured permeability in the Caco-2 assay to a moderate calculated P_{eff} leads to a significant increase in predicted exposure. The sensitivity of the simulated exposure to a hypothetical solubility increase to BCS class I level is also different between the two permeability estimates of vemurafenib and lapatinib. Moreover, higher than observed exposure can be achieved in the model using a hypothetically high permeability as well as solubility. Therefore, solubility or permeability limitation are non-identifiable for these compounds.

4.2.1.3. Dose linearity and food effect in human

Exposure of all model compounds, except for pazopanib > 800 mg (24, 31) and M1, single dose PK is reported to be dose-proportional or more than dose-proportional (Table 19). The exposure of crizotinib increases less-than-dose-proportionally according to the FDA's Clinical Pharmacology and Biopharmaceutics Review (19), but the data presented suggests dose-linearity. These data can indicate solubility-limited absorption at higher doses, when the exposure increases in a less than dose proportional manner or non-solubility-limited absorption when the PK is linear or increases more than dose proportionally.

The food effect data were collected to investigate the coherence of solubility-limited absorption and food effect of the model drugs, which is discussed in 4.2.3. The AUC and C_{max} fed/fasted ratios reported in the literature are presented in Table 19. Concomitant food intake has only a strong impact on the exposure of lapatinib, vemurafenib and pazopanib (strong positive food effect). In the erlotinib food study at 150 mg (43), the change in AUC in the fed state compared to the fasted state differs in the two periods of the study (97 % AUC increase in period 1 and 7 % AUC decrease in period 2). The small observed food effect of gefitinib is confounded by a very high inter-subject variability (32).

4.2.2. Analysis of preclinical PK data

4.2.2.1. Results of the in vivo rat PK studies

The calculated PK parameters resulting from the rat PK study are presented in Table 21. The clearance, volume of distribution, and amount of parent drug excreted in the feces after IV administration are presented along with the absolute and gut bioavailability, as well as the percentage of the dose excreted in the feces after oral administration. The variability (indicated by the range of the parameters) was lower after IV than oral administration. The percentage of AUC extrapolation provides information on the reliability of the extrapolated AUC_{0-inf} and therefore the calculated bioavailability. Extrapolation of $\leq 20\%$ is generally considered uncritical, but higher values provide risk for miscalculation of PK parameters based on the extrapolation. The extrapolated AUC from the last measured time point to infinity ($AUC_{last-inf}$) was higher than 20% for the long half-life drugs trametinib, gefitinib, vemurafenib, and pazopanib.

The oral absorption of vemurafenib and ground Zelboraf[®] was so much delayed in one of the three animal each, that the plasma concentration after 24 h represented the C_{max} of the profile, these animals were also excluded from the analysis. Due to the low oral trametinib dose (0.04 mg/mL), several plasma concentrations in the individual profiles were lower than the limit of quantification (0.5 ng/mL). The analysis was performed based on the mean profile resulting from the available values. The IV PK parameters of dabrafenib and gefitinib are only based on 2 animals, as the third animal was dosed extravascular.

A common practice for PK characterization in drug discovery is cassette IV PK testing at a low dose (147, 148), e.g. 0.2 mg/kg like in the present study. The low dose enables the quantitative contribution of all eliminating mechanisms to capture the full pharmacokinetic potential. At a higher, clinically relevant dose, the clearance might be lower if some of these mechanisms get saturated. In this work, the IV clearance is directly used for the calculation of oral bioavailability and in the oral PBPK models. Therefore, a similar degree of metabolic saturation and comparable clearance after oral and IV dosing is crucial for compounds with non-linear PK. For the model drugs erlotinib and crizotinib, non-linear clearance in the rat was strongly suspected. The elimination slopes in the oral profiles were less steep than after the low IV dose of 0.2 mg/kg. Moreover, bioavailability of $> 300\%$ was calculated for erlotinib based on the AUC after 0.2 mg/kg IV (data not shown). IV PK testing at doses closer to the oral dose generated better data for both drugs to use in the presented analysis of rat PK data to identify solubility-limited absorption.

Table 21: Results of the rat PK studies. The numbers in brackets represent the range of the values.

Parameters	Crizotinib	Dabrafenib	Erlotinib	Gefitinib	Imatinib	Lapatinib	M1	Pazopanib	Votrient®	Trametinib	Vemura-fenib	Zelboraf®
IV dose [mg/kg]	4.9	0.2	3.0	0.2	0.2	0.2	0.2	0.2	n.a.	0.2	0.2	n.a.
Clearance [L/h/kg]	3.94 (3.42-4.70)	0.70 (0.71-0.70)	0.26 (0.24-0.29)	0.57 (0.47-0.72)	0.67 (0.64-0.69)	0.19 (0.15-0.32)	7.93 (n.a.)	0.01 (0.01-0.02)	n.a.	0.33 (0.29-0.35)	0.03 (0.03-0.04)	n.a.
V _{ss} [L/kg]	25.2 (22.3-29.2)	0.71 (0.62-0.76)	1.28 (1.18-1.39)	3.49 (2.90-4.41)	2.09 (2.07-2.13)	0.87 (0.73-0.86)	19.6 (n.a.)	0.17 (0.17-0.17)	n.a.	6.79 (6.54-7.00)	0.21 (0.20-0.22)	n.a.
% of dose as parent in feces 0-24 h (IV)	9.1 (1.8-16.4)	< 1	4.6 (3.0-6.9)	11.4 (0.7-22.1)	1.8 (0.1-4.3)	< 1	43 (n.a.)	1.7 (0.1-3.9)	n.a.	< 1	< 1	n.a.
Oral dose [mg/kg]	4.4	3.5	3.0	4.1	6.0	34.8	0.5	13.0	14.9	0.04	12.0	15.4
Absolute bioavailability	0.41 (0.16-0.56)	0.63 (0.50-0.77)	0.65 (0.52-0.81)	0.73 (0.40-1.67)	1.5 (1.24-1.76)	0.43 (0.32-0.52)	0.17 (n.a.)	0.73 ^e (0.32-1.78)	0.40 (0.26-0.56)	0.36 ^b	0.010 ^c (0.003-0.022)	0.13 ^c (0.14-0.15)
Gut bioavailability	1	0.75	0.69	0.84	1	0.45	1	0.73	0.40	0.39	0.010	0.13
% of dose as parent in feces 0-24 h (oral)	13 (0.0-34.0)	9.5 (0.3-18.6)	7.3 (4.5-10.0)	< 1	3.6 (0.8-5.5)	6.4 (0.0-7.0)	51 (n.a.)	15.8 (0.4-42.9)	1.5 (0.0-2.5)	80 (11.3-135.2)	47 ^c (8.2-56.0)	27.6 ^c (0.0-55.1)
% of dose as parent in feces 24-48 h (oral)	not measured	1.1 (1.5-0.6)	4.7 (2.1-3.8)	not measured	not measured	not measured	not measured	not measured	29.3 (16.5-41.8)	41 (17.8-74.4)	not measured	32.7 ^c (6.7-58.6)
% AUC extrapolation (oral) ^a	< 20	< 20	< 20	59	< 20	< 20	n.a.	51	20	68	122	43

^a The fraction of the extrapolated AUC_{last-inf} is presented as percent of the measured AUC_{0-last}.

^b plasma concentrations at many time points < LOQ, only the mean profile was analyzed

^c absorption in 1 animal was so much delayed, that the plasma concentration after 24 h represented the C_{max} of the profile, this animal was excluded from the analysis

The rat clearance of dabrafenib (2 mg/kg) (73) and imatinib (10 mg/kg) (149) reported in the literature are in accordance with the measured clearance in this study at 0.2 mg/kg. However, the clearances reported for gefitinib (5 mg/kg) (150), pazopanib (10 mg/kg) (151), and lapatinib (10 mg/kg) (96) are higher than in the current rat study. As the doses in the literature are much higher, this was unexpected as elimination mechanisms might get saturated at higher concentrations leading to a slower clearance of the drug. The crizotinib clearance at 5 mg/kg is with 29 ± 8 mL/min/kg (152) approximately 2-fold lower than in the current study at the same dose. The differences in between the clearances measured within this work and the literature values could be explained by different animal strains or genders between the studies. The absolute bioavailability in this study does not deviate more than $\pm 10\%$ from the reports in the literature of dabrafenib (4 mg/kg) (73), erlotinib (dose unknown) (70), pazopanib (10 mg/kg) (151), and trametinib (3 mg/kg) (153). For crizotinib (25 mg/kg) (152), lapatinib (10 mg/kg) (96), the bioavailability reported in the literature did not deviate by more than $\pm 20\%$ from the results in this study. Same is true for vemurafenib (30 mg/kg) when considering the lower value of 18% bioavailability in the source (98). An approximately -23% lower oral bioavailability of 49.8% after 5 mg/kg oral gefitinib in female rats has been reported in (150), and a lower estimated imatinib bioavailability of approximately 53% (149). The differences can be explained by the above addressed differences in clearance, different oral or IV doses, the formulations or food-state in the studies.

The mean plasma concentration-time profiles are shown in Figure 14. The t_{max} in all mean oral PK profiles of this study is unusually late (at the 4 h or 6 h sampling point). This delay in oral absorption is related to the capsule dosage form. Saphier et al. (154) investigated the gastric emptying of enteric coated PCcaps[®] in the original size of 7.18 mm length as well as shortened capsules in rats with X-ray imaging. The capsules of 7.18 mm length, the same size as the capsules used in this work, were retained in the stomach for > 5 h. The gastric residence time of almost all shortened capsules of 4.8 mm length administered in the fasted state and approximately two-thirds of the 4.8 mm capsules tested with free food-intake was > 2.5 h. High variability between the rats and different study days has been reported (154). Even though the capsules prepared for the PK study in this research were not coated, these findings explain the delay in oral absorption. This assumption is supported by the fact, that even smaller particles of 0.5 mm-2 mm can be retained in the rat stomach for at least 4 h (155), sizes that occur upon the disintegration of the capsules. Furthermore, Jang et al. (155) found that mini gelatin capsules of size 9 can stick to the esophagus for up to 1 h. Even though M1 was administered as an oral suspension, its absorption was delayed as well. The same phenomenon occurs in human and is not fully understood. The particle size was homogenized (to < 10 μ m for the most part) among the different APIs to exclude this factor as a covariate. Such particle sizes are common to enhance the dissolution kinetics of poorly soluble drugs (156). However, the gastric emptying kinetics turned out to be the absorption rate-limiting step.

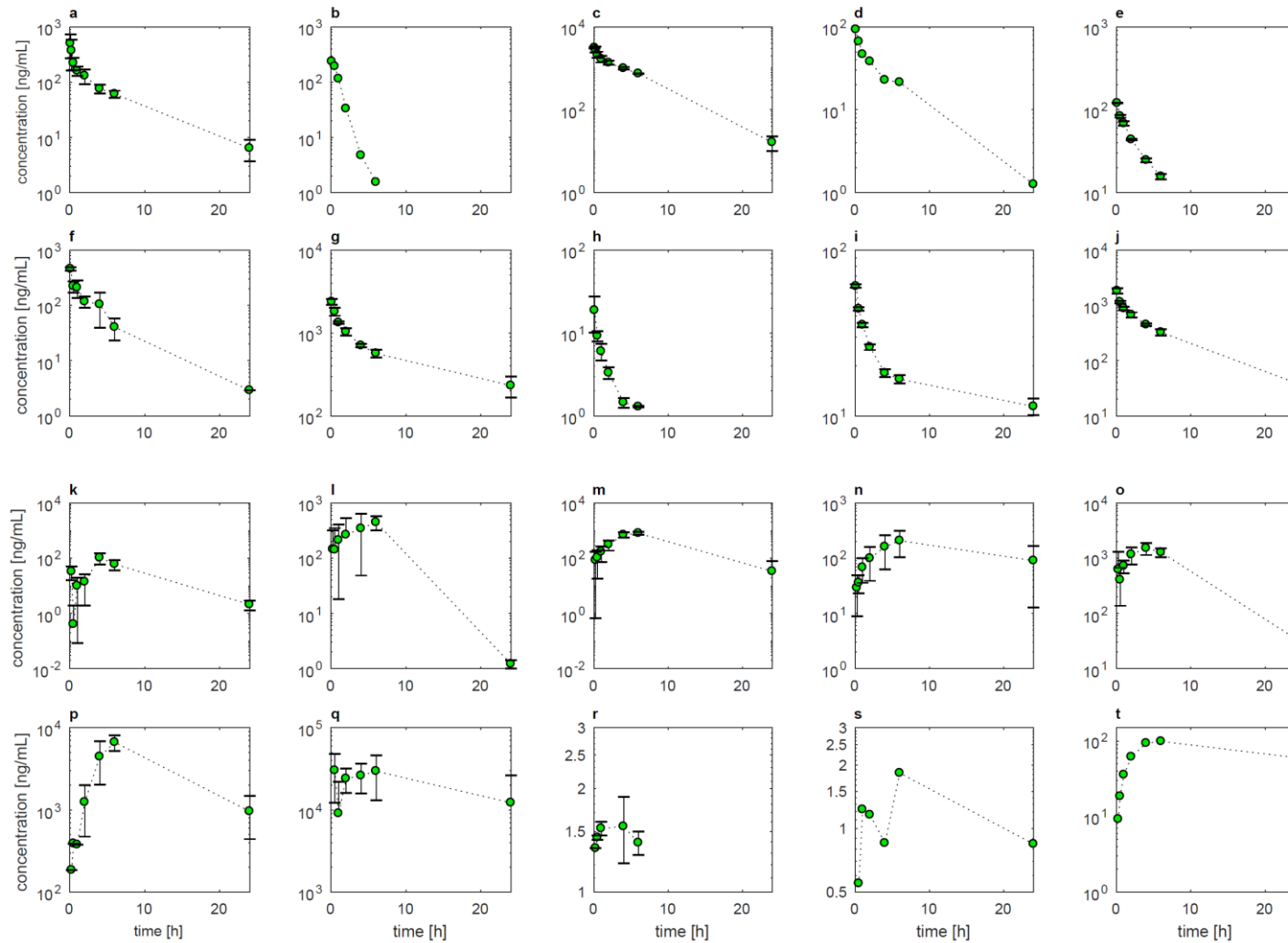


Figure 14: Mean (SD) plasma concentration-time profiles after IV and oral (capsules) administration in the rat, (a) 4.9 mg/kg crizotinib iv; (b) 0.2 mg/kg dabrafenib iv; (c) 2.97 mg/kg erlotinib iv; (d) 0.2 mg/kg gefitinib iv; (e) 0.2 mg/kg imatinib iv; (f) 0.2 mg/kg lapatinib iv; (g) 0.2 mg/kg pazopanib iv; (h) 0.2 mg/kg M1 iv; (i) 0.2 mg/kg trametinib iv; (j) 0.2 mg/kg vemurafenib iv; (k) 4.4 mg/kg crizotinib p.o.; (l) 3.5 mg/kg dabrafenib p.o.; (m) 3.0 mg/kg erlotinib p.o.; (n) 4.1 mg/kg gefitinib p.o.; (o) 6.0 mg/kg imatinib p.o.; (p) 34.8 mg/kg lapatinib p.o.; (q) 13.0 mg/kg pazopanib p.o.; (r) 0.5 mg/kg M1 p.o.; (s) 0.044 mg/kg trametinib p.o. (oral suspension); (t) 12.0 mg/kg vemurafenib p.o.

In some of the individual rat PK profiles of different model compounds, the plasma concentrations drop temporarily during the absorption phase. In the cases of crizotinib (Figure 14k) and pazopanib (Figure 14q), this issue is so pronounced that it is visible even in the mean profiles. It can be explained by discontinuation of the intestinal drug supply through the delayed, variable and unsteady gastric emptying. As it does not affect the overall AUC, it will have a negligible impact on the identification of solubility-limited absorption.

The late C_{max} in combination with a lack of measured plasma concentrations between 6 h and 24 h is hampering an accurate half-life estimation when the terminal slope of the log-profile is only based on 2-3 data points. This impacts the AUC extrapolation to infinity and, therefore, the bioavailability calculation, especially for drugs with long estimated half-lives (trametinib, gefitinib, vemurafenib, and pazopanib). The bioavailability calculated from the measured AUC_{0-last} provides the minimum expected bioavailability in vivo, which is 0.33, 0.46 (0.23-0.67), 0.006 (0.001-0.015) and 0.59 (0.35-1.02) for trametinib, gefitinib, vemurafenib, and pazopanib, respectively. The uncertainty in trametinib, gefitinib, vemurafenib, and pazopanib bioavailability affects the gut bioavailability calculation and is discussed in the next section (4.2.2.2).

The ground market products of pazopanib (Votrient® 400 g film-coated tablets) and vemurafenib (Zelboraf® 240 mg film-coated tablets) were administered at the same dose as the APIs to investigate the potential effect of the formulation on the extent of absorption. In the case of pazopanib, the performance of the ground tablets was similar to the API, as expected according to the composition of the market formulation containing crystalline API (134). For vemurafenib, however, the ground tablet was superior due to its amorphous state within Zelboraf® (Table 21) (19).

4.2.2.2. Gut bioavailability in the rat

Imatinib, M1, crizotinib, dabrafenib, and gefitinib have good gut bioavailability > 0.75 in the rat at the dose tested (Table 21), whereas the gut bioavailability of trametinib, erlotinib, lapatinib, vemurafenib, and pazopanib API in capsule is < 0.75 . This indicates a loss of the long half-life drugs trametinib, vemurafenib and pazopanib in the gut (whose bioavailability is uncertain to some degree) even with the bioavailability calculated based on AUC_{0-inf} , which is higher than the bioavailability based on AUC_{0-last} . For trametinib, the apparent low gut bioavailability could also come from the approximately 5-times higher IV than oral dose. Higher systemic clearance after oral administration could have led to lower bioavailability in general, not necessarily lower gut bioavailability. For gefitinib, the gut bioavailability based on the extrapolated AUC_{0-inf} (0.84) (Table 21) is significantly higher than the value calculated with the measured AUC_{0-last} (0.53). The use of extrapolated AUC indicates the absence of an intestinal loss of drug, while the use of AUC_{0-last} suggests otherwise.

4.2.2.3. Rat top-down PBPK analysis

The IV PBPK simulations provided the CL_{int} and K_p factors (Table S 7) for the use in the oral PK simulations for all compounds except for pazopanib and vemurafenib. The clearance of these two compounds is very low (0.01 L/h/kg and 0.03 L/h/kg, respectively) and cannot be captured in the PBPK model, as the simulations get insensitive to further CL_{int} reduction at some point. Therefore, pazopanib and vemurafenib were excluded from the rat PBPK simulations. For the oral PK simulations of dabrafenib, only one animal (rat 1) was used as the variability in the absorption phase is extremely high and the mean profile is therefore not representative. The second animal had extremely delayed absorption and the third animal with a very fast onset died between 4 h and 6 h after administration (Figure S 2).

The oral PBPK simulations at the body weight-scaled doses of their human food effect studies could capture the observed AUC of M1, crizotinib, trametinib, dabrafenib, gefitinib, and erlotinib adequately, using the in vitro FaSSIF solubility and either of the two permeability estimates (i.e. Caco-2 permeability or calculated P_{eff}) (Table 22). The exposure of lapatinib was overpredicted by approximately 2-fold, which could be related to gut first pass metabolism. The imatinib AUC was underpredicted by approximately 2-fold, although it was completely absorbed. This is probably because the input CL_{int} derived from the 0.2 mg/kg IV PK profile is higher than after 6.0 mg/kg p.o. in vivo due to saturation of eliminating mechanisms. This theory is supported by the fact, that an imatinib bioavailability of 1.5 was calculated based on these data, as it leads to a smaller dose-normalized IV AUC than oral AUC. Reducing the imatinib CL_{int} in the model by one third as a test, resulted in good C_{max} and AUC prediction. The PBPK simulations identified complete absorption for all compounds except for trametinib, with a fraction absorbed of 47 % simulated with Caco-2 permeability and 38 % with calculated P_{eff} .

In contrast to the AUC, the shape of all simulated plasma concentration time profiles, except for trametinib, did not match the observed. The initial upswing was faster and resulted in higher C_{max} and earlier t_{max} , than in vivo, while the later time points were under-predicted, indicating prolonged absorption. This behavior is typical when gastric emptying is delayed in vivo (99), which is caused by capsules used in the current study, as discussed earlier. The default gastric emptying rate in the model is 0.37 min^{-1} (61) and the values used for the individual simulations are shown in Table 22.

Table 22: Observed vs predicted rat pharmacokinetic parameters and simulation using hypothetical BCS class I-like solubility

	Observed PK parameters			PBPK simulated PK Parameters using Caco-2 Permeability				PBPK simulated PK using calculated P _{eff}				AUC and C _{max} ratios (hypothetical BCS class I like solubility to best-fit solubility) from PBPK simulations			
	AUC _{0-24 h}	C _{max}	t _{max}	AUC _{0-24 h}	C _{max}	t _{max}	GER	AUC _{0-24 h}	C _{max}	t _{max}	GER	Caco-2 permeability		Calculated P _{eff}	
	[h*μM]	[μM]	[h]	[h*μM]	[μM]	[h]	[min ⁻¹]	[h*μM]	[μM]	[h]	[min ⁻¹]	AUC _{0-24 h} ratio	C _{max} ratio	AUC _{0-24 h} ratio	C _{max} ratio
Crizotinib	1.348	0.133	4	1.4	0.17	1.84	0.006	1.4	0.17	1.92	0.006	1.0	1.0	1.0	1.0
Dabrafenib (R1) *	9.684	1.11	4	6.87	1.2	2.16	0.005	6.86	1.2	2.24	0.005	1.0	1.0	1.0	1.0
Erlotinib	24.21	1.87	6	19.8	2.15	3.36	0.005	19.7	2.14	3.52	0.005	1.0	1.0	1.0	1.0
Gefitinib	7.969	0.466	6	9.1	0.481	8	0.001	9.19	0.487	7.92	0.001	1.0	1.0	1.0	1.0
Imatinib	31.72	2.57	4	16.8	2.08	2.64	0.006	16.8	2.08	2.72	0.006	1.0	1.0	1.0	1.0
Lapatinib	93.16	7.19	6	permeability too low				192	14.4	5.84	0.0025	n.a.	n.a.	1.0	1.0
M1	0.0175	0.0032	4	0.0152	0.0045	1.1	0.01	0.0152	0.0045	1.06	0.01	1.0	1.0	1.0	1.0
Trametinib	0.0438	0.0026	6	0.0553	0.0030	5.36	0.37	0.0537	0.0023	6.72	0.37	2.3	4.8	2.3	5.6

* The PBPK analysis as only performed for one animal (R1). The second animal (R2) had a fast onset but died 4-6 h after administration and R3 had extremely delayed absorption.

Like in the human PBPK simulations, the effect of solubility on the oral absorption was investigated by simulating the PK metrics with a hypothetical BCS class I-like solubility in the established PBPK models. The ratios of C_{\max} and AUC between increased hypothetical BCS class I-like solubility input to the in vitro solubility input are summarized in

Table 22. The PBPK simulations of all compounds except for trametinib are insensitive to an increase in the input solubility with an AUC or C_{\max} ratio of 1. The exposure and C_{\max} in the trametinib model are increased using the BCS class I solubility, with either the Caco-2 permeability or the calculated P_{eff} by > 2-fold and indicate therefore solubility-limited absorption behavior. This explains also why the simulations are not affected by the delay in gastric emptying, which is only the rate-limiting step for the absorption of readily soluble and permeable drugs. The dabrafenib absorption in the PBPK model was non-solubility-limited for rat 1. Therefore it is likely, that this is generally the case for dabrafenib and could be proven based on further rat PK profiles, where the elimination slope is characterized using time points beyond the absorption phase (unlike in rat), and the actual C_{\max} is better captured than in rat 3, leading to a more representative measured $\text{AUC}_{0-\text{last}}$ (Figure S 2).

As expected according to their high-medium permeability, there is only a minor difference between the simulations using the two different permeability values of imatinib, M1, crizotinib, trametinib, dabrafenib, gefitinib, and erlotinib. In contrast, changing from the moderate calculated P_{eff} to the very low Caco-2 derived value decreases the simulated exposure of lapatinib immensely. Even when increasing the input solubility to the BCS class I level, the simulation using the Caco-2 permeability underestimated the observed PK profile by approximately 40 % and a curve fit cannot be obtained.

4.2.2.4. Dose linearity of exposure in the rat

The information on dose proportionality of exposure in the rat available in the FDA's Clinical Pharmacology and Biopharmaceutics Reviews differ in the dose range tested (including two or more doses), the dosing schemes (i.e. steady state or single dose) and the vehicles used. Single-dose PK is preferred for the discussion of solubility-limited absorption because accumulation and saturation effects at steady state can cover effects observed at a single dose. However, these data are not always published. Vehicle components can increase the solubility (e.g. SDS) or inhibit the precipitation (e.g. HPMC) of the drug, and therefore enhance absorption (156) and result in a different dose-exposure relationship compared to administration of pure API. The exposure of imatinib, trametinib, gefitinib, erlotinib, and lapatinib is reported to be dose-proportional or more than dose-proportional, whereas a less than dose-proportional relationship was reported for crizotinib, dabrafenib, and vemurafenib (Table 23). The data is not available in the rat for pazopanib and M1.

Table 23: Evaluation of the model compounds' dose proportionality of exposure in the rat available the FDA's Pharmacology Reviews. The numbers in brackets represent the reference numbers.

	Dose range tested	Dosing schedule	Formulation/ Vehicle	Increase in exposure
Crizotinib	50-500 mg/kg	steady state (day 7)	no formulation info	less than proportional (157)
Dabrafenib	5 vs. 10 mg/kg	single dose	HPMC suspension	less than proportional (158)
Erlotinib	20 vs. 100 mg/kg	single dose	no formulation info	± proportional (159)
Gefitinib	5 vs. 12.5 mg/kg	single dose	0.5% HPMC in 0.1% Polysorbate 80 for oral dosing	dose proportional (150)
Imatinib	60 → 300 → 750 mg/m ²	steady state	purified water, USP	more than proportional (149)
Lapatinib	2 vs. 10 mg/kg	single dose	no formulation info	more than proportional (96)
M1	not available	not available	not available	not available
Pazopanib	not available	not available	not available	not available
Trametinib	1 → 5 mg/m ²	single dose	i.a. 1.5% HPMC, 5% mannitol 60 and 0.2% SDS	more than proportional (153)
Vemurafenib	30-800 mg/kg crystalline API 30-250 mg/kg co-precipitate	steady state	2% hydroxypropyl cellulose (Klucel LF) in deionized water adjusted to pH 4 (± 0.2) with 1 N HCl	less than proportional (160)

4.2.3. Solubility-limited absorption and food effect in human and rat

4.2.3.1. Identification of solubility-limited exposure and food effect in human

Table 24 summarizes the properties within the biopharmaceutic frameworks (BCS and DCS) coupled with properties/methods used in the analysis (gut bioavailability, PBPK simulations, and dose linearity) for the identification of solubility-limited oral pharmacokinetics in human. Every property/method is color-coded for the drugs selected in this study to distinguish solubility-limited drugs (red) from those that are not (green). On the far right, the food effect for these drugs is also color-coded red or green to distinguish drugs that show a positive food effect from those that do not.

Table 24: Heatmap presenting the properties in the BCS and DCS frameworks along with properties/methods used in the analysis of human pharmacokinetic data (51)

	Dose number (BCS)	SLAD (DCS)	Human gut Bioavailability ($F_a * F_g$)	Human PBPK model sensitive to solubility increase	Dose proportionality in human single-dose PK studies	Food effect
Imatinib	II	I	IIa			
M1	likely IV	likely IV				
Crizotinib	IV	IV				
Gefitinib	II	IIa				
Trametinib	II	IIb				
Dabrafenib	II	IIb				
Erlotinib	II	IIb				
Lapatinib	IV	IV	IV PK data required for the calculation is not available	solubility and/or permeability		
Vemurafenib	IV	IV		solubility and/or permeability		
Pazopanib	II	IIb				

Table 25: Heatmap presenting the dose/solubility relationship in the rat along with properties/methods used in the analysis of rat pharmacokinetic data

	Required volume of FaSSIF to dissolve the dose [mL]	Rat gut Bioavailability ($F_a * F_g$)	% of dose excreted as parent drug in the feces after p.o. vs. IV dosing	Rat PBPK model sensitive to solubility increase	Dose proportionality of exposure in the rat
Imatinib					
M1					not available
Crizotinib					
Gefitinib					
Trametinib					
Dabrafenib					
Erlotinib					
Lapatinib					
Vemurafenib				not available	
Pazopanib				not available	not available

Legend Table 24 and Table 25:

Green - No solubility limitation: Dose number < 1 (BCS I/III), SLAD > clinical dose, required volume of FaSSIF to dissolve the dose for a rat with 0.25 kg body weight is < 2 mL, gut bioavailability > 0.75, % of dose excreted as parent drug in the feces in the rat after p.o. ≤ IV dosing, PBPK model is not sensitive to increase in solubility, dose-proportional or supra proportional increase of AUC and C_{max} in the food effect dose range, absence of positive food effect (AUC and C_{max} fed/fasted ratio ≤ 1)

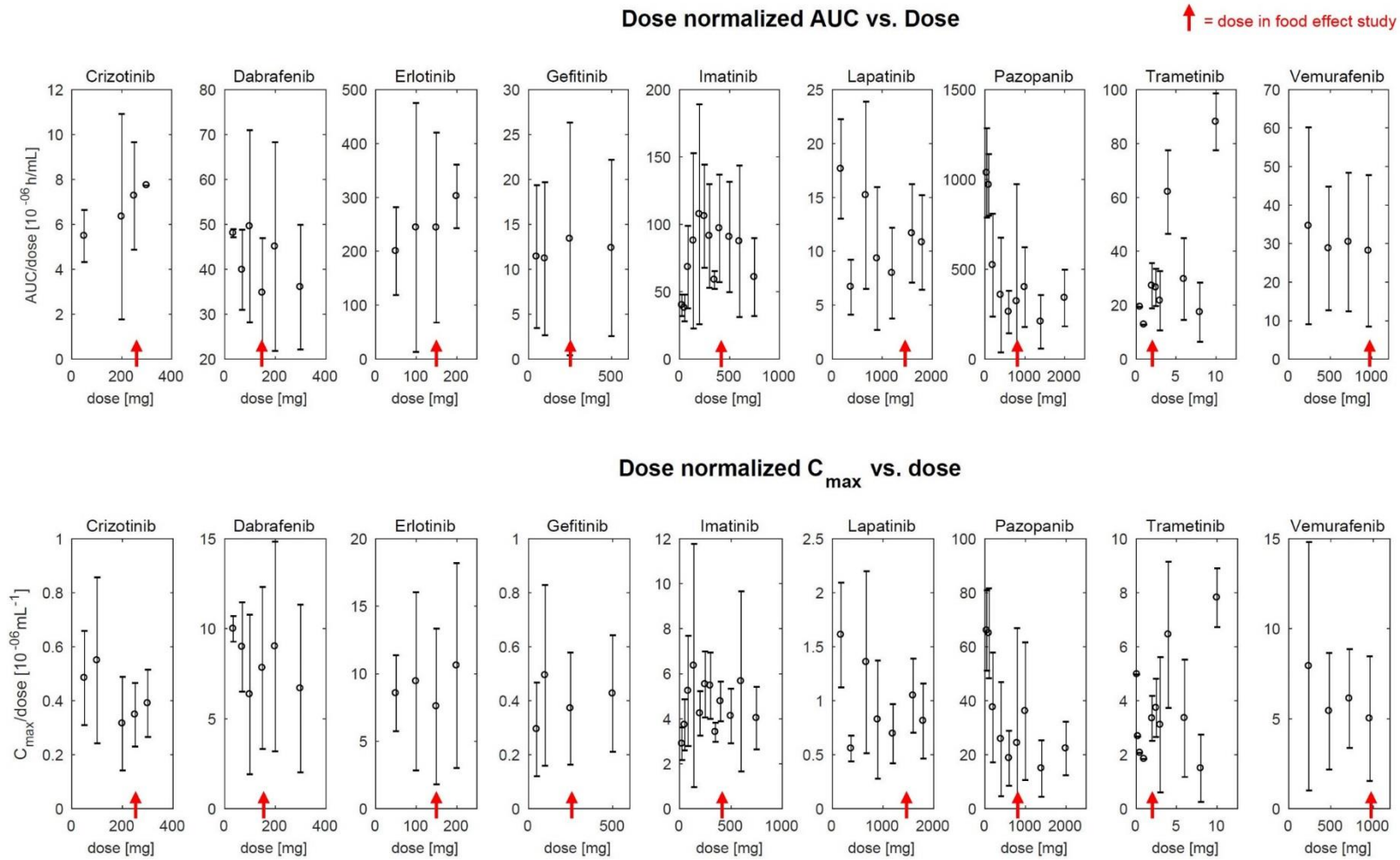
Red – solubility-limited: Dose number > 1 (BCS II/IV), SLAD < clinical dose, required volume of FaSSIF to dissolve the dose for a rat with 0.25 kg body weight is > 2 mL, gut bioavailability < 0.75, % of dose excreted as parent drug in the feces in the rat after p.o. > IV dosing, better exposure in PBPK model using increased input solubility (solubility and/or permeability limitation of vemurafenib and lapatinib absorption is non-identifiable), less than dose proportional increase of AUC and C_{max} , ≥ 2-fold positive food effect

Yellow: The human food effect of gefitinib (approx. 30 % increase in AUC and C_{max} (44)) is confounded by a high inter-subject variability, the human food effect of erlotinib is inconsistent (97 % AUC increase in period 1 and 7 % AUC decrease in period 2 (43)) between the two periods of the 150 mg single dose food effect study; the rat gut bioavailability of gefitinib was estimated between 0.53 and 0.84

BCS classification for regulatory purposes, based on in vitro solubility in aqueous buffers and effective permeability suggests that all model drugs are expected to show solubility-limited exposure. Imatinib could qualify as a BCS class I drug based on the dose number in FaSSIF (Table 18). The less conservative DCS classification for drug development purposes, however, identifies imatinib, M1, crizotinib and gefitinib as drugs having sufficient solubility at their food effect doses for complete oral absorption, which aligns better with the clinical outcomes. The gut bioavailability calculation and PBPK modeling are possible when IV and oral PK data from Phase I clinical studies become available. Both these assessment methods show the same trends regarding solubility-limited absorption for all model drugs except for erlotinib. A reduced gut bioavailability of < 1 indicates an intestinal loss of drug, but it cannot identify the responsible mechanism. Insufficient solubilization, gut first pass metabolism or efflux by intestinal transporters are the possible causes. Hypothesis testing with PBPK analysis can identify insoluble drugs whose poor oral bioavailability is due to the intestinal loss mediated by gut metabolism rather than the poor aqueous solubility, as exemplified earlier by erlotinib (Figure 13). Another advantage of the PBPK approach over the gut bioavailability is that it can be applied even when IV data are not available, provided the oral profile is sufficiently well characterized. Single ascending dose PK can confirm the results from the PBPK analysis to distinguish solubility limitation (less than dose proportional PK) from gut metabolism and efflux (supra dose proportional). However, as pointed out earlier, it is difficult to establish a dose-exposure relationship as the analysis is often challenged by high variability and insufficient dose groups, commonly encountered in oncology drug development (Figure 15). This seems to be the case for the BCS class IV model drugs vemurafenib and lapatinib, where the dose linearity is not in line with the PBPK outcome. The doses of the food effect studies of both these compounds at the upper end of the dose range tested in the dose-escalating studies so that they are not well covered. The solubility-limited exposure of pazopanib was adequately predicted by all assessment methods.

Table 24 shows that the compounds for which the PBPK analysis identified solubility-limited exposure are also those for which a positive food effect was observed. The AUC and C_{max} ratios from the PBPK exercise comparing hypothetical BCS class I-like solubility to best-fit solubility correlate with the extent of observed food effect. This demonstrates that the proposed analysis of clinical PK data can predict the solubilization-driven food effect of drugs identified as solubility-limited.

The type, amount and quality of the available PK data are important to estimate the gut bioavailability and conduct the PBPK analysis, especially for more complicated scenarios. For example, if the elimination is concentration-dependent, it is important that the intravenous and oral PK studies are conducted using a similar plasma concentration range. Alternatively, intravenous administration of a radiolabeled concomitant micro-dose in addition to a clinically relevant orally administered dose could help distinguish between hepatic and intestinal extractions. Although the IV and oral doses in the

Figure 15: Dose proportionality of AUC and C_{\max} in human single-dose PK studies confounded by high inter-subject variability (51)

absolute bioavailability studies were not identical in the absolute bioavailability studies (Table 9), the similar elimination slopes in the log PK profiles (Figure S 1) indicate suitability. The terminal slope of the oral dabrafenib PK simulation is steeper than the observed because it was derived from the observed IV PK that is characterized by a shorter half-life than the oral PK (74). Therefore, prolonged absorption is hypothesized (74). If intravenous administration is not feasible, sufficiently characterized single-dose oral PK profiles with less than 20 % AUC extrapolation, ideally after different doses, are necessary to estimate the elimination parameters. A mass balance study at the clinically relevant dose with quantification of parent drugs in the feces can also provide information about the extent of absorption in form of the unabsorbed amount excreted in the feces. An additional analysis of parent drug in the feces after intravenous administration is required to confirm the absence of biliary excretion. With regards to inter-subject variability in clinical studies, the common design in dose escalation with three to ten subjects per dose group in Phase I studies may not be sufficient to capture the full range of intra- and inter-subject variability (especially for patients with liver or colon carcinoma), as illustrated in Figure 15. In the practice, full PK characterization (e.g. at very high doses or IV) as described might not always be feasible in human, which is why the use of preclinical species is especially interesting.

4.2.3.2. Identification of solubility-limited exposure in the rat

Table 25 presents the combined results of the rat PK analysis in a heatmap equivalent to Table 24 that shows the outcomes in human. The red color-code indicates solubility-limited absorption, while green points to sufficient solubilization in the rat at the dose tested. As there is no BCS-equivalent classification system in the rat, the required volume of FaSSIF to dissolve the dose for a 0.25 kg animal was calculated. A physiological water content in the rat GI in the fasted state of 3.2 ± 1.8 mL and 7.8 ± 1.5 mL in the fed state was found by McConnell et al. (161) and a stomach volume of 0.2 mL fasted and 1.3 mL fed was reported in (162). Therefore, the cut-off volume < 2 mL for the green color code indicating non-solubility-limited absorption was chosen. Only the selected doses of crizotinib, M1 and imatinib, can be dissolved in this volume of FaSSIF in vitro so that this parameter indicates solubility-limited absorption for all other model drugs at their doses. Like in human, the calculated gut bioavailability is less conservative than the classification based on in vitro solubility, but as already discussed in 4.2.3.1, it cannot distinguish between a loss of drug through gut first pass or solubility-limitation. The amount of parent drug excreted in feces the after IV and oral administration was quantified in this study to support this distinction. If the percentage of the recovered dose in the feces is greater after oral administration than after IV, it is possibly due to unabsorbed or effluxed material. This was the case for trametinib, vemurafenib and pazopanib. However, full quantification and mass balancing cannot be assured with this study design, which is why solubility-limited absorption can still not be excluded with certainty for erlotinib and lapatinib, as well as gefitinib that has uncertain gut

bioavailability between 0.53 and 0.84. As described for the human PK analysis, the proposed PBPK approach can identify solubility-limited absorption as the cause of an intestinal drug loss. If the AUC and C_{\max} simulated with hypothetically high solubility of BCS class I standard are not significantly higher than the observed, the drug loss is likely caused by gut metabolism or efflux, which seems to be the case for erlotinib, lapatinib and gefitinib (if any). Rat PBPK modeling of pazopanib and vemurafenib were not possible due to the very low observed clearance. However, the PK was sufficiently characterized in the rat to conclude solubility-limited absorption (reduced gut bioavailability and higher percentage of dose as parent in the feces compared to IV). The dose-exposure relationship in the rat was assumed to comply with the results from the PBPK analysis to confirm solubility-limited (less than dose proportional PK) or non-solubility-limited (proportional or more than dose proportional increases in exposure) absorption. For all compounds except for lapatinib, the lowest dose of the dose range tested was higher than the dose in the rat PK study within this research. This suggests non-solubility-limited absorption of imatinib, gefitinib, and erlotinib even at higher doses than tested in this research and explains the apparent contradiction with the PBPK results in the cases of crizotinib and dabrafenib. However, certain vehicle components can enhance the solubility and promote dose-linear absorption, which might be the case for trametinib, where the current PK analysis suggests solubility-limited absorption from the API in capsules but supra-proportional PK in the rat is reported in the literature (153).

To summarize, the proposed approach to analyze rat PK data (based on gut bioavailability, percentage of dose as parent in the feces after oral compared to IV administration, PBPK analysis and dose-linearity of exposure) identifies solubility-limited absorption in the rat for trametinib, pazopanib, and vemurafenib from capsules filled with API of the clinically relevant salt form at the body weight-scaled human food effect study doses. Non-solubility-limited absorption behavior was identified for imatinib, M1, crizotinib, dabrafenib, gefitinib, erlotinib, and lapatinib in the same setting. As the rat is not a common model to test the effect of food on the oral dosage forms of drugs (12), the food effect is only discussed in human in this work.

4.2.3.3. The rat as a model for solubility-limited exposure in human and its use in drug development

The rat as a model for human absorption has been extensively studied and intestinal permeability in the rat and intestinal permeability or fraction absorbed in human were found to correlate by different groups (163). However, the levels of enzyme expression and systemic as well as gut metabolism differ in human and rat (163, 164), which is why the rat is not necessarily a good model to predict human bioavailability. In this research, the rat PK data was processed to identify the extent of and solubility-impact on the absorption.

The proposed analysis of pharmacokinetic data using PBPK modeling identifies the same solubility or non-solubility-limited absorption behavior in human and rat at body-weight equivalent doses for imatinib, M1, crizotinib, dabrafenib, gefitinib, erlotinib, vemurafenib, and pazopanib (8 of 10 compounds). While the human PK was generated by different (in some cases solubility-optimized) formulations, the rat PK analysis was based on pure API in capsules. In this setting, trametinib showed solubility-limited absorption behavior in the rat, but not in human. As the human formulation (Mekinist®) contains SDS (90), a potential solubility-limited absorption behavior of the pure API might be overcome by the formulation and the possibility for a positive food effect ruled out. However, the example of vemurafenib shows that even after optimizing the formulation, the absorption can still be solubility-limited.

Lapatinib is the only model drug, where the results regarding solubility-limited absorption are not in line in human and rat, and cannot be explained by the different formulations. The high sensitivity of its solubility to the bile salt concentration might be the cause for the misprediction of the rat, as it is a species with higher bile flow rate (165) and intestinal bile salt concentrations (166, 167) compared to human or dog. The difference in the model drugs' solubility in the presence and absence of taurocholate and lecithin is presented in (Figure 8 and Table 15). With 87-fold solubility difference in regular FaSSIF and the FaSSIF blank buffer, it is the most TC/ lecithin-sensitive of the included drugs. Vemurafenib solubility is also quite sensitive but the FaSSIF solubility is still very low compared to its dose. The gefitinib solubility in both FaSSIF and FaSSIF blank is generally higher, while the dose is lower so that the better bile salt mediated solubilization is less critical for absorption and might not create a difference in rat and human absorption.

A quantitative comparison of rat and human "in vivo solubility" derived from best-fit PBPK simulations was unfortunately not possible in our study due to the capsule-induced delay in gastric emptying in the rat, rendering the best-fit solubility.

To summarize, the analysis of early human PK data demonstrates that deconvolution of key mechanisms driving intestinal loss with PBPK analysis reliably identifies poorly water-soluble drugs whose oral absorption is truly solubility-limited and are therefore likely to show a positive food effect. The analog analysis based on rat PK, which is available earlier on in discovery and can be studied more extensively (e.g. higher dose range, IV testing almost always possible), delivered the same outcomes for 8 out of 10 examined oral anticancer drugs. The rat PK analysis can identify drugs where solubility-optimized formulations might increase the absorption or even mitigate a positive food effect in human. This suggests, that this approach to analyze preclinical and early clinical data can be considered to guide decisions in formulation development, on conducting food interaction studies or to negotiate study waivers with the regulatory agencies for drugs beyond the BCS class I. The rat PK study in this

research was performed in capsules to monitor the performance of the API in a solid dosage form, free of excipient/ formulation effects, at the relevant dose to predict the human food effects of the model drugs reported in the literature. However, the analysis can also be performed based on the data that is routinely generated in drug discovery.

4.3. Predicting the food effect on drug exposure using GastroPlus®

4.3.1. Target fraction absorbed and input gut first pass for the model drugs

PBPK models for the use of prospective predictions of untested clinical scenarios need to be mechanistically correct. To allow this, the fraction absorbed (F_a) and the fraction metabolized in the gut (F_g) are identified in the first step of the developed workflow (Figure 6). As these fractions cannot be measured directly, the assessment is based on available clinical PK data and top-down PBPK analysis, as described in 3.6. The combination of bottom-up and top-down PBPK approaches is not new (168-170). However, its use for the quantification of F_a and F_g has not been previously reported to improve PBPK food effect predictions. The results are presented in Table 26.

Crizotinib, gefitinib, imatinib, M1, dabrafenib, and trametinib have been identified as drugs with non-solubility-limited absorption at the dose of their food effect studies by an analysis of available clinical PK data (4.2.3). The presence of gut metabolism for these drugs could be excluded, as the gut bioavailability is high (> 0.75). The amount of unmetabolized drug recovered in the feces can be attributed to biliary excreted drug, as it was mainly collected after more than 24 h. Therefore, a fraction absorbed of one was targeted in the GastroPlus® PBPK models and no gut first-pass metabolism was implemented (Table 26). Pazopanib and erlotinib were found to have reduced gut bioavailability, which was attributed to gut first-pass metabolism in the case of erlotinib and poor absorption in the case of pazopanib (4.2.3). This is supported by the fact that 67.3 % of unmetabolized radiolabeled pazopanib was recovered in the feces (the majority of radioactivity was recovered < 48 h) (84), but only 1 % of erlotinib parent drug (145). Therefore, it was assumed that the fraction absorbed of pazopanib equals the calculated gut bioavailability of 0.21 and the fraction absorbed of 1 was targeted for erlotinib, while 39 % gut first-pass metabolism was implemented in the PBPK model (Table 26).

In the absence of IV PK data for lapatinib and vemurafenib, the fraction absorbed can only be roughly estimated. In the case of vemurafenib, a radiolabeled mass balance study at the same dose like the food effect study is available. It reports 38 % excretion of vemurafenib parent drug in the feces, which might be partially biliary excreted and partially unabsorbed (171). However, food increases the vemurafenib exposure by approximately 5-fold (46). This is likely to be solubility mediated, as the vemurafenib half-life is very long 71.7 h (171). Any inhibiting effects of the food on elimination and metabolism might therefore have only limited effect on the overall exposure. The vemurafenib fraction

absorbed was estimated with 0.2 (Table 26) based on the food effect. As the mass balance study of lapatinib was performed at a 6-times lower dose than the relevant dose in the food effect study, only limited conclusions can be drawn. 27 % of the dose were recovered as parent drug in the feces at 250 mg (146), but the unabsorbed amount of drug after intake of 1500 mg could be even higher. Therefore, the fraction absorbed was estimated as 0.25 based on the approximately 4-fold food effect on lapatinib exposure (82) (Table 26). This procedure is of course not feasible in the absence of a clinical food effect study and highlights again the importance of good PK characterization that enables mechanistic insights to the human PK. As already pointed out earlier (4.2.3), IV PK characterization is particularly essential. For both, lapatinib and vemurafenib, the extent of gut first-pass metabolism cannot be estimated based on the available data.

Estimating the fraction absorbed and extent of gut first-pass metabolism supports building PBPK models closer to the in vivo situation. In addition to the observed plasma concentration time profile, it provides information on the target condition.

Table 26: Target fraction absorbed and input gut first pass for the GastroPlus® models. The numbers in brackets represent the reference numbers.

Compound	F _a *F _g	F _a *F _g @ dose [mg]	% dose parent drug in feces	parent in feces @ dose [mg]	Gut first pass reported	CYP3A4 metabolism	Target F _a	Input % gut first pass
Crizotinib	0.9	250	53 (172)	250	no	yes (72)	1	0
Dabrafenib	1	150	21.8 (173)	95	no	yes (76)	1	0
Erlotinib	0.61	150	1 (145)	100	yes (145)	yes (145)	1	39
Gefitinib	1	250	12.1 (174)	50	yes (175)	yes (176)	1	0
Imatinib	1	400	23 (177)	200	no	yes (81)	1	0
Lapatinib	not available	1500	27 (146)	250	yes (82)	yes (83)	estimated 0.25 ^b	n.a.
M1	0.86	500			no	yes	1	0
Pazopanib	0.21	800	67.3 (84)	400	no	yes (87)	0.21	0
Trametinib	0.75	2	27.4; 45.0 (178) ^a	2	no	no (90)	1	0
Vemurafenib	not available	960	55 (171)	960	no	5% (179) (minor contribution)	estimated 0.2 ^b	n.a.

^a individual data of the two patients in this study. Due to poor total dose recovery, the fraction of parent dose recovered in the feces is given as % of the excreted dose

^b in the absence of IV PK data, the fraction absorbed was estimated based on the food effect on AUC

4.3.2. Bottom-up oral PK prediction, model optimization and verification

4.3.2.1. Bottom-up oral PK prediction

After fitting the compartmental PK parameters to the IV PK data, the oral bottom-up predictions were performed. The anticipated target fraction absorbed (Table 26) was achieved in the bottom-up

predicted models of the compounds crizotinib as well as imatinib and was adequately approached by M1 with 89.4 % (Table 27). Imatinib AUC and C_{max} were predicted within the predefined limit of 1.5-fold of the observed values (Table 28). There was no need for further model optimization to reproduce the observed plasma concentration-time profile in the fasted state. Despite the accurate prediction of crizotinib and M1 fraction absorbed, the crizotinib C_{max} and M1 C_{max} as well as AUC were not well captured. The models required further optimization. The other model drugs' anticipated target fraction absorbed was underpredicted (Table 27). Underperformance of simulations from poorly soluble compounds was previously reported in the literature and attributed to an over-sensitivity to the low aqueous solubility (180) or fixed by adjusting the precipitation time (168).

Table 27: PBPK models with absorption related compound characteristics in the bottom-up oral PK prediction and their changes during model optimization

Model Name	Particle size (μm)	Precipitation time (s)	Bile salt Solubilization Ratio	Gut first pass (%)	Other	Fraction absorbed (%)
Crizotinib bottom up	25	900	0	0	-	100
Dabrafenib bottom up	25	900	16,200	0	-	9.8
Dabrafenib Opt 1	2.5	1,000,000	0	0	Reference solubility*10	99.9
Erlotinib bottom up	25	900	36,400	39	-	33.7
Gefitinib bottom up	25	900	473,000	0	-	48.7
Gefitinib Opt 1	25	1,000,000	473,000	0	-	99.6
Gefitinib Opt 2	25	900	4,830,000	0	-	93.6
Imatinib bottom up	25	900	6062,1	0	-	100
Lapatinib bottom up	25	900	2,040,000	0	-	0.7
M1 bottom up	6.2	900	140,000	0	-	89.4
Pazopanib bottom up	25	900	32,900	0	-	5.4
Pazopanib Opt 1	25	1,000,000	32,900	0	-	17.8
Pazopanib Opt 2	2.5	1,000,000	32,900	0	-	30.2
Trametinib bottom up	25	900	71,800	0	-	3.0
Trametinib Opt 1	2.5	900	68,500	0	Reference solubility*10	100
Vemurafenib bottom up	25	900	2,860,000	0	-	3.3
Vemurafenib Opt 1	1	900	2,860,000	58	-	15.9
Vemurafenib Opt 2	25	900	22,900,000	58	-	18.5

Table 28: Acceptance criteria in the verification simulations (fold of the observed value). The references for the studies considered are given in Table 11.

Compound	Food effect study	Higher/lower dose	ARA study
Crizotinib	1.5	2	not available
Dabrafenib	1.5	2	not available
Erlotinib	2	3	single dose not available ^c
Gefitinib	2	2	2
Imatinib	1.5	1.5	1.5
Lapatinib	no variability information ^a	2 ^b	single dose not available ^c
M1			not available
Pazopanib	1.5	3	single dose not available ^c
Trametinib	1.5	1.5	not available
Vemurafenib	2	2	not available

^a No information in the variability was given in the reference presenting the food effect study, the same criterion as for the lower/higher dose was applied

^b The coefficient of variation (CV%) was not given in the reference presenting the dose escalation, but the parameters AUC and C_{max} were in a range of approximately 2-fold.

^c Single dose ARA (acid-reducing agents) study was not available, therefore the simulations were verified using the 90 % confidence interval of AUC and C_{max} ratios without ARA to with ARA

Initially, the idea was to use measured in vitro dissolution data in GastroPlus[®]. For the IR formulations of the model drugs, the use of the Z-Factor dissolution model is appropriate. However, the measured dissolution data did not seem to represent the in vivo release well (4.1.3), especially for M1 with very pronounced coning effects, even with 100 rpm paddle speed. Z-Factors were fitted to the different release profiles of gefitinib, erlotinib, pazopanib, and vemurafenib and applied in the bottom-up PBPK simulations. However, the bottom-up underprediction of erlotinib and pazopanib was not fixed by using the z-Factor - not even in the case of gefitinib, where the release is extremely fast (Figure 9). Only the simulated vemurafenib exposure was massively increased, but the observed AUC was overpredicted by approximately 3-fold.

Although there are successful reports about the use of in vitro dissolution data in GastroPlus[®] (181) or other PBPK models (40) in the literature, the present study indicates that it does not generally improve the simulation performance. It might require testing of various dissolution conditions (or even fitting of the dissolution data to the observed PK (182)) until the data contributes to the simulation of the desired results. However, the verification and justification of such an approach might be questionable.

4.3.2.2. Optimization of the bottom-up PBPK models

The aim of the model optimization procedure was to identify the parameters responsible for the misfit of the bottom-up PBPK simulations. The parameters to be adjusted were selected based on their reliability. The underprediction of the observed PK appears to be based on the parameters determining the solubilization in the models. This phenomenon was also observed in the top-down PBPK approach (4.2.1.2). Therefore, the solubilization-related parameters were included in the PSA.

API micronization is often used to increase the oral bioavailability of poorly soluble drugs via an accelerated dissolution rate through increasing the available surface area. Common milling techniques are capable of generating mean particle sizes of $< 10 \mu\text{m}$, with individual particles of $2\text{-}5 \mu\text{m}$ (156). Therefore, the lower limit for particle radius in the PSA of $2.5 \mu\text{m}$ was chosen. The default value of 900 s precipitation time was used in the bottom-up simulations, as there is no recognized common method available to identify it in human. The full range of precipitation time (up to the maximum possible value of 1,000,000 s) in GastroPlus® was tested in the PSA. The variability of human intestinal fluid (HIF) solubility and the differences in HIF and simulated intestinal fluids (SIF) solubility in fasted and fed state have been investigated by different groups. The results of these intestinal solubility tests in different media were often within a range of 2-fold, but in some cases, 6-20-fold variation was observed. (30, 119). Therefore, the bile salt solubilization ratio was increased based on the assumption that FaSSIF and FeSSIF solubility might vary up to 10-fold in vivo. The reference solubility was tested within the default range suggested by the software, which is 10-fold variation of the initial value.

The model optimization process is exemplified by the case of pazopanib (Figure 16). The results of the PSA identify the sensitive parameters to be optimized. The pazopanib bottom up PBPK model (with fraction absorbed of 5.4 %) is especially sensitive to an increase in precipitation time and reference solubility, followed by a decrease in particle size. As illustrated in Figure 16, a fraction absorbed of approximately 18 %, which is close to the target fraction absorbed, can be achieved when increasing

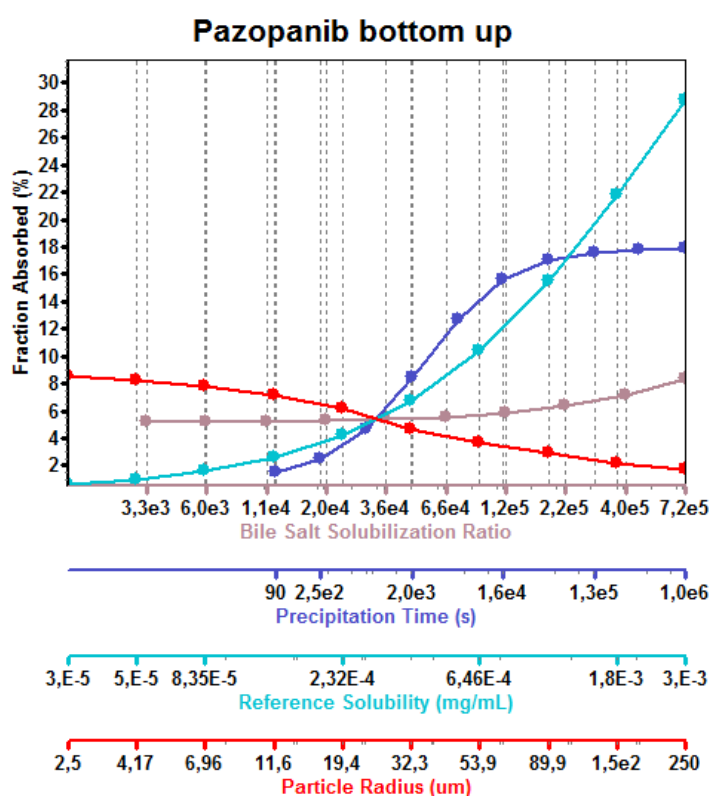


Figure 16: PSA of the fraction absorbed to optimize the bottom-up predicted pazopanib model in the fasted state

the precipitation time to the maximum of 1,000,000 s. Therefore, this setting was used to build the optimized model, “Pazopanib Opt 1” (Table 27). Decreasing the particle size to 2.5 μm in addition, results in a fraction absorbed of 0.30 in the model “Pazopanib Opt 2” (Table 27) and an even better fit to the observed plasma concentration-time profile. The reference solubility remained unchanged, as it is the parameter with the highest confidence among the ones tested in the PSA.

An overview of the bottom-up predicted as well as optimized models of all model drugs is provided in Table 27, along the parameters that have been adjusted to build these models. Besides the pazopanib bottom-up model, the bottom-up model of gefitinib was especially sensitive to an increase in precipitation time, which led to “Gefitinib Opt 1”. The gefitinib model was also sensitive to an increase in bile salt solubilization ratio, resulting in “Gefitinib Opt 2”. The vemurafenib bottom up PK simulation provided a good AUC prediction but a delayed and underpredicted C_{max} . To optimize this model, the particle size was decreased to 1 μm in “Vemurafenib Opt 1”, as its market formulation contains amorphous vemurafenib coprecipitate. There are no actual API particles whose size could be absorption-limiting. In the model “Vemurafenib Opt 2”, the bile salt solubilization ratio was increased, as the bottom-up model was sensitive to this parameter as well. Both, decreasing the particle size and increasing the bile salt solubilization ratio, led to an increased predicted C_{max} of vemurafenib as desired - but at the same time to an AUC increase, which is overcome by introducing gut first pass metabolism to “Vemurafenib Opt 1” and “Vemurafenib Opt 2”. Optimization of particle size, precipitation time and bile salt solubilization ratio alone each or in combination was not sufficient to enable complete absorption of dabrafenib and trametinib in the PBPK models. Therefore, the reference solubility of these compounds had to be increased in addition. The crizotinib AUC bottom-up prediction was good and the underprediction of C_{max} and early t_{max} was overcome by increasing the stomach transit time to 2 h. This is analog to the previous top-down PBPK analysis (4.2.1.2).

If there are different possibilities to simulate the fasted state exposure adequately and no way to further validate them on a mechanistic basis (like in the cases of gefitinib, pazopanib, and vemurafenib), it is necessary to consider all possible input parameter combinations for the food effect predictions. In the cases of erlotinib and lapatinib, there is the need to change the particle size, precipitation time and bile salt solubilization ratio at the same time to reproduce the observed plasma concentration-time profiles. Optimizing one factor alone or two factors in combination cannot account for the observed PK. This results in numerous possible fasted state models and the proposed workflow is therefore not applicable to these compounds in the practice.

The fraction absorbed of M1 was accurately predicted by the bottom-up PBPK model, however, C_{max} and AUC were over-predicted. M1 simulated t_{max} was too early. The PSA to optimize the M1 model did

not provide improvements that reduce C_{\max} and AUC without reducing the fraction absorbed. Therefore, the proposed workflow is not applicable to M1.

For low permeability drugs, the effective permeability is usually also included in a PSA. However, all model compounds in this work except for lapatinib and vemurafenib exhibit high permeability. For those BCS class II drugs, low sensitivity to changes in permeability is anticipated, and was confirmed by the top-down PBPK analysis (4.2.1.2). Therefore, the effective permeability for vemurafenib and lapatinib is discussed separately. Changes in P_{eff} within a 2-fold range (GastroPlus® default in the PSA module), affects the bottom-up predicted fraction absorbed of both lapatinib and vemurafenib less pronounced than the solubility related parameters (only + 0.6 % in fraction absorbed of lapatinib and + 4.4 % for vemurafenib). Moreover, an increase in permeability is associated with a simultaneous AUC and C_{\max} increase, which is why changing the permeability does not overcome the challenges related to optimizing the vemurafenib PBPK model (i.e. increasing the C_{\max} without increasing the AUC). In the case of lapatinib, additional variation of the permeability would have increased the number of possible models even more.

Besides the parameters that can be covered by the PSA, the extent of gut first pass metabolism (if not evident from clinical PK data) needs to be considered and adapted during the model optimization. To this aim, several models with different extent of gut first-pass metabolism were built. However, this can eventually result in a large number of models with different input parameter combinations but similar PK. In the case of lapatinib, this circumstance hinders the practical application of the entire suggested procedure for food effect predictions. The input gut first-pass metabolism for vemurafenib of 58 % was chosen, as it reduces the AUC overprediction to comply with the anticipated acceptance range of vemurafenib simulations of 2-fold (Table 28) after the C_{\max} was improved. 58 % of gut first pass metabolism is a very high estimate for a low clearance compound like vemurafenib. However, considering the low fraction absorbed, the absolute amount of dose involved is low (\ll 58 % of the total dose). Higher concentrations in the intestine than in the liver and different enzyme expression could contribute to quantitative differences in hepatic and intestinal metabolism.

In general, the bottom-up predicted PBPK models of most model drugs could be optimized by adjusting the input parameters with low confidence. Thereby, modulation of the precipitation time was particularly important. It was increased for all three weakly basic drugs, whose bottom-up model needed optimization (dabrafenib, gefitinib, pazopanib). However, no general conclusions on the model optimization can be drawn based on the limited number of 10 model drugs.

4.3.2.3. Verification of the optimized PBPK models

Model verification is important to increase the confidence in the simulations. To verify the absorption model, different simulation exercises of clinical situations, that were not used to build the PBPK models, were performed as described (lower dose, higher dose, and acid reduced conditions). If a previous food effect study of this drug is available, the model should be verified against this data as well (62).

The simulations were performed according to the available data. The limits of acceptance for the verification simulations, based on inter and intra-study variability (CV %), were 1.5-fold or 2-fold of the observed value in most cases (Table 28). All optimized models, except for the “Trametinib Opt 1” did not fail in more than 1 verification simulation (Table S 14). When there were two optimized models of the same compound, the performance in the verification simulations was similar.

Even though, the verification exercise did not identify the best model, it is still recommended to challenge the models to find out for what purposes they might be valid. For example, in the case of trametinib, where “Trametinib Opt 1” underpredicted the PK at the lower dose (0.5 mg) and overpredicted the PK at the higher dose (10 mg) by more than 1.5-fold, the absorption model enabled a fraction absorbed of 100 % at both doses. The AUC and C_{max} mispredictions are apparently caused by non-linear systemic PK, and the model might still be used for absorption related predictions. However, it should be acknowledged, that simulating the fed state, is a more complex scenario than the ones tested in the verification simulations.

4.3.3. Predicting the effect of food on the model compounds' exposure

4.3.3.1. Food effect prediction using different fed state physiologies

The effect of food on the simulated PK in the optimized models was first tested using the default Human-Physiological-Fed physiology (Table S 10). However, this is only one possible constellation of parameters. In vivo, the GI physiology in the fed state is highly dynamic and variable. For example, gastric pH values of > pH 5 change to pH 1 and lesser directly after the meal (100). Gastric transit times of 4.3 h - 20.2 h (100) and 69 min - 583 min (with a mean of 308 min) (183) have been reported, and highly variable bile salt concentrations of 0.74 mM - 86.14 mM in the fed state have been observed in HIF of healthy volunteers (184).

The fed stomach physiology reported by Koziolk et al. (100) was translated into an alternative stomach physiology for the application in PBPK food effect predictions to test the impact of the physiology. This alternative fed stomach physiology is more dynamic than in the default Human-Physiological-Fed physiology. It covers the reacidification of the stomach pH after the meal intake and uses a longer stomach transit time of 4.5 h. The predicted food effects using the different fed stomach

physiologies are compared in Table 29, along with the 90 % confidence intervals of the observed AUC and C_{\max} fed/fasted ratios determined in the clinical food effect studies. When two models of one compound were available, the predicted AUC or C_{\max} fed/ fasted ratio is presented in the form of a range between these two values.

Table 29: Food effect prediction using the default Human-Physiological-Fed physiology and fed stomach physiology derived from Koziolk et al. (100). The numbers in brackets represent the reference numbers. AUC ratio (90% CI) - 90 % confidence interval of the AUC fed/fasted ratio, C_{\max} ratio (90% CI) - 90 % confidence interval of the C_{\max} fed/fasted ratio

	<u>Observed Food effect</u>				<u>Predicted food effect using Human-Physiological-Fed physiology</u>		<u>Predicted food effect using a fed stomach physiology derived from Koziolk et al. (100)</u>	
	AUC ratio (90% CI)	C_{\max} ratio (90% CI)	t_{\max} fasted [h]	t_{\max} fed [h]	AUC ratio	C_{\max} ratio	AUC ratio	C_{\max} ratio
Crizotinib	0.789-0.933 (71)	0.779-0.954 (71)	5 (71)	5 (71)	1.00 ^a	0.78 ^a	1.00 ^a	0.39 ^a
Dabrafenib	0.57-0.85 (140)	0.35-0.69 (140)	2 (140)	6 (140)	1	0.69	1	0.46
Gefitinib	1.239-1.508 (44)	1.16-1.498 (44)	5 (44)	5 (44)	1.00-1.00	0.90-0.93	1.00-1.04	0.58-0.61
Imatinib	0.89 ^b (144)	0.93 ^b (144)	not available	1.5 h later than fasted (144)	1	1	1	0.43
Pazopanib	1.64-3.35 (45)	1.51-2.98 (45)	4 (45)	6 (45)	0.08-0.35	0.06-0.24	2.23-3.09	1.46-2.00
Trametinib	0.697-0.828 ^c (141)	0.243-0.371 (141)	1.5 (141)	4.03 (141)	1.00 ^{c,d}	0.77 ^d	0.98 ^{c,d}	0.34 ^d
Vemurafenib	2.8-8.0 (46)	1.8-3.4 (46)	4 (46)	8 (46)	1.92-5.13	1.91-5.70	2.01-5.30	1.80-5.26

^a AUC and C_{\max} fed/fasted ratio was calculated for the crizotinib bottom-up prediction without prolonged stomach transit time, as the stomach transit time in the Human-Physiological-Fed physiology of 1 h would be otherwise shorter than in the fasted state simulation with 2 h stomach transit time to reproduce the C_{\max} appropriately, and lead to distortion of the ratio

^b 90% CI not available

^c AUC₀₋₁₆₈

^d the predefined acceptance criteria in the verification simulations (4.3.2.3) were not met by this model

The Human-Physiological-Fed physiology provides prediction of the AUC fed/fasted ratio within or close to 90% CI in the clinical studies of all compounds except for pazopanib, where a strong negative food effect was predicted, but a strong positive food effect observed (Table 29). Moreover, it provides predictions of the food effect on the C_{max} within or close to the 90% CI in the clinical studies for all compounds except for pazopanib (like the AUC prediction) and trametinib, where the negative effect on C_{max} is not captured.

The fed stomach physiology derived from Koziolk et al. (100) provides a good food effect prediction on the AUC of all model drugs. Using this physiology, the strong positive food effect on pazopanib AUC and C_{max} is adequately simulated. The fed state C_{max} prediction is improved for dabrafenib and trametinib with a negative food effect on C_{max} . However, a negative food effect on crizotinib, gefitinib, and imatinib C_{max} is falsely predicted using the alternative fed stomach physiology.

The fact that different physiologies are required to get a good food effect prediction might be related to the study design. Gastric emptying rate is a function of the caloric content of the meal (185). The emptying process of the drug depends on its distribution within the stomach and the mixing with the food, which is related to the relative timing of the food and dosage form intake. Effective gastric mixing is assumed to take primarily place in the distal part of the stomach (5). Therefore, gastric emptying of the drug might be more delayed, when taking the drug after full completion of the meal, compared to an earlier intake. Exact information on the relative timing of the food and drug intake is not reported for all studies. However, the following example shows that the timing of drug and food intake might not be the only explanation why different physiologies are required to get a good food effect prediction. Crizotinib was administered 30 minutes after starting the meal (71) and trametinib within 5 minutes after completion of the meal (141), which might be equivalent. However, the Human-Physiological-Fed physiology provided the better prediction for crizotinib, whereas the fed stomach physiology derived from Koziolk et al. (100) was superior in the case of trametinib. In this research, food effect studies with a standardized high-fat meal were selected for all model drugs (for imatinib, the meal type is not clarified in (144)). Therefore, the meal type might not be responsible for the differences. Further differences can come from the concomitant fluid intake or the position of the dosage form in the stomach with regard to the so called "Magenstrasse" (186) for accelerated gastric emptying of liquids.

The superiority of one of the two applied fed state physiologies cannot be confirmed. Therefore, it is recommended to simulate the fed state PK with both physiologies and consider all eventualities.

When the food effect was simulated with two different fasted state models in this work (in the cases of gefitinib, pazopanib, and vemurafenib), the results using the two models were similar. Therefore,

the better way to optimize the bottom-up predicted fasted state models cannot be derived retrospectively, after the food effect simulations.

When it comes to the differentiation of negative food effect and absence of food effect (for completely absorbed drugs in the fasted state), it is noteworthy that the model drugs with relatively late t_{\max} in the fasted state have similar t_{\max} in the fed state (e.g. crizotinib, gefitinib, imatinib). Therefore, these drugs show similar C_{\max} with and without concomitant meal intake. In the cases of trametinib and dabrafenib with early fasted state t_{\max} , in contrast, the fed state t_{\max} is significantly delayed leading to a negative food effect on the C_{\max} (Table 29). This might be related to the stomach transit time, which is discussed in the following section 4.3.3.2.

4.3.3.2. Food-PSA

To further investigate the impact of the multiple parameters that change in the presence of food, the Food-PSA of the absorption relevant parameters provides information on the impact of each factor separately. It helps to understand the food effect simulation outcome and the observed food effect in vivo. Moreover, the Food-PSA can identify the critical parameters responsible for good or misleading food effect predictions within this research.

As previously described, the stomach pH, stomach transit time and intestinal bile salt concentrations are among the highly variable properties in the fed state GI. Therefore, they were selected as variables for the Food-PSA (Table 14). The upper limit for the stomach pH of pH 5 was chosen according to (100). A stomach transit time in the upper middle range of 6 h was chosen as the maximum value of the PSA. Technically, the bile salt solubilization ratio is not a physiological parameter that changes in the presence of food. It was varied in the Food-PSA by 10-fold to investigate whether it can be used as a surrogate for testing different levels of intestinal bile salt concentrations (which is more complex).

The Food-PSA is exemplified by the models Pazopanib Opt 1 (AUC) (Figure 17) and Dabrafenib Opt 1 (C_{\max}) (Figure 18) to illustrate the causes of the inconsistent food effect predictions using the different physiologies (default Human-Physiological-Fed physiology vs. fed stomach physiology derived from Koziol et al. (100)).

The model Pazopanib Opt 1 suggests that the observed absorption-related positive effect of food on pazopanib AUC (45) is caused by the prolonged stomach residence time rather than better bile salt solubilization. Although the solubility of pazopanib HCl increases when sodium taurocholate and lecithin are added to the buffer, it is still very low (even in FeSSIF with 5 $\mu\text{g}/\text{mL}$) (Figure 8). The buffer pH, however, has a stronger effect of on pazopanib solubility than the bile salt/ lecithin concentration. Pazopanib solubility increases by several orders of magnitude when in decreasing the pH from pH 6.5 (solubility 0.3 $\mu\text{g}/\text{mL}$) to pH 1.6 (solubility 1 mg/mL) (Figure 7). Therefore, the increased residence time

in the stomach with lower pH than the intestine (as it is reacidified) enhances the solubilization of pazopanib. As a BCS II high permeability drug (87), the dissolved pazopanib is directly absorbed after its emptying into the duodenum. Moreover, the Food-PSA reveals the cause for the poor food effect prediction of pazopanib using the Human-Physiological-Fed physiology: In the model, the negative effect of the increased gastric pH on pazopanib AUC overrules the positive effect of the prolonged stomach transit time. In Figure 17, the small increase in simulated AUC following a stomach pH increase to pH 3 is caused by the pK_a -fitted solubility profile. It allows slightly better solubility as the pH increases beyond the basic pK_a value of 2.1 (87) before it is reduced again when approaching the basic pK_a value of 6.4 (87). Since pazopanib solubility is extremely pH dependent and its absorption depends strongly on the solubilization in the stomach, the positive food effect can only be simulated when gastric reacidification and a reasonably long fed state gastric emptying time are implemented in the fed state physiology.

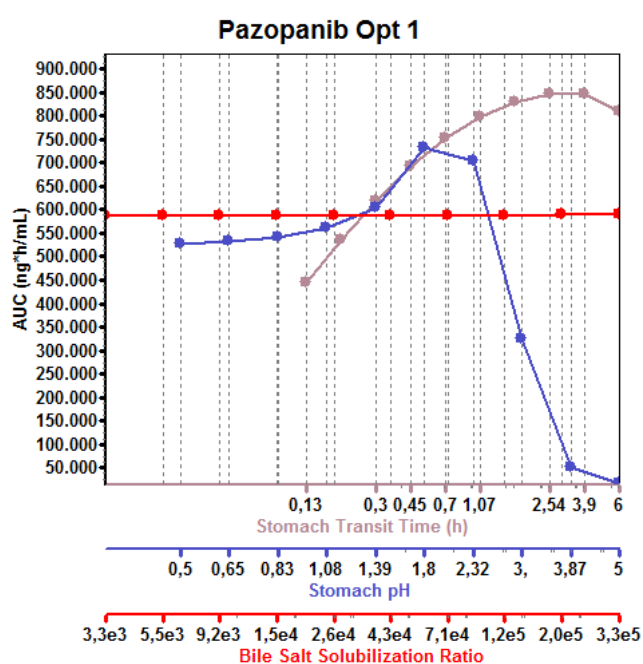


Figure 17: The impact of the physiological changes in the presence of food on the simulated AUC of the model Pazopanib Opt 1

Although the solubility of dabrafenib mesylate is influenced by the bile salt and lecithin concentration, changes in bile salt solubilization cannot increase the extent or rate absorption (Figure 18). Its absorption is already relatively fast (t_{max} of 2 h (140)) and complete (gut bioavailability of 1.09) in the fasted state, when administered with a HPMC capsule shell. Dabrafenib mesylate solubility is pH dependent and therefore, an increased stomach pH slows down the absorption in the model, resulting in a decreased C_{max} . However, the pH shift alone can only decrease the C_{max} by approximately 25 % in the model (Figure 18, Table 30). An increase in stomach residence time results in stronger C_{max} reduction following the delayed presentation of the drug to the absorption site. To simulate the dabrafenib C_{max} decrease (by approximately 50 %) that is observed in vivo in the fed state compared to the fasted state (140), the increase in stomach transit time is essential. Gastric emptying delay has not been reported as a possible reason for the food effect, which is hypothesized to be related to precipitation in the fed stomach with elevated pH (140). However, the dabrafenib fasted and fed state PK profiles cross each other in the characteristic way for different gastric emptying rates (140) - with a slower absorption rate but higher terminal concentrations of the delayed fed state profile. Using a stomach transit time of 4.5 h in combination with a dynamic gastric pH (fed stomach physiology derived from Koziolok et al. (100)) provides a better fed state C_{max} prediction than 1 h stomach transit time in combination with a static gastric pH of 4.9 (Human-Physiological-Fed physiology) (Table 29).

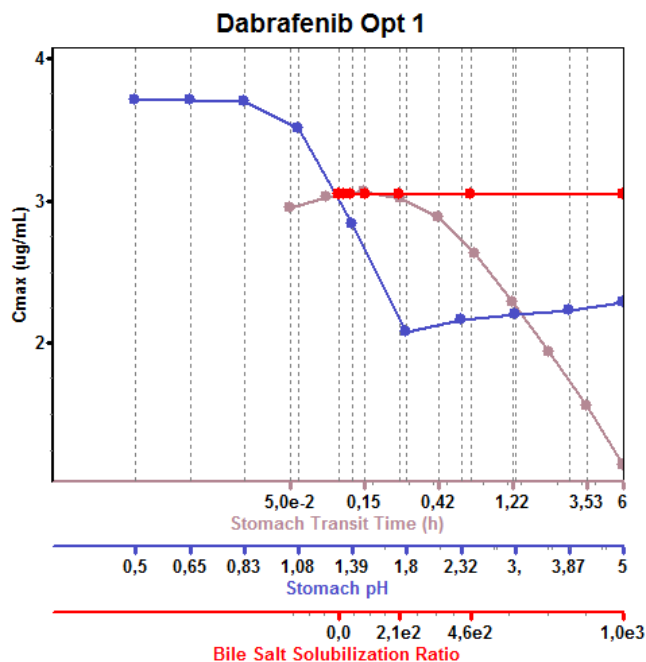


Figure 18: The impact of the physiological changes in the presence of food on the simulated C_{max} of the model Dabrafenib Opt 1

An overview of the Food-PSA results of all compounds is provided in Table 30. For better visualization, the parameters that changed by < 20 % are highlighted in green, and > 20 % in red. The 20 % limit was selected corresponding to the traditional bioequivalence limit of 80 % - 125 %.

Table 30: Percentage deviation of AUC and C_{max} following the physiology related changes in the Food PSA for all compounds' optimized fasted state models (Bile salt SR- Bile salt solubilization ratio, double fed intestinal bile salts - double bile salt concentrations in each compartment than in Human-Physiological-Fed physiology in GastroPlus®)

Model Name	AUC				C_{max}			
	Stomach transit time 6 h	Stomach pH pH 5	Bile salt SR *10	Double fed intestinal bile salts	Stomach transit time 6 h	Stomach pH pH 5	Bile salt SR *10	Double fed intestinal bile salts
Crizotinib bottom up	±0	-2	±0	±0	-67	±0	±0	±0
Dabrafenib Opt 1	-1	-1	±0	±0	-62	-25	±0	+1
Gefitinib Opt 1	-1	-66	±0	±0	-45	-69	+2	+2
Gefitinib Opt 2	+2	-50	+3	+3	-47	-57	+1	+1
Imatinib bottom up	-14	±0	±0	±0	-63	±0	±0	±0
Pazopanib Opt 1	+38	-97	±0	±0	-16	-98	±0	±0
Pazopanib Opt 2	-11	-97	+2	+2	-45	-98	±0	±0
Trametinib Opt 1	-6	±0	±0	±0	-66	±0	±0	+1
Vemurafenib Opt 1	+119	±0	+150	+149	+94	±0	+151	+151
Vemurafenib Opt 2	+14	±0	+109	+122	±0	±0	+110	+122

The stomach transit time was identified as a critical parameter in most of the PBPK models. Prolonged gastric transit delays and reduces the C_{max} of rapidly dissolving and absorbed drugs. Therefore, crizotinib, gefitinib, dabrafenib, imatinib, and trametinib, show BCS class I-like behavior. Moreover, prolonged gastric residence time can enhance the absorption of poorly soluble weakly basic drugs (like pazopanib), as the drug has more time to dissolve in the stomach with a lower pH than the intestine. Delayed gastric emptying might have a positive effect on the exposure of the poorly permeable vemurafenib administered as acid insoluble HPMC-AS coprecipitate (19), through increasing the time window for intestinal permeation and absorption.

Although all model drugs except for trametinib and vemurafenib have pH dependent solubility (weak bases), an increase in stomach pH from pH 1.3 to pH 5 does not significantly affect the simulation of these model drugs. Only gefitinib and pazopanib AUC and C_{max} are reduced by more than 20%. However, the exposure of these two drugs is not reduced after food intake in vivo (44, 45). As discussed, a constant stomach pH of pH 5 might be too conservative to explain the pazopanib food effect. This could also be true for gefitinib, as its AUC and C_{max} remain unchanged up to stomach pH of pH 3.9 in the Food-PSA, but then decreases dramatically with further pH increase. The results are in line with the lack of connection between negative food effect and pH dependent solubility discussed in 4.1.3. Interestingly, pazopanib and gefitinib exposure decreases when co-administered with an ARA

(109, 115), suggesting that their solubility is in principle pH dependent in vivo, but the negative effect is ruled out by other meal triggered processes.

As the models of crizotinib, gefitinib, imatinib, dabrafenib, and trametinib were optimized to have a fraction absorbed of 100 %, better bile salt solubilization (either by increasing the bile salt solubilization ratio or the intestinal bile salt concentrations) was not expected to increase the exposure of these drugs. Only the models of vemurafenib, whose solubility is stronger affected by the bile salt concentrations than pazopanib (Table 15), are sensitive to better bile salt solubilization. Increasing the bile salt solubilization ratio or the intestinal bile salt concentrations in each gut compartment led to an increase in simulated vemurafenib AUC and C_{max} . The good quantitative agreement of the simulation results with 10-fold increased bile salt solubilization ratio vs. double fed intestinal bile salt concentrations (which are also approximately 10-fold higher than in the fasted state) is related to the fact that both factors contribute equally to the drug solubility in the presence of bile salts (Equation 14). The high vemurafenib bile salt sensitivity is in line with the strong absorption related effect of food on exposure in vivo (46).

To summarize, the stomach transit time has emerged as a crucial parameter that can promote a positive as well as a negative effect of food on the drug absorption. The prediction of a negative food effect on the exposure of some model drugs mediated by an increased stomach pH was not in line with the observed in vivo PK data. Improved solubilization mediated by increased bile salt concentrations can be identified with a PSA of the bile salt solubilization ratio. The Food-PSA can identify the parameters most critical to the absorption in the presence of food. However, the identification of the most important factor might not always be possible. When one parameter in the baseline setting changes, the sensitivity of the other parameters could be altered. The observed food effect in vivo might only be explained by a combination of parameters. This could be the case for the model "Pazopanib Opt 2", where a positive food effect is simulated using the fed stomach physiology derived from Koziolk et al. (100), but not indicated by the Food-PSA. Moreover, it must be acknowledged, that the mechanistic validity of the Food-PSA is limited by the validity of the model, i.e. the input parameters. However, the Food-PSA aids in understanding the behavior of the PBPK model, which is beneficial in any case.

4.3.4. Summary of the bottom-up PBPK food effect predictions

Prospective food effect predictions require consideration of all uncertain parameters - compound-wise as well as physiology-wise - to come up with a range of possible predicted food effects. For this purpose, GastroPlus® is a useful tool for absorption modeling, as it provides the mechanistic basis to account for different possible scenarios. Uncertainty related to compound input parameters can be clarified by a PSA and worked around by building different possible models, if necessary. The various physiological aspects that change in the presence of food can be covered by the proposed Food-PSA and by creating customized fed physiologies according to the current state of science.

A workflow has been developed to improve prospective food effect predictions that do not require the fitting of the model to the observed fed state PK profile. For the first time, bottom-up PBPK predictions were combined with a top-down PBPK approach to enable model optimization not only based on the observed plasma concentration time profile, but also the fraction absorbed, after assessing the risk and extent of possible gut first pass metabolism.

The workflow has proven useful when gut bioavailability was complete in the fasted state so that the space for a positive food effect through solubilization was limited. The decrease in stomach pH showed minor or no effect on the exposure of the model drugs. The highly variable stomach transit time appeared to be a common cause for a potential negative food effect. The proposed approach focuses on solubility related food effects, so that additional effects of the food on first pass metabolism and efflux might not be detected.

Food effect prediction of drugs with gut bioavailability < 1 represent the greater challenge, because many of these drugs are sensitive to multiple uncertain parameters in the models. When more than two parameters need to be altered at the same time to reproduce the PK in the fasted state, for example in the cases of erlotinib and lapatinib, it ends up in numerous potential models, whose input parameter combinations can hardly be scientifically justified. This limitation is more likely to affect the models of low permeability compounds (BCS class III and IV), as the P_{eff} is an additional sensitive parameter in the model (in contrast to BCS class I and II drugs). The intestinal fluid volume in the PBPK absorption model, a recent topic (14), could especially influence the PK prediction of poorly soluble drugs and can be included in the workflow in the future. The success of the proposed approach is limited when the PK is not sufficiently characterized. For example, the fraction absorbed cannot be distinguished in the absence of IV PK. Moreover, the gut first pass cannot be precisely estimated, which increases as an additional covariate the number of possible models. As discussed earlier (4.2.3), suitable doses in the IV PK study, the mass balance study and dose range in escalation are crucial for proper PK characterization, especially of drugs with non-linear PK.

The quality of the simulation outcomes, as well as PSA results, depends on the quality and in vivo relevance of the input parameters in the model. The problem of non-identifiability of the relevant combination of compound-related input parameters, an issue for all model drugs except for imatinib and crizotinib, was addressed by considering different possible parameter combinations. Thus, following the proposed workflow, the risk for significant solubility-related food effect on the AUC of all model drugs (except for erlotinib, lapatinib, and M1) could be correctly indicated. It can support, for example, the decision, whether a preliminary food effect study with the non-market formulation or dose is necessary. However, it is not recommended to make decisions in drug development only based on PBPK predictions for compounds with high sensitivity to multiple uncertain input parameters. More model compounds with well-characterized PK required to further probe the proposed approach.

5. Summary and Outlook

In the drug development of oral drugs, food effect investigations are mandatory. Clinical food effect studies are resource intensive and are, currently, not subject to biowaivers. Therefore, several research groups work on the prediction of food effect. This work provides insights into the performance of in vitro solubility and dissolution testing and PBPK modeling in food effect predictions. Moreover, it provides rationales for potential biowaivers in the future based on a mechanistic analysis of clinical and preclinical PK data to identify drugs with solubility-limited absorption. This is connected to a high risk for a positive food effect on drug exposure and relevant for proper design of clinical trials.

5.1. Importance of in vitro solubility and dissolution data in food effect predictions

The solubility and dissolution data generated for the model drugs of this work considered in isolation did not reflect the observed food effects in the clinical studies. The relative difference between FaSSIF and FeSSIF solubility or dissolution parameters are greater than the differences in fed and fasted AUC or C_{max} in the clinical studies. Generally, a stronger positive food effect was predicted than observed. Based on the selected model drugs, the common biorelevant dissolution conditions cannot be recommended as a screening method. The pH dependent solubility in vitro is not associated with a negative effect on AUC or C_{max} in the clinical food studies of the model drugs. The in vitro models cannot mimic the exact in vivo conditions and therefore do not always deliver a good food effect prediction when considered as an isolated factor. In these cases, the use of in vitro release profiles in PBPK absorption models for the prediction of unknown scenarios is also not reasonable. However, when it can be shown, that a drug has solubility-limited absorption in vivo, enhanced solubility in the fed state simulated in vitro, is also meaningful in vivo. For other biopharmaceutical questions, coupling the in vitro solubility and dissolution data with other factors has been recommended as well, for example in the assessment of relative bioavailability as suggested by Aburub et al. (187). The need to test several dissolution conditions to obtain an IVIVC (142) also underlines the fact that there is not one specific in vitro test setting, that always represents the in vivo situation.

In vitro solubility is important for the biopharmaceutical classification of drugs. The hypothesis that food increases the exposure of most BCS class II drugs (188) could not be confirmed by the selected model anticancer drugs. Most of them are categorized in BCS class II and still do not exhibit a strong positive food effect (17). This research suggests that the BCS classification system is too strict when it comes to the identification of drugs with true solubility-limited absorption in vivo. The DCS classification system has a more liberal solubility class threshold. Therefore, fewer model drugs are categorized as solubility-limited in the DCS than the BCS, which aligns better with their clinical observations related to solubility (e.g. gut bioavailability, dose linearity of exposure or food effect).

Solubility is a crucial input parameter in PBPK models, for top-down analysis of observed clinical PK or bottom-up PK predictions. The PBPK models simulate the dynamic interplay of dissolution, permeation and absorption permeation that the current in vitro models cannot deliver. In both PBPK platforms used in this research (generic PBPK model in MATLAB® and GastroPlus®), the in vitro data tended to underpredict the observed PK, but the models could be optimized and used for their specific purpose within this work to assess and understand the food effect of the model drugs.

To summarize, solubility measurements are (among multiple other applications in drug discovery and development) useful for food effect assessments. However, the actual solubility in vivo might be better than in vitro, which is why clinical/ preclinical PK data should be considered to identify drugs with solubility-limited absorption that are susceptible to food effects.

5.2. Prediction of food effect on exposure through understanding the mechanisms underlying the absorption in human and rat

This work clearly shows a correlation between solubility-limited absorption and food effect. It was demonstrated that deconvolution of key mechanisms driving an intestinal loss of drug with PBPK analysis reliably identifies poorly water-soluble drugs whose oral absorption is truly solubility-limited. These drugs are therefore likely to show a positive food effect or benefit from a solubility-enhancing formulation development. Not all poorly water-soluble (defined under the biopharmaceutic framework) and weak basic compounds have solubility-limited oral absorption. The ARA effect has not been entirely investigated as the clinical studies are not available for all model drugs, but a negative effect of ARA on the absorption might also be less probable if solubility is not absorption limiting. A more realistic approach based on the totality of evidence from in silico modeling and early clinical data may be considered in the future as the basis of regulatory requirement for food and ARA interaction study biowaivers.

The analog analysis to assess solubility-limited absorption based on rat PK delivered the same outcomes than in human for 8 out of 10 examined oral anticancer drugs. Drugs with strongly bile salt sensitive drug solubility might be susceptible to misfits between human and rat due to the different intestinal bile salt levels. The rat PK analysis can identify drugs that may benefit from solubility-optimized formulations to increase absorption or mitigate a positive food effect in human.

5.3. Predicting the of food effect on exposure using GastroPlus®

Combining the learnings from the top-down PBPK analysis and the measured solubility data, a workflow has been developed in GastroPlus® to improve prospective food effect predictions and does not require the fitting of the model to the observed fed state PK profile as the full range in drug-related input parameters and physiological variability is considered.

The workflow has proven useful when gut bioavailability was complete in the fasted state so that the space for a positive food effect through solubilization was limited. The decrease in stomach pH showed minor or no effect on the exposure of the model drugs and the highly variable stomach transit time was discussed as a cause for a potential negative food effect. Food effect prediction of compounds, with gut bioavailability < 1, represent the greater challenge, as many of these are sensitive to multiple uncertain parameters in the models. The feasibility is limited when more than two parameters need to be altered at the same time to reproduce the PK in the fasted state, resulting in numerous potential models, whose input parameter combinations can hardly be scientifically justified. It can be used to support for example the decision, whether early food effect study with non-market formulation/dose is necessary. However, it is important to characterize the sensitivity of the models to input parameters with low confidence. It is not recommended to make decisions in drug development only based on PBPK predictions for compounds with high sensitivity to multiple uncertain input parameters.

5.4. Conclusions

Food effect predictions based solely on in vitro solubility and dissolution data were found to be poor and are not recommended. The elaborated workflow for food effect predictions via bottom-up PBPK modeling using GastroPlus® overcomes the current scientific challenges regarding the uncertainty in compound input parameters and the highly variable fed state GI physiology for most model drugs. However, gaps like the intestinal fluid volumes remained uncovered and the non-identifiability of the relevant input parameters remains a problem if the model is sensitive to several uncertain parameters. The mechanistic analysis of human and rat PK data using top-down PBPK modeling provides valuable rationales to guide decisions on conducting food interaction studies and in formulation development. It can be easily adopted in the current drug development and bears the potential to negotiate study waivers with the regulatory agencies in the future. The approach may be especially useful in the development of anti-cancer drugs, where the clinical food effect investigations are often limited by high toxicity and studies in healthy volunteers are not possible. Investigations of the effect of food on drug metabolism will help to complement this research. The objective of this work to evaluate and improve the current food effect prediction strategies based on ten oral anticancer model drugs was met and the learnings may also be applied to other poorly soluble drugs or drug candidates.

References

- (1) Lipinski, C.A., Lombardo, F., Dominy, B.W. & Feeney, P.J. Experimental and computational approaches to estimate solubility and permeability in drug discovery and development settings. *Advanced drug delivery reviews* **23**, 3-25 (1997).
- (2) Lipinski, C.A. Drug-like properties and the causes of poor solubility and poor permeability. *Journal of pharmacological and toxicological methods* **44**, 235-49 (2000).
- (3) OBrien, Z. & F Moghaddam, M. A Systematic Analysis of Physicochemical and ADME Properties of All Small Molecule Kinase Inhibitors Approved by US FDA from January 2001 to October 2015. *Current medicinal chemistry* **24**, 3159-84 (2017).
- (4) Di, L., Fish, P.V. & Mano, T. Bridging solubility between drug discovery and development. *Drug Discovery Today* **17**, 486-95 (2012).
- (5) Koziolok, M. *et al.* The mechanisms of pharmacokinetic food-drug interactions—A perspective from the UNGAP group. *European Journal of Pharmaceutical Sciences* **134**, 31-59 (2019).
- (6) *U.S. Food and Drug Administration: Guidance for Industry - Food-Effect Bioavailability and Fed Bioequivalence* *Studies* <<https://www.fda.gov/downloads/drugs/guidancecomplianceregulatoryinformation/guidances/ucm070241.pdf>> (2002). Accessed February 8 2019.
- (7) European Medicines Agency: Guideline on the investigation of drug interactions - CPMP/EWP/560/95/Rev. 1 Corr. 2**. (2012).
- (8) Lennernas, H. *et al.* Oral biopharmaceutics tools - time for a new initiative - an introduction to the IMI project OrBiTo. *European journal of pharmaceutical sciences : official journal of the European Federation for Pharmaceutical Sciences* **57**, 292-9 (2014).
- (9) Nicolaidis, E., Galia, E., Efthymiopoulos, C., Dressman, J.B. & Reppas, C. Forecasting the In Vivo Performance of Four Low Solubility Drugs from Their In Vitro Dissolution Data. *Pharmaceutical Research* **16**, 1876-82 (1999).
- (10) Kostewicz, E.S., Wunderlich, M., Brauns, U., Becker, R., Bock, T. & Dressman, J.B. Predicting the precipitation of poorly soluble weak bases upon entry in the small intestine. *Journal of pharmacy and pharmacology* **56**, 43-51 (2004).
- (11) Fleisher, D., Li, C., Zhou, Y., Pao, L.-H. & Karim, A. Drug, Meal and Formulation Interactions Influencing Drug Absorption After Oral Administration. *Clinical Pharmacokinetics* **36**, 233-54 (1999).
- (12) Lentz, K.A. Current methods for predicting human food effect. *The AAPS journal* **10**, 282-8 (2008).
- (13) Sjogren, E. *et al.* In vivo methods for drug absorption - comparative physiologies, model selection, correlations with in vitro methods (IVIVC), and applications for formulation/API/excipient characterization including food effects. *European journal of pharmaceutical sciences : official journal of the European Federation for Pharmaceutical Sciences* **57**, 99-151 (2014).

- (14) Li, M., Zhao, P., Pan, Y. & Wagner, C. Predictive performance of physiologically based pharmacokinetic models for the effect of food on oral drug absorption: current status. *CPT: pharmacometrics & systems pharmacology* **7**, 82-9 (2018).
- (15) Parsad, S. & Ratain, M. Food effect studies for oncology drug products. *Clinical Pharmacology & Therapeutics* **101**, 606-12 (2017).
- (16) Singh, B.N. & Malhotra, B.K. Effects of Food on the Clinical Pharmacokinetics of Anticancer Agents. *Clinical Pharmacokinetics* **43**, 1127-56 (2004).
- (17) Willemsen, A.E.C.A.B., Lubberman, F.J.E., Tol, J., Gerritsen, W.R., Van Herpen, C.M.L. & Van Erp, N.P. Effect of food and acid-reducing agents on the absorption of oral targeted therapies in solid tumors. *Drug Discovery Today* **21**, 962-76 (2016).
- (18) Amidon, G.L., Lennernas, H., Shah, V.P. & Crison, J.R. A theoretical basis for a biopharmaceutic drug classification: the correlation of in vitro drug product dissolution and in vivo bioavailability. *Pharm Res* **12**, 413-20 (1995).
- (19) *US Food and drug administration. Vemurafenib (Zelboraf) Clinical Pharmacology and Biopharmaceutics Review.* <https://www.accessdata.fda.gov/drugsatfda_docs/nda/2011/202429Orig1s000ClinPharmR.pdf> (2011). Accessed January 27 2017.
- (20) Leuner, C. & Dressman, J. Improving drug solubility for oral delivery using solid dispersions. *European journal of Pharmaceutics and Biopharmaceutics* **50**, 47-60 (2000).
- (21) Wagner, J.G. Biopharmaceutics: Absorption aspects. *Journal of Pharmaceutical Sciences* **50**, 359-87 (1961).
- (22) Butler, J.M. & Dressman, J.B. The developability classification system: Application of biopharmaceutics concepts to formulation development. *Journal of Pharmaceutical Sciences* **99**, 4940-54 (2010).
- (23) *European Medicines Agency: Guideline on the investigation of bioequivalence - CPMP/EWP/QWP/1401/98 Rev. 1/ Corr **.* <https://www.ema.europa.eu/en/documents/scientific-guideline/guideline-investigation-bioequivalence-rev1_en.pdf> (2010). Accessed June 14th 2019.
- (24) *U.S. Food and Drug Administration: Guidance for Industry - Waiver of In Vivo Bioavailability and Bioequivalence Studies for Immediate-Release Solid Oral Dosage Forms Based on a Biopharmaceutics Classification System.* <<https://www.fda.gov/regulatory-information/search-fda-guidance-documents/waiver-vivo-bioavailability-and-bioequivalence-studies-immediate-release-solid-oral-dosage-forms>> (2017). Accessed February 10 2019.
- (25) Winiwarter, S., Bonham, N.M., Ax, F., Hallberg, A., Lennernas, H. & Karlén, A. Correlation of human jejunal permeability (in vivo) of drugs with experimentally and theoretically derived parameters. A multivariate data analysis approach. *Journal of medicinal chemistry* **41**, 4939-49 (1998).
- (26) Koziolok, M. *et al.* Investigation of pH and Temperature Profiles in the GI Tract of Fasted Human Subjects Using the Intellicap® System. *Journal of Pharmaceutical Sciences* **104**, 2855-63 (2015).

- (27) Galia, E., Nicolaidis, E., Hörter, D., Löbenberg, R., Reppas, C. & Dressman, J. Evaluation of various dissolution media for predicting in vivo performance of class I and II drugs. *Pharmaceutical Research* **15**, 698-705 (1998).
- (28) Dressman, J., Vertzoni, M., Goumas, K. & Reppas, C. Estimating drug solubility in the gastrointestinal tract. *Advanced drug delivery reviews* **59**, 591-602 (2007).
- (29) Jantratid, E., Janssen, N., Reppas, C. & Dressman, J.B. Dissolution Media Simulating Conditions in the Proximal Human Gastrointestinal Tract: An Update. *Pharmaceutical Research* **25**, 1663 (2008).
- (30) Fuchs, A., Leigh, M., Kloefer, B. & Dressman, J.B. Advances in the design of fasted state simulating intestinal fluids: FaSSIF-V3. *European Journal of Pharmaceutics and Biopharmaceutics* **94**, 229-40 (2015).
- (31) Zoeller, T. & Klein, S. Simplified biorelevant media for screening dissolution performance of poorly soluble drugs. *Dissolution Technol* **14**, 8-13 (2007).
- (32) Stegemann, S., Leveiller, F., Franchi, D., de Jong, H. & Lindén, H. When poor solubility becomes an issue: From early stage to proof of concept. *European Journal of Pharmaceutical Sciences* **31**, 249-61 (2007).
- (33) Bergstrom, C.A. *et al.* Early pharmaceutical profiling to predict oral drug absorption: current status and unmet needs. *European journal of pharmaceutical sciences : official journal of the European Federation for Pharmaceutical Sciences* **57**, 173-99 (2014).
- (34) *US Food and Drug Administration: Guidance for Industry - Dissolution Testing of Immediate Release Solid Oral Dosage Forms.* <<https://www.fda.gov/regulatory-information/search-fda-guidance-documents/dissolution-testing-immediate-release-solid-oral-dosage-forms>> (1997). Accessed February 8 2019.
- (35) *U.S. Food and Drug Administration: Guidance for Industry - Immediate Release Solid Oral Dosage Forms, Scale-Up and Postapproval Changes: Chemistry, Manufacturing, and Controls, In Vitro Dissolution Testing, and In Vivo Bioequivalence Documentation.* <<https://www.fda.gov/regulatory-information/search-fda-guidance-documents/supac-ir-immediate-release-solid-oral-dosage-forms-scale-and-post-approval-changes-chemistry>> (1995). Accessed February 8 2019.
- (36) Kostewicz, E.S. *et al.* In vitro models for the prediction of in vivo performance of oral dosage forms. *European journal of pharmaceutical sciences : official journal of the European Federation for Pharmaceutical Sciences* **57**, 342-66 (2014).
- (37) Shono, Y., Jantratid, E. & Dressman, J.B. Precipitation in the small intestine may play a more important role in the in vivo performance of poorly soluble weak bases in the fasted state: case example nelfinavir. *European Journal of Pharmaceutics and Biopharmaceutics* **79**, 349-56 (2011).
- (38) Shono, Y., Jantratid, E., Kesisoglou, F., Reppas, C. & Dressman, J.B. Forecasting in vivo oral absorption and food effect of micronized and nanosized aprepitant formulations in humans. *European Journal of Pharmaceutics and Biopharmaceutics* **76**, 95-104 (2010).
- (39) Berlin, M., Przyklenk, K.-H., Richtberg, A., Baumann, W. & Dressman, J.B. Prediction of oral absorption of cinnarizine—a highly supersaturating poorly soluble weak base with borderline permeability. *European Journal of Pharmaceutics and Biopharmaceutics* **88**, 795-806 (2014).

- (40) Wagner, C., Jantratid, E., Kesisoglou, F., Vertzoni, M., Reppas, C. & Dressman, J.B. Predicting the oral absorption of a poorly soluble, poorly permeable weak base using biorelevant dissolution and transfer model tests coupled with a physiologically based pharmacokinetic model. *European Journal of Pharmaceutics and Biopharmaceutics* **82**, 127-38 (2012).
- (41) Mann, J. *et al.* Validation of dissolution testing with biorelevant media: an OrBiTo study. *Molecular pharmaceutics* **14**, 4192-201 (2017).
- (42) Ruff, A., Fiolka, T. & Kostewicz, E.S. Prediction of Ketoconazole absorption using an updated in vitro transfer model coupled to physiologically based pharmacokinetic modelling. *European Journal of Pharmaceutical Sciences* **100**, 42-55 (2017).
- (43) Ling, J., Fettner, S., Lum, B.L., Riek, M. & Rakhit, A. Effect of food on the pharmacokinetics of erlotinib, an orally active epidermal growth factor receptor tyrosine-kinase inhibitor, in healthy individuals. *Anti-Cancer Drugs* **19**, 209-16 (2008).
- (44) Swaisland, H.C. *et al.* Single-Dose Clinical Pharmacokinetic Studies of Gefitinib. *Clinical Pharmacokinetics* **44**, 1165-77 (2005).
- (45) Heath, E.I. *et al.* A Phase I Study of the Pharmacokinetic and Safety Profiles of Oral Pazopanib With a High-Fat or Low-Fat Meal in Patients With Advanced Solid Tumors. *Clinical Pharmacology & Therapeutics* **88**, 818-23 (2010).
- (46) Ribas, A. *et al.* The effects of a high-fat meal on single-dose vemurafenib pharmacokinetics. *The Journal of Clinical Pharmacology* **54**, 368-74 (2014).
- (47) Nicolaidis, E., Symillides, M., Dressman, J.B. & Reppas, C. Biorelevant Dissolution Testing to Predict the Plasma Profile of Lipophilic Drugs After Oral Administration. *Pharmaceutical Research* **18**, 380-8 (2001).
- (48) Butler, J. *et al.* In vitro models for the prediction of in vivo performance of oral dosage forms: Recent progress from partnership through the IMI OrBiTo collaboration. *European Journal of Pharmaceutics and Biopharmaceutics* **136**, 70-83 (2019).
- (49) Kambayashi, A., Yasuji, T. & Dressman, J.B. Prediction of the precipitation profiles of weak base drugs in the small intestine using a simplified transfer (“dumping”) model coupled with in silico modeling and simulation approach. *European Journal of Pharmaceutics and Biopharmaceutics* **103**, 95-103 (2016).
- (50) Sjögren, E. *et al.* In vivo methods for drug absorption – Comparative physiologies, model selection, correlations with in vitro methods (IVIVC), and applications for formulation/API/excipient characterization including food effects. *European Journal of Pharmaceutical Sciences* **57**, 99-151 (2014).
- (51) Fink, C. *et al.* Evaluating the role of solubility in oral absorption of poorly water-soluble drugs using physiologically based pharmacokinetic (PBPK) modeling. *Clin Pharmacol Ther*, (2019). <https://doi.org/10.1002/cpt.1672>
- (52) Yazdanian, M., Briggs, K., Jankovsky, C. & Hawi, A. The “high solubility” definition of the current FDA guidance on biopharmaceutical classification system may be too strict for acidic drugs. *Pharmaceutical research* **21**, 293-9 (2004).
- (53) Faassen, F. & Vromans, H. Biowaivers for oral immediate-release products. *Clinical pharmacokinetics* **43**, 1117-26 (2004).

- (54) Brunton, L.L., Chabner, B.A. & Knollmann, B.C. *Goodman and Gilman's The Pharmacological Basis of Therapeutics*. 12th edn. (McGraw-Hill Education / Medical: 2011).
- (55) Kuentz, M., Nick, S., Parrott, N. & Röthlisberger, D. A strategy for preclinical formulation development using GastroPlus™ as pharmacokinetic simulation tool and a statistical screening design applied to a dog study. *European journal of pharmaceutical sciences* **27**, 91-9 (2006).
- (56) Thummel, K.E. *et al.* Oral first-pass elimination of midazolam involves both gastrointestinal and hepatic CYP3A-mediated metabolism. *Clinical Pharmacology & Therapeutics* **59**, 491-502 (1996).
- (57) Peters, S.A. Identification of intestinal loss of a drug through physiologically based pharmacokinetic simulation of plasma concentration-time profiles. *Clinical pharmacokinetics* **47**, 245-59 (2008).
- (58) Jones, H. *et al.* Physiologically based pharmacokinetic modeling in drug discovery and development: a pharmaceutical industry perspective. *Clinical Pharmacology & Therapeutics* **97**, 247-62 (2015).
- (59) Agoram, B., Woltosz, W.S. & Bolger, M.B. Predicting the impact of physiological and biochemical processes on oral drug bioavailability. *Advanced Drug Delivery Reviews* **50**, S41-S67 (2001).
- (60) Jamei, M., Dickinson, G.L. & Rostami-Hodjegan, A. A Framework for Assessing Inter-individual Variability in Pharmacokinetics Using Virtual Human Populations and Integrating General Knowledge of Physical Chemistry, Biology, Anatomy, Physiology and Genetics: A Tale of 'Bottom-Up' vs 'Top-Down' Recognition of Covariates. *Drug Metabolism and Pharmacokinetics* **24**, 53-75 (2009).
- (61) Peters, S.A. Evaluation of a generic physiologically based pharmacokinetic model for lineshape analysis. *Clinical pharmacokinetics* **47**, 261-75 (2008).
- (62) Tistaert, C., Heimbach, T., Xia, B., Parrott, N., Samant, T. & Kesisoglou, F. Food Effect Projections via Physiologically Based Pharmacokinetic Modeling: Predictive Case Studies. *Journal of pharmaceutical sciences*, (2018).
- (63) Parrott, N.J., Li, J.Y., Takano, R., Nakamura, M. & Morcos, P.N. Physiologically based absorption modeling to explore the impact of food and gastric pH changes on the pharmacokinetics of alectinib. *The AAPS journal* **18**, 1464-74 (2016).
- (64) Andreas, C.J., Pepin, X., Markopoulos, C., Vertzoni, M., Reppas, C. & Dressman, J.B. Mechanistic investigation of the negative food effect of modified release zolpidem. *European Journal of Pharmaceutical Sciences* **102**, 284-98 (2017).
- (65) Heimbach, T., Xia, B., Lin, T.-h. & He, H. Case Studies for Practical Food Effect Assessments across BCS/BDDCS Class Compounds using In Silico, In Vitro, and Preclinical In Vivo Data. *The AAPS journal* **15**, 143-58 (2013).
- (66) Lu, A.T.K., Frisella, M.E. & Johnson, K.C. Dissolution Modeling: Factors Affecting the Dissolution Rates of Polydisperse Powders. *Pharmaceutical Research* **10**, 1308-14 (1993).
- (67) Takano, R. *et al.* Oral Absorption of Poorly Water-Soluble Drugs: Computer Simulation of Fraction Absorbed in Humans from a Miniscale Dissolution Test. *Pharmaceutical Research* **23**, 1144-56 (2006).

- (68) Klein, S. & Shah, V.P. A standardized mini paddle apparatus as an alternative to the standard paddle. *Aaps Pharmscitech* **9**, 1179-84 (2008).
- (69) Ranson, M. *et al.* A phase I dose-escalation and bioavailability study of oral and intravenous formulations of erlotinib (Tarceva[®], OSI-774) in patients with advanced solid tumors of epithelial origin. *Cancer Chemotherapy and Pharmacology* **66**, 53-8 (2010).
- (70) Frohna, P. *et al.* Evaluation of the Absolute Oral Bioavailability and Bioequivalence of Erlotinib, an Inhibitor of the Epidermal Growth Factor Receptor Tyrosine Kinase, in a Randomized, Crossover Study in Healthy Subjects. *The Journal of Clinical Pharmacology* **46**, 282-90 (2006).
- (71) Xu, H. *et al.* Evaluation of crizotinib absolute bioavailability, the bioequivalence of three oral formulations, and the effect of food on crizotinib pharmacokinetics in healthy subjects. *The Journal of Clinical Pharmacology* **55**, 104-13 (2015).
- (72) US Food and Drug Administration. Crizotinib (Xalkori) Clinical Pharmacology and Biopharmaceutics Review. <http://www.accessdata.fda.gov/drugsatfda_docs/nda/2011/202570Orig1s000TOC.cfm> (2011). Accessed July 6 2016.
- (73) Denton, C.L. *et al.* Concomitant Oral and Intravenous Pharmacokinetics of Dabrafenib, a BRAF Inhibitor, in Patients with BRAF V600 Mutation-Positive Solid Tumors. *The Journal of Clinical Pharmacology* **53**, 955-61 (2013).
- (74) GSK. Clinical Study Report 113479 - Determination of the Absolute Bioavailability of GSK2118436 Following a Single Oral Dose Co-Administered with an Intravenous Radiolabelled Microtracer of GSK2118436 in Subjects with BRAF Mutant Solid Tumors. <https://www.gsk-clinicalstudyregister.com/study/113479?search=study&search_terms=113479#csr> (2012). Accessed August 31 2017.
- (75) GSK. Clinical Study Report 113468 - An Open-Label Study to Examine the Effects of a High-Fat Meal and Particle Size on the Pharmacokinetics of Orally Administered GSK2118436 in Subjects with BRAF Mutation-Positive Tumor. <https://www.gsk-clinicalstudyregister.com/study/113468?search=study&search=study&search_terms=113468#csr> (2012). Accessed February 13 2018.
- (76) US Food and Drug Administration. Dabrafenib (Tafinlar) Clinical Pharmacology and Biopharmaceutics Review. <http://www.accessdata.fda.gov/drugsatfda_docs/nda/2013/202806Orig1s000TOC.cfm> (2013). Accessed February 20 2017.
- (77) US Food and Drug Administration. Erlotinib (Tarceva) Clinical Pharmacology and Biopharmaceutics Review. <http://www.accessdata.fda.gov/drugsatfda_docs/nda/2004/21-743_Tarceva.cfm> (2004). Accessed January 25 2017.
- (78) US Food and Drug Administration. Gefitinib (Iressa) Clinical Pharmacology and Biopharmaceutics Review. <http://www.accessdata.fda.gov/drugsatfda_docs/nda/2003/021399_iressa.cfm> (2002). Accessed May 17 2017.
- (79) Peng, B. *et al.* Absolute Bioavailability of Imatinib (Glivec[®]) Orally versus Intravenous Infusion. *The Journal of Clinical Pharmacology* **44**, 158-62 (2004).

- (80) Peng, B., Lloyd, P. & Schran, H. Clinical Pharmacokinetics of Imatinib. *Clinical Pharmacokinetics* **44**, 879-94 (2005).
- (81) US Food and Drug Administration. Imatinib (Gleevec) Clinical Pharmacology and Biopharmaceutics Review. <https://www.accessdata.fda.gov/drugsatfda_docs/nda/2003/021588s000_GleevecTOC.cfm> (2003). Accessed January 25 2017.
- (82) Koch, K.M. *et al.* Effects of Food on the Relative Bioavailability of Lapatinib in Cancer Patients. *Journal of Clinical Oncology* **27**, 1191-6 (2009).
- (83) US Food and Drug Administration. Lapatinib (Tykerb) Clinical Pharmacology and Biopharmaceutics Review. <http://www.accessdata.fda.gov/drugsatfda_docs/nda/2007/022059s000TOC.cfm> (2007). Accessed July 07 2018.
- (84) Deng, Y. *et al.* Bioavailability, metabolism and disposition of oral pazopanib in patients with advanced cancer. *Xenobiotica* **43**, 443-53 (2013).
- (85) GSK. Clinical Study Report VEG10004 - An Open-Label, Two-Part Study to Characterize the Pharmacokinetics of a Single Intravenous Dose of Pazopanib (GW786034) and the Absorption, Distribution, Metabolism and Elimination of a Single Oral [14C] Labeled Dose of Pazopanib in Subjects with Solid Tumor Malignancies. <https://www.gsk-clinicalstudyregister.com/study/VEG10004?search=study&search_terms=10004#csr> (2009). Accessed January 27 2017.
- (86) GSK. Clinical Study Report VEG10005 - An Open-Label, Two-Period, Randomized, Crossover Study to Evaluate the Effect of Food on the Pharmacokinetics of Single Doses of Pazopanib in Cancer Patients. <https://www.gsk-clinicalstudyregister.com/study/VEG10005?search=study&search_terms=veg10005#csr> (2008). Accessed June 28 2017.
- (87) US Food and Drug Administration. Pazopanib (Votrient) Clinical Pharmacology and Biopharmaceutics Review. <http://www.accessdata.fda.gov/drugsatfda_docs/nda/2009/022465s000TOC.cfm> (2008). Accessed August 12 2016.
- (88) Leonowens, C. *et al.* Concomitant oral and intravenous pharmacokinetics of trametinib, a MEK inhibitor, in subjects with solid tumours. *British Journal of Clinical Pharmacology* **78**, 524-32 (2014).
- (89) GSK. Clinical Study Report 113709 - An Open-Label, Two-Period, Randomized, Crossover Study to Evaluate the Effect of Food on the Single Dose Pharmacokinetics of the MEK Inhibitor, GSK1120212, in Subjects with Solid Tumors. <https://www.gsk-clinicalstudyregister.com/study/113709?search=study&search_terms=113709#csr> (2012). Accessed February 13 2018.
- (90) US Food and drug administration. Trametinib (Mekinist) Clinical Pharmacology and Biopharmaceutics Review. <http://www.accessdata.fda.gov/drugsatfda_docs/nda/2013/204114Orig1s000TOC.cfm> (2013). Accessed January 11 2017.
- (91) Rowland, M. & Tozer, T.N. *Clinical Pharmacokinetics and Pharmacodynamics: Concepts and Applications*. 4th edn. (Lippincott Williams&Wilki 2010).

- (92) Davies, B. & Morris, T. Physiological parameters in laboratory animals and humans. *Pharmaceutical research* **10**, 1093-5 (1993).
- (93) Simcyp® Version 13. *Certara, Princeton, New Jersey, USA*, (2013).
- (94) Peters, S.A. & Dolgos, H.J.C.P. Requirements to Establishing Confidence in Physiologically Based Pharmacokinetic (PBPK) Models and Overcoming Some of the Challenges to Meeting Them. (2019).
- (95) Berry, L.M., Li, C. & Zhao, Z. Species differences in distribution and prediction of human Vss from preclinical data. *Drug Metabolism and Disposition*, dmd. 111.040766 (2011).
- (96) *US Food and Drug Administration. Lapatinib (Tykerb) Pharmacology Review - Part 1.* <https://www.accessdata.fda.gov/drugsatfda_docs/nda/2007/022059s000TOC.cfm> (2007). Accessed August 3 2017.
- (97) Mittapalli, R.K., Vaidhyanathan, S., Sane, R. & Elmquist, W.F. Impact of P-glycoprotein (ABCB1) and breast cancer resistance protein (ABCG2) on the brain distribution of a novel BRAF inhibitor: vemurafenib (PLX4032). *Journal of Pharmacology and Experimental Therapeutics* **342**, 33-40 (2012).
- (98) *European Medicines Agency. Zelboraf : EPAR - Public assessment report.* <http://www.ema.europa.eu/docs/en_GB/document_library/EPAR_-_Public_assessment_report/human/002409/WC500124400.pdf> (2011). Accessed June 14 2017.
- (99) Peters, S.A. & Hultin, L. Early identification of drug-induced impairment of gastric emptying through physiologically based pharmacokinetic (PBPK) simulation of plasma concentration-time profiles in rat. *Journal of pharmacokinetics and pharmacodynamics* **35**, 1-30 (2008).
- (100) Koziolok, M. *et al.* Intra-gastric pH and pressure profiles after intake of the high-caloric, high-fat meal as used for food effect studies. *Journal of controlled release* **220**, 71-8 (2015).
- (101) Chaddock, G. *et al.* Novel MRI tests of oro-cecal transit time and whole gut transit time: studies in normal subjects. *Neurogastroenterology & Motility* **26**, 205-14 (2014).
- (102) Paine, M.F., Hart, H.L., Ludington, S.S., Haining, R.L., Rettie, A.E. & Zeldin, D.C. The human intestinal cytochrome P450 "pie". *Drug metabolism and disposition*, (2006).
- (103) Lin, J.H. Drug–drug interaction mediated by inhibition and induction of P-glycoprotein. *Advanced Drug Delivery Reviews* **55**, 53-81 (2003).
- (104) *European Public Assessment Report (EPAR) Xalkori (Crizotinib) - Product information.* <http://www.ema.europa.eu/ema/index.jsp?curl=pages/medicines/human/medicines/002489/human_med_001592.jsp&mid=WC0b01ac058001d124> (2012). Accessed September 11 2018.
- (105) GSK. *Clinical Study Report 113220 - An Open- Label, Dose Escalation, Phase I/II Study to Investigate the Safety, Pharmacokinetics, Pharmacodynamics and Clinical Activity of the BRAF Inhibitor GSK2118436 in Combination with the MEK Inhibitor GSK1120212 in Subjects with BRAF Mutant Metastatic Melanoma (Preliminary Data as of Clinical Cut-off Date of SEP 2011).* <<https://www.gsk-studyregister.com/study/3867>> (2012). Accessed April 15 2019.

- (106) GSK. *Clinical Study Report 113463 - An Open-Label Study to Characterize the Absorption, Distribution, Metabolism and Elimination of a single Oral 14C Labeled Dose of GSK2118436 in Subjects with BRAF mutant Solid tumors.* <<https://www.gsk-studyregister.com/study/3930>> (2011). Accessed April 15 2019.
- (107) Hidalgo, M. *et al.* Phase I and pharmacologic study of OSI-774, an epidermal growth factor receptor tyrosine kinase inhibitor, in patients with advanced solid malignancies. *Journal of clinical oncology* **19**, 3267-79 (2001).
- (108) Kletzl, H., Giraudon, M., Ducray, P.S., Abt, M., Hamilton, M. & Lum, B.L. Effect of gastric pH on erlotinib pharmacokinetics in healthy individuals: omeprazole and ranitidine. *Anti-Cancer Drugs* **26**, 565-72 (2015).
- (109) Tang, W., Tomkinson, H. & Masson, E. Effect of Sustained Elevated Gastric pH Levels on Gefitinib Exposure. *Clinical Pharmacology in Drug Development*, n/a-n/a (2017).
- (110) Peng, B. *et al.* Pharmacokinetics and pharmacodynamics of imatinib in a phase I trial with chronic myeloid leukemia patients. *Journal of Clinical Oncology* **22**, 935-42 (2004).
- (111) Egorin, M.J. *et al.* Effect of a proton pump inhibitor on the pharmacokinetics of imatinib. *British Journal of Clinical Pharmacology* **68**, 370-4 (2009).
- (112) GSK. *Clinical Study Report EGF10003- A Phase I, Open-Label, Multiple Dose, Dose Escalation Study of GW572019 in Patients with Solid Tumors.* <<https://www.gsk-studyregister.com/study/7491>> (2006). Accessed January 27 2019.
- (113) Koch, K.M. *et al.* Effects of Esomeprazole on the Pharmacokinetics of Lapatinib in Breast Cancer Patients. *Clinical Pharmacology in Drug Development* **2**, 336-41 (2013).
- (114) Hurwitz, H.I. *et al.* Phase I trial of pazopanib in patients with advanced cancer. *Clinical cancer research* **15**, 4220-7 (2009).
- (115) Tan, A.R. *et al.* Effects of ketoconazole and esomeprazole on the pharmacokinetics of pazopanib in patients with solid tumors. *Cancer Chemotherapy and Pharmacology* **71**, 1635-43 (2013).
- (116) GSK. *Clinical Study Report 115064 - Determination of the Absolute Bioavailability of GSK1120212 Following a Single Oral Dose Co-Administered with an Intravenous Radiolabelled Microdose of GSK1120212 in Subjects with Solid Tumors.* <<https://www.gsk-studyregister.com/study/4412>> (2012). Accessed September 1 2017.
- (117) Grippo, J.F. *et al.* A phase I, randomized, open-label study of the multiple-dose pharmacokinetics of vemurafenib in patients with BRAF V600E mutation-positive metastatic melanoma. *Cancer Chemotherapy and Pharmacology* **73**, 103-11 (2014).
- (118) Mithani, S.D., Bakatselou, V., TenHoor, C.N. & Dressman, J.B. Estimation of the increase in solubility of drugs as a function of bile salt concentration. *Pharmaceutical research* **13**, 163-7 (1996).
- (119) Augustijns, P., Wuyts, B., Hens, B., Annaert, P., Butler, J. & Brouwers, J. A review of drug solubility in human intestinal fluids: implications for the prediction of oral absorption. *European Journal of Pharmaceutical Sciences* **57**, 322-32 (2014).

- (120) Tolman, K.G., Sanders, S.W., Buchi, K.N., Karol, M.D., Jennings, D.E. & Ringham, G.L. The Effects of Oral Doses of Lansoprazole and Omeprazole on Gastric pH. *Journal of Clinical Gastroenterology* **24**, 65-70 (1997).
- (121) Budha, N.R. *et al.* Drug Absorption Interactions Between Oral Targeted Anticancer Agents and PPIs: Is pH-Dependent Solubility the Achilles Heel of Targeted Therapy? *Clinical Pharmacology & Therapeutics* **92**, 203-13 (2012).
- (122) Lindahl, A., Ungell, A.-L., Knutson, L. & Lennernäs, H. Characterization of Fluids from the Stomach and Proximal Jejunum in Men and Women. *Pharmaceutical Research* **14**, 497-502 (1997).
- (123) Banwell, J.G., Gorbach, S.L., Pierce, N.F., Mitra, R. & Mondal, A. Acute undifferentiated human diarrhea in the tropics: II. Alterations in intestinal fluid and electrolyte movements. *Journal of Clinical Investigation* **50**, 890-900 (1971).
- (124) Litou, C. *et al.* Characteristics of the Human Upper Gastrointestinal Contents in the Fasted State Under Hypo- and A-chlorhydric Gastric Conditions Under Conditions of Typical Drug – Drug Interaction Studies. *Pharmaceutical Research* **33**, 1399-412 (2016).
- (125) GlaxoSmithKline. *Tykerb (lapatinib) Highlights of prescribing information.* <https://www.accessdata.fda.gov/drugsatfda_docs/label/2010/022059s007lbl.pdf>.
- (126) Serajuddin, A.T. Salt formation to improve drug solubility. *Advanced drug delivery reviews* **59**, 603-16 (2007).
- (127) Berben, P. *et al.* Biorelevant dissolution testing of a weak base: Interlaboratory reproducibility and investigation of parameters controlling in vitro precipitation. *European Journal of Pharmaceutics and Biopharmaceutics* **140**, 141-8 (2019).
- (128) *Biorelevant.com - Web page.* <<https://biorelevant.com/about-us/>>. Accessed June 12 2019.
- (129) Arndt, M., Chokshi, H., Tang, K., Parrott, N.J., Reppas, C. & Dressman, J.B. Dissolution media simulating the proximal canine gastrointestinal tract in the fasted state. *European Journal of Pharmaceutics and Biopharmaceutics* **84**, 633-41 (2013).
- (130) Wiest, J. *et al.* Geometrical and structural dynamics of Imatinib within biorelevant colloids. *Molecular pharmaceutics* **15**, 4470-80 (2018).
- (131) *U.S. Food and Drug Administration Dissolution Database.* <<https://www.accessdata.fda.gov/scripts/cder/dissolution/index.cfm>>.
- (132) Grimm, M. *et al.* Gastric emptying and small bowel water content after administration of grapefruit juice compared to water and isocaloric solutions of glucose and fructose: a four-way crossover MRI pilot study in healthy subjects. *Molecular pharmaceutics* **15**, 548-59 (2018).
- (133) Mudie, D.M. *et al.* Quantification of gastrointestinal liquid volumes and distribution following a 240 mL dose of water in the fasted state. *Molecular pharmaceutics* **11**, 3039-47 (2014).
- (134) *Novartis Pharma GmbH. Fachinformation Votrient® 400 mg Filmtabletten (Stand: Mai 2018).* <https://www.gelbe-liste.de/produkte/Votrient-400-mg-Filmtabletten_527528/fachinformation> (2018).

- (135) Jede, C. *et al.* Application of an automated small-scale in vitro transfer model to predict in vivo precipitation inhibition. *International Journal of Pharmaceutics* **565**, 458-71 (2019).
- (136) Davis, S., Hardy, J. & Fara, J. Transit of pharmaceutical dosage forms through the small intestine. *Gut* **27**, 886-92 (1986).
- (137) Nicolaidis, E., Hempenstall, J.M. & Reppas, C. Biorelevant dissolution tests with the flow-through apparatus? *Dissolution Technologies* **7**, 8-15 (2000).
- (138) Sunesen, V.H., Pedersen, B.L., Kristensen, H.G. & Müllertz, A. In vivo in vitro correlations for a poorly soluble drug, danazol, using the flow-through dissolution method with biorelevant dissolution media. *European journal of pharmaceutical sciences* **24**, 305-13 (2005).
- (139) Bønløkke, L., Hovgaard, L., Kristensen, H.G., Knutson, L., Lindahl, A. & Lennernäs, H. A comparison between direct determination of in vivo dissolution and the deconvolution technique in humans. *European Journal of Pharmaceutical Sciences* **8**, 19-27 (1999).
- (140) Ouellet, D. *et al.* Effects of particle size, food, and capsule shell composition on the oral bioavailability of dabrafenib, a BRAF inhibitor, in patients with BRAF mutation-positive tumors. *Journal of pharmaceutical sciences* **102**, 3100-9 (2013).
- (141) Cox, D.S. *et al.* Evaluation of the Effects of Food on the Single-Dose Pharmacokinetics of Trametinib, a First-in-Class MEK Inhibitor, in Patients with Cancer. *The Journal of Clinical Pharmacology* **53**, 946-54 (2013).
- (142) Mistry, B., Patel, N., Jamei, M., Rostami-Hodjegan, A. & Martinez, M.N. Examining the Use of a Mechanistic Model to Generate an In Vivo/In Vitro Correlation: Journey Through a Thought Process. *The AAPS journal* **18**, 1144-58 (2016).
- (143) Flaherty, K.T. *et al.* Inhibition of Mutated, Activated BRAF in Metastatic Melanoma. *New England Journal of Medicine* **363**, 809-19 (2010).
- (144) European Medicines agency. *European Public Assessment Report (EPAR) Glivec - Summary of Product Characteristics (Annex 1)*. www.ema.europa.eu/docs/en_GB/document_library/EPAR_-_Product_Information/human/000406/WC500022207.pdf (2009). Accessed August 31 2017.
- (145) Johnson, K. *et al.* Metabolism and excretion of erlotinib, a small molecule inhibitor of epidermal growth factor receptor tyrosine kinase, in healthy male volunteers. *Drug metabolism and disposition*, (2005).
- (146) Castellino, S., O'Mara, M.J., Koch, K.M., Borts, D., Bowers, G.D. & MacLauchlin, C. Human metabolism of lapatinib, a dual kinase inhibitor: implications for hepatotoxicity. *Drug Metabolism and Disposition*, dmd. 111.040949 (2011).
- (147) White, R.E. & Maniatisitkul, P. Pharmacokinetic Theory of Cassette Dosing in Drug Discovery Screening. *Drug Metabolism and Disposition* **29**, 957-66 (2001).
- (148) Smith, N.F., Raynaud, F.I. & Workman, P. The application of cassette dosing for pharmacokinetic screening in small-molecule cancer drug discovery. *Molecular Cancer Therapeutics* **6**, 428-40 (2007).

- (149) US Food and Drug Administration. Imatinib (Gleevec) Pharmacology Review - Part 1. <https://www.accessdata.fda.gov/drugsatfda_docs/nda/2001/21335_Gleevec.cfm> (2001). Accessed June 14 2017.
- (150) US Food and Drug Administration. Gefitinib (Iressa) Pharmacology Review - Part 1. <https://www.accessdata.fda.gov/drugsatfda_docs/nda/2003/021399_iressa.cfm> (2002). Accessed June 14 2017.
- (151) US Food and Drug Administration. Pazopanib (Votrient) Pharmacology Review. <https://www.accessdata.fda.gov/drugsatfda_docs/nda/2009/022465s000TOC.cfm> (2008). Accessed June 14 2017.
- (152) Yamazaki, S. *et al.* Prediction of Oral Pharmacokinetics of cMet Kinase Inhibitors in Humans: Physiologically Based Pharmacokinetic Model versus Traditional One Compartment Model. *Drug Metabolism and Disposition*, (2010).
- (153) US Food and Drug Administration. Trametinib (Mekinist) Pharmacology Review. <https://www.accessdata.fda.gov/drugsatfda_docs/nda/2013/204114Orig1s000TOC.cfm> (2013). Accessed June 01 2017.
- (154) Saphier, S., Rosner, A., Brandeis, R. & Karton, Y. Gastro intestinal tracking and gastric emptying of solid dosage forms in rats using X-ray imagining. *International journal of pharmaceutics* **388**, 190-5 (2010).
- (155) Jang, S.F., Goins, B.A., Phillips, W.T., Santoyo, C., Rice-Ficht, A. & McConville, J.T. Size discrimination in rat and mouse gastric emptying. *Biopharmaceutics & drug disposition* **34**, 107-24 (2013).
- (156) Williams, H.D. *et al.* Strategies to address low drug solubility in discovery and development. *Pharmacological reviews* **65**, 315-499 (2013).
- (157) US Food and Drug Administration. Crizotinib (Xalkori) Pharmacology Review. <https://www.accessdata.fda.gov/drugsatfda_docs/nda/2011/202570Orig1s000TOC.cfm> (2011). Accessed May 31 2017.
- (158) US Food and Drug Administration. Dabrafenib (Tafinlar) Pharmacology Review. <https://www.accessdata.fda.gov/drugsatfda_docs/nda/2013/202806Orig1s000TOC.cfm> (2013). Accessed June 30 2017.
- (159) US Food and Drug Administration. Erlotinib (Tarceva) Pharmacology Review. <https://www.accessdata.fda.gov/drugsatfda_docs/nda/2004/21-743_Tarceva.cfm> (2004). Accessed June 30 2017.
- (160) US Food and Drug Administration. Vemurafenib (Zelboraf) Pharmacology Review. <https://www.accessdata.fda.gov/drugsatfda_docs/nda/2011/202429s000TOC.cfm> (2011). Accessed June 30 2017.
- (161) McConnell, E.L., Basit, A.W. & Murdan, S. Measurements of rat and mouse gastrointestinal pH, fluid and lymphoid tissue, and implications for in-vivo experiments. *Journal of Pharmacy and Pharmacology* **60**, 63-70 (2008).
- (162) Grignard, E., Taylor, R., McAllister, M., Box, K. & Fotaki, N. Considerations for the development of in vitro dissolution tests to reduce or replace preclinical oral absorption studies. *European Journal of Pharmaceutical Sciences* **99**, 193-201 (2017).

- (163) Cao, X. *et al.* Why is it challenging to predict intestinal drug absorption and oral bioavailability in human using rat model. *Pharmaceutical research* **23**, 1675-86 (2006).
- (164) Jones, C.R., Hatley, O.J.D., Ungell, A.-L., Hilgendorf, C., Peters, S.A. & Rostami-Hodjegan, A. Gut Wall Metabolism. Application of Pre-Clinical Models for the Prediction of Human Drug Absorption and First-Pass Elimination. *The AAPS journal* **18**, 589-604 (2016).
- (165) Holm, R., Müllertz, A. & Mu, H. Bile salts and their importance for drug absorption. *International Journal of Pharmaceutics* **453**, 44-55 (2013).
- (166) Kararli, T.T. Comparison of the gastrointestinal anatomy, physiology, and biochemistry of humans and commonly used laboratory animals. *Biopharmaceutics & Drug Disposition* **16**, 351-80 (1995).
- (167) Staggers, J.E., Frost, S.C. & Wells, M.A. Studies on fat digestion, absorption, and transport in the suckling rat. III. Composition of bile and evidence for enterohepatic circulation of bile salts. *Journal of lipid research* **23**, 1143-51 (1982).
- (168) Lu, T. *et al.* Combining “bottom-up” and “top-down” approaches to assess the impact of food and gastric pH on pictilisib (GDC-0941) pharmacokinetics. *CPT: pharmacometrics & systems pharmacology* **6**, 747-55 (2017).
- (169) Tsamandouras, N., Rostami-Hodjegan, A. & Aarons, L. Combining the ‘bottom up’ and ‘top down’ approaches in pharmacokinetic modelling: fitting PBPK models to observed clinical data. *British Journal of Clinical Pharmacology* **79**, 48-55 (2015).
- (170) Feng, S. *et al.* Combining ‘Bottom-Up’ and ‘Top-Down’ Methods to Assess Ethnic Difference in Clearance: Bitopertin as an Example. *Clinical Pharmacokinetics* **55**, 823-32 (2016).
- (171) Goldinger, S.M. *et al.* A single-dose mass balance and metabolite-profiling study of vemurafenib in patients with metastatic melanoma. *Pharmacology research & perspectives* **3**, (2015).
- (172) Johnson, T.R. *et al.* Metabolism, excretion and pharmacokinetics of [14C] crizotinib following oral administration to healthy subjects. *Xenobiotica* **45**, 45-59 (2015).
- (173) Bershas, D.A. *et al.* Metabolism and disposition of oral dabrafenib in cancer patients: proposed participation of aryl nitrogen in carbon-carbon bond cleavage via decarboxylation following enzymatic oxidation. *Drug Metabolism and Disposition* **41**, 2215-24 (2013).
- (174) McKillop, D. *et al.* Metabolic disposition of gefitinib, an epidermal growth factor receptor tyrosine kinase inhibitor, in rat, dog and man. *Xenobiotica* **34**, 917-34 (2004).
- (175) Scheffler, M., Di Gion, P., Doroshenko, O., Wolf, J. & Fuhr, U. Clinical pharmacokinetics of tyrosine kinase inhibitors. *Clinical pharmacokinetics* **50**, 371-403 (2011).
- (176) Swaisland, H.C. *et al.* Pharmacokinetic drug interactions of gefitinib with rifampicin, itraconazole and metoprolol. *Clinical pharmacokinetics* **44**, 1067-81 (2005).
- (177) Gschwind, H.-P. *et al.* Metabolism and disposition of imatinib mesylate in healthy volunteers. *Drug metabolism and disposition* **33**, 1503-12 (2005).
- (178) Ho, M.Y. *et al.* Trametinib, a first-in-class oral MEK inhibitor mass balance study with limited enrollment of two male subjects with advanced cancers. *Xenobiotica* **44**, 352-68 (2014).

-
- (179) van Leeuwen, R.W., van Gelder, T., Mathijssen, R.H. & Jansman, F.G. Drug–drug interactions with tyrosine-kinase inhibitors: a clinical perspective. *The Lancet Oncology* **15**, e315-e26 (2014).
- (180) Darwich, A.S. *et al.* IMI–Oral biopharmaceutics tools project–Evaluation of bottom-up PBPK prediction success part 3: Identifying gaps in system parameters by analysing In Silico performance across different compound classes. *European Journal of Pharmaceutical Sciences* **96**, 626-42 (2017).
- (181) Parrott, N., Lukacova, V., Fraczkiwicz, G. & Bolger, M. Predicting pharmacokinetics of drugs using physiologically based modeling—application to food effects. *The AAPS journal* **11**, 45-53 (2009).
- (182) Xia, B. *et al.* Utility of Physiologically Based Modeling and Preclinical In Vitro/In Vivo Data to Mitigate Positive Food Effect in a BCS Class 2 Compound. *AAPS PharmSciTech* **14**, 1255-66 (2013).
- (183) Weitschies, W., Blume, H. & Mönnikes, H. Magnetic Marker Monitoring: High resolution real-time tracking of oral solid dosage forms in the gastrointestinal tract. *European Journal of Pharmaceutics and Biopharmaceutics* **74**, 93-101 (2010).
- (184) Riethorst, D., Mols, R., Duchateau, G., Tack, J., Brouwers, J. & Augustijns, P. Characterization of Human Duodenal Fluids in Fasted and Fed State Conditions. *Journal of Pharmaceutical Sciences* **105**, 673-81 (2016).
- (185) Hunt, J.N. & Stubbs, D.F. The volume and energy content of meals as determinants of gastric emptying. *The Journal of Physiology* **245**, 209-25 (1975).
- (186) Koziolk, M. *et al.* Navigating the human gastrointestinal tract for oral drug delivery: Uncharted waters and new frontiers. *Advanced Drug Delivery Reviews* **101**, 75-88 (2016).
- (187) Aburub, A., Sperry, D.C., Bhattachar, S., Lobo, E., Ding, X. & Rose, J.P. Relative Bioavailability Risk Assessment: A Systematic Approach to Assessing In Vivo Risk Associated With CM&C-Related Changes. *Journal of Pharmaceutical Sciences* **108**, 8-17 (2019).
- (188) Gu, C.-H. *et al.* Predicting Effect of Food on Extent of Drug Absorption Based on Physicochemical Properties. *Pharmaceutical Research* **24**, 1118-30 (2007).

Acknowledgements

First, I would like to thank Prof. Karsten Mäder for the great support of my PhD research. In spite of the geographical distance between Halle and Darmstadt, our interactions were frequent and valuable.

I would also like to thank my mentors at Merck Healthcare KGaA, Dr. Sheila-Annie Peters, Dr. Knut Wagner, Melanie Schneider, and Dr. Holger Bauer, who provided me the opportunity to perform this research in an industrial and academic collaboration. Many thanks to Holger for initiating this project together with Sheila, and for your interest in my work - even after changing the department. Knut and Melanie, thank you for providing this great framework in the lab, your regular input and open doors for my questions. Sheila, thank you so much for being so passionate about my work, for your motivation, ideas and almost 24/7 support me.

The leaderships of Analytical Development, Dr. Johannes Dasenbrock and Dr. Anette Partheil, as well as the former Quantitative Pharmacology and Drug Disposition, Dr. Hugues Dolgos, may also be acknowledged for supporting this research.

I would like to thank Simulations Plus who supported this work with an academic GastroPlus® license. It was very much appreciated.

Furthermore, I would like thank the colleagues from DMPK department that who contributed to my project. Special thanks to Dr. Marc Lecomte and Dr. Lassina Badolo for enabling the rat PK study and the numerous scientific discussions. Thanks also to the colleagues who provided me with the Caco-2 permeability data of the model drugs.

Many thanks to my fellow labmates, especially to the (former) dissolution team with Sabrina Wacker, Vanessa Stroh, Eckard Garrandt, Maria Schandel and Antje Brunner for their technical support and for always encouraging me. Special thanks also to Andreas Töpel for his HPLC support and to Annabel Mehl for the great help during her internship.

I would also like to thank my Co-PhD students, Carolin Auch, Christian Jede, Karsten Flügel, Melinda Kern, Lara Rosenberger, Nadine Gottschalk, Lena Preiss, Katharina Krollik, Florian Johann, Steffen Wöll und Magdalena Münster, for helping me out with any issues and making these 3 years and 3 months even more unforgettable. Moreover, I would like to acknowledge all other colleagues from Pharmtech who supported me. Special thanks to Dr. Christian Wagner and Dr. Simone Hansmann for their help with GastroPlus®.

Thanks to Dr. Anita Nair and Dr. Dajun Sun for their input to my first publication, and to Sabrina Wacker and Sebastian Alarcon Salinas for reviewing this thesis carefully and for being there as friends.

I would also like to thank all other friends, who were always there for me and supported a proper work-life balance during the PhD time. Thank you for making me laugh and cheering me up so many times. Special thanks to: Sabrina Burk, Antonia Spahn, Madlen Jacob, Franziska Zeyda, Franziska Carle, Dorit Köhler, Volker Jelinek and Mira Otto!

Finally, I would like to thank my family for their permanent support. Thank you for always being there for me, motivating me and providing me a safety net. Because of you, I took everything much calmer and focused on this project without worries. You have substantially contributed to this work.

Last but not least, I would like to thank Arnold. Thank you for being so incredibly patient with me, for being so proud of me and for always believing in me.

Curriculum Vitae

Persönliche Daten

Geburtsdatum: 03. Juni 1990
Geburtsort: 35398 Gießen
Familienstand: ledig
Staatsangehörigkeit: Bundesrepublik Deutschland
Anschrift: Elisabethenstraße 50, 64283 Darmstadt

Bildungsgang

Schulische Bildung: 2000 – 2009 Abitur an der Liebigschule in Gießen

Berufliche Bildung: Oktober 2010 – Oktober 2014: Studium der Pharmazie an der Philipps Universität Marburg

September 2012: Erwerb des ersten Staatsexamens Pharmazie

Oktober 2014: Erwerb des zweiten Staatsexamens Pharmazie

November 2014 – April 2015: Pharmazeut im Praktikum bei Merck KGaA in Darmstadt, Abteilung: Chemical & Pharmaceutical Development (Analytical Development)

Mai 2015 – Oktober 2015: Pharmazeut im Praktikum in der Alpha Apotheke Darmstadt

November 2015: Erwerb des dritten Staatsexamens Pharmazie

Dezember 2015: Approbation zum Apotheker

Januar 2016 - April 2016: Apothekerin in der Rehberg Apotheke in Roßdorf

Mai 2016: Beginn Promotion (Dr. rer. nat.) in pharmazeutischer Technologie bei Merck Healthcare KGaA in Darmstadt, Abteilungen: Analytical Development und Quantitative Pharmacology

Thema: Predicting the effect of food on drug exposure through an understanding of the impact of in vitro solubility and dissolution on the human

in vivo absorption using physiologically based pharmacokinetic (PBPK) modelling

universitäre Betreuung: Prof. Dr. Karsten Mäder (Martin-Luther-Universität Halle-Wittenberg)

seit August 2019: QC Referent Solida (Deviations) bei Merck Healthcare KGaA in Darmstadt, Abteilung: Healthcare Quality Darmstadt

Veröffentlichungen

Artikel (Peer-review):

September 2019: Fink, C. *et al.* Evaluating the role of solubility in oral absorption of poorly water-soluble drugs using physiologically based pharmacokinetic (PBPK) modeling. *Clin Pharmacol Ther*, (2019). <https://doi.org/10.1002/cpt.1672>

Poster:

März 2019: "Performance of in vitro solubility and dissolution testing in food effect predictions" (3rd European Conference on Pharmaceutics, Bologna, Italien)

Declaration under Oath/ Eidesstattliche Erklärung

Martin-Luther-Universität Halle-Wittenberg

Naturwissenschaftliche Fakultät I - Biowissenschaften

Ich erkläre gemäß § 5 der Promotionsordnung der Naturwissenschaftlichen Fakultäten I, II & III der Martin-Luther-Universität Halle-Wittenberg an Eides statt, dass ich die Arbeit selbstständig und ohne fremde Hilfe verfasst habe, keine anderen als die von mir angegebenen Quellen und Hilfsmittel benutzt habe und die den benutzten Werken wörtlich oder inhaltlich entnommenen Stellen als solche kenntlich gemacht habe. Weiterhin erkläre ich, dass ich mich mit der vorliegenden Dissertationsarbeit erstmals um die Erlangung eines Doktorgrades bewerbe.

Datum

Unterschrift des Antragstellers

Appendix

Table S 1: Potential issues arising from poor drug solubility and their consequences (51)

Potential issues	Consequences
Low and highly variable oral bioavailability	<ul style="list-style-type: none"> • High inter-patient variability in clinical response leading to inefficient treatment or poor patient safety • Need for dose augmentation leading to increased risk of GI toxicity and poor patient compliance
Poor dose-exposure proportionality	<ul style="list-style-type: none"> • Hampering clinical translation • Nonlinear dose-exposure relationship
Accurate measure of free concentration limited by precipitation, adsorption or binding in in vitro assays	<ul style="list-style-type: none"> • Poor tolerability of biological matrices to solubilizing components limits the possibility for improving solubility. Therefore, performance of in vitro assays (e.g., activity screening in cell culture, metabolic stability and transporter assays, binding and displacement assays, enzyme inhibition etc.) is compromised by the variability and inconsistency of the measured concentrations.
Inability to achieve high concentrations	<ul style="list-style-type: none"> • Limits the range of concentrations that can be tested in preclinical in vivo toxicological assessment • Complete binding and inhibition profiles cannot be obtained.
Need for advanced formulation development	<ul style="list-style-type: none"> • As compounds progress through discovery and into development, the solid-state properties will almost certainly change solid-state properties of material will not be the final, or optimal • Increase cost of drug product
Need for additional in vitro solubility and dissolution tests	<ul style="list-style-type: none"> • Use of more physiological (biorelevant) media to get the most realistic characterization and avoid under prediction by compendial buffers • Two-stage dissolution and precipitation testing for weak bases
Need for additional clinical studies	<ul style="list-style-type: none"> • Food effect studies • Acid-reducing agent (ARA) studies • Bioequivalence studies

Table S 2: Overview of the compound specific HPLC parameters detection wave length, injection volume and solvent for the preparation of a 0.1 mg/mL standard solution

	Detection wave length [nm]	Injection volume [μ L]	Solvent for standard solution
Crizotinib	264	40	Methanol/ Water 50:50 + 0.1% 1 N HCl
Dabrafenib	331	30	Methanol/ Water 50:50
Erlotinib	247	5	Methanol/ Water 70:30
Gefitinib	252	10	Methanol
Imatinib	265	8	Methanol/ Water 50:50
Lapatinib	268	99	Acetonitrile/ Water 50:50
M1	260	15	Acetonitrile/ Water 30:70
Pazopanib	267	10	Acetonitrile/ Water 50:50
Trametinib	245	5	Acetonitrile + 1 % DMSO
Vemurafenib	249	10	Acetonitrile/ Water 80:20

Table S 3: Applied gradient in HPLC Method 1

Time [min]	Eluent A [%]	Eluent B [%]	Flow rate [mL/min]
0	90	10	0.85
0.6	90	10	0.85
4	10	90	0.85
5.5	10	90	0.85
5.6	90	10	2.5
8	90	10	2.5
8.1	90	10	0.85
8.5	90	10	0.85

Table S 4: Applied gradient in HPLC Method 2

Time [min]	Eluent A [%]	Eluent B [%]	Flow rate [mL/min]
0	85	15	3
4	45	55	3
4.1	5	95	3
5	5	95	3
5.1	85	15	3
7	85	15	3

Table S 5: Introduced compound specific changes to optimize the presented basic HPLC methods

Compound	Optimizations of the Basic HPLC method
Dabrafenib	Dabrafenib elutes after 5.5 min, therefore the period of 10 % Eluent A/ 90 % Eluent B in Method 1 was extended up to 6.0 min
Gefitinib	Gefitinib elutes already after 2.4 min, so the gradient of Method 2 is changed back to the initial conditions after 4.1 min instead of 5.1 min to shorten the run time to 6 min
Lapatinib	The expected lapatinib sample concentrations were very low. To enable the use of higher injection volumes the column of Method 1 was changed to Chromolith High Resolution; RP-18e, 100 x 4.6 mm and a flow rate of 1.5 mL/min was used instead of 0.85 mL/min
Trametinib	Trametinib elutes after 5.8 min, therefore the period of 10 % Eluent A/ 90 % Eluent B in Method 1 was extended up to 6.5 min
Vemurafenib	The flow rate of Method 1 was increased to 1.5 mL/min and kept constant to avoid baseline noise during the peak elution.

Table S 6: Summary of input parameters for the human physiologically based pharmacokinetic simulations with the generic PBPK model in MATLAB®

	Crizotinib	Dabrafenib	Erlotinib	Gefitinib	Imatinib	Lapatinib	M1	Pazopanib	Trametinib	Vemurafenib
Molecular weight	450.34 (72)	615.68 (76)	429.90 (77)	446.9 (78)	589.7 (80)	943.48 (113)	547.1	473.99 (87)	693.5 (90)	489.93 (19)
logP	4.28 (72)	2.9 (76)	3.2 ^a	4.15 (78)	1.99 (80)	6 (113)	3	3.55 ^a	4.99 (90)	3.0 (19)
Basic pK_a values	9.4, 5.6 (72)	2.2, 1.5 (76)	5.42 (77)	7.2, 5.4 (78)	8.07, 1.52 (80)	4.6, 6.7 (113)	9.5, 2.8	6.4, 2.1 (87)	n.a.	n.a.
Acidic pK_a values	n.a.	6.6 (76)	n.a.	n.a.	n.a.	n.a.	n.a.	10.2 (87)	n.a.	7.9, 11.1 (19)
Unbound fraction in plasma	0.093 (72)	0.003 (76)	0.065 ^b	0.089 (174)	0.05 [*]	0.01 [§]	0.0215	0.001 (87)	0.026 (90)	0.0014 (19)
Blood to Plasma Ratio	1.14 (72)	0.54 (76)	0.71 [‡]	0.76 [†]	1.1 (95)	0.84 (96)	0.8	0.76 ^c	3.2 (90)	0.58 (19)
Caco-2 P_{app} passive [10⁻⁶ cm^{s-1}]	15.35	12.45	40.43	10.41	25.9	0.21	14.7	28.46	15.44	0.11
cP_{eff} [10⁻⁴ cms⁻¹]	2.22	2.38	3.58	5.23	2.61	1.84	6.19	0.85	1.07	2.54
Input solubility [mg/mL]	0.7430	0.0037	0.0124	0.0887	5	0.0350	0.0728	0.0012	0.0008 (90)	0.0054
pH input solubility refers to	6.5	6.5	6.5	6.5	6.5	6.5	6.5	6.5	6.3 (90)	6.5
Gastric solubility [mg/mL]	10 (121)	0.0117	0.1665	21 (78)	5	0.0055	0.0213	1.0779	0.0004 (90)	0.0003
pH gastric solubility refers to	1.6 (121)	1.6	1.6	1 (78)	1.6	1.6	1.6	1.6	2 (90)	1.6
Hypothetical BCS class I-like solubility [mg/mL]	1.0	1.0	3.5	1.9	n.a. ^d	1.0	9.7	3.8	1.0	1.0
CL_{int}^e [μl/min/mg protein]	250	3,150	40	800	100	720	365	175	19	80
K_p factor^e	1	20	0.45	0.8	18	0.45	13	1	0.22	0.3

^a sourced from Drug Bank (<https://www.drugbank.ca/>)

^b plasma protein binding 92-95 % (77) → mean value 93.5 % → unbound fraction 0.065

^c blood to plasma concentration ratio 0.59 - 0.93 (87) → mean value 0.76

^d solubility is already BCS class I niveau

^e fitted to observed intravenous pharmacokinetic profile

Abbreviations: HCl - hydrochloride, logP - decadic logarithm of the partition coefficient, pK_a - acid dissociation constant, Caco-2 P_{app} passive - apparent passive permeability determined in Caco-2 assay, cP_{eff} - calculated effective permeability, CL_{int} - intrinsic microsomal clearance, K_p factor - multiplicative factor, to scale the tissue distribution coefficients, DMSO - dimethyl sulfoxide

References:

The numbers in brackets represent the reference numbers from the main text.

- * US Food and Drug Administration. *Imatinib (Gleevec) Clinical Pharmacology and Biopharmaceutics Review - Part 1*. <https://www.accessdata.fda.gov/drugsatfda_docs/nda/2001/21335_Gleevec.cfm> (2001). Accessed July 7 2018.
- § US Food and Drug Administration. *Lapatinib (Tykerb) Medical Review - Part 1*. <https://www.accessdata.fda.gov/drugsatfda_docs/nda/2007/022059s000_MedR_P1.pdf> (2007). Accessed July 27 2017.
- ‡ Gruber, A. *et al.* Monitoring of erlotinib in pancreatic cancer patients during long-time administration and comparison to a physiologically based pharmacokinetic model. *Cancer chemotherapy and pharmacology* **81**, 763-71 (2018).
- † Li, J., Brahmer, J., Messersmith, W., Hidalgo, M. & Baker, S.D. Binding of gefitinib, an inhibitor of epidermal growth factor receptor-tyrosine kinase, to plasma proteins and blood cells: in vitro and in cancer patients. *Investigational new drugs* **24**, 291-7 (2006).

Table S 7: Summary of input parameters for the rat physiologically based pharmacokinetic simulations with the generic PBPK model in MATLAB®

	Crizotinib	Dabrafenib	Erlotinib	Gefitinib	Imatinib	Lapatinib	M1	Pazopanib	Trametinib	Vemurafenib
Molecular weight	450.34 (72)	615.68 (76)	429.90 (77)	446.9 (78)	589.7 (80)	943.48 (96)	547.1	473.99 (87)	693.5 (90)	489.922 (19)
Dose [mg/kg]	4.4	3.47	2.97	4.13	5.95	34.79	0.5	12.95	0.044	11.98
logP	4.28 (72)	2.9 (76)	3.2 ^a	4.15 (78)	1.99 (80)	6 (113)	3	3.55 (87)	4.99 (90)	3.0 (19)
Basic pK_a values	9.4, 5.6 (72)	2.2, 1.5 (76)	5.42 (77)	7.2, 5.4 (78)	8.07, 1.52 (80)	4.6, 6.7 (113)	9.5, 2.8	6.4, 2.1 (87)	n.a.	n.a.
Acidic pK_a values	n.a.	6.6 (76)	n.a.	n.a.	n.a.	n.a.	n.a.	10.2 (87)	n.a.	7.9, 11.1 (19)
Unbound fraction in plasma	0.057 (157)	0.016 [◇]	0.085 [•]	0.038 [†]	0.055 [£]	0.01 (96)	0.07	0.0042 (151)	0.04 (153)	0.0015 (98)
Blood to Plasma Ratio	0.88 (152)	0.58 ^{c, ◇}	0.71 ^{b, ‡}	1.25 (150)	1.1 (95) ^b	0.41 (96)	0.72	0.76 (87) ^b	0.88 (153)	0.6 (98)
Caco-2 P_{app} passive [10⁻⁶ cm^s⁻¹]	15.35	12.45	40.43	10.41	25.9	0.21	14.7	28.46	15.44	0.11
cP_{eff} [10⁻⁴ cms⁻¹]	2.22	2.38	3.58	5.23	2.61	1.84	6.19	0.85	1.07	2.54
Input solubility [mg/mL]	0.7430	0.0037	0.0124	0.0887	5	0.0350	0.0728	0.0012	0.0008 (90)	0.0054
pH input solubility refers to	6.5	6.5	6.5	6.5	6.5	6.5	6.5	6.5	6.3 (90)	6.5
Gastric solubility [mg/mL]	≥ 10	0.0040	0.0726 ^d	2.6 (78)	≥ 20	0.0047	0.0131 ^d	0.0359	0.0003 (90)	<0.00026 (19)
pH gastric solubility refers to	4	4	4	4	4	4	4	4	4	4
Hypothetical BCS class I-like solubility [mg/mL]	1.0	1.0	3.5	1.9	n.a. ^e	1.0	9.7	3.8	1.0	1.0
CL_{int}^f [μl/min/mg protein]	1200	710	40	100	90	280	9000	n.a.	53	n.a.
K_p factor^f	3	8	1.2	0.7	17	0.45	21	n.a.	2.15	n.a.

^a sourced from Drug Bank (<https://www.drugbank.ca/>)

^b blood to plasma ratio in the rat is not available, human value used

^c blood to plasma concentration ratios ranged from 0.45 to 0.71 in all tested species (value of 0.58 - in the middle - is used)

^d solubility in acetate buffer pH 4.5 + 130mM NaCl

^e solubility is already BCS class I level

^f fitted to observed intravenous pharmacokinetic profile

Abbreviations: logP - decadic logarithm of the partition coefficient, pK_a - acid dissociation constant, Caco-2 Papp passive - apparent passive permeability determined in caco-2 assay, cP_{eff} - calculated effective permeability, CL_{int} - intrinsic microsomal clearance, K_p factor - multiplicative factor, to scale the tissue distribution coefficients, DSMO - dimethyl sulfoxide

References:

The numbers in brackets represent the reference numbers from the main text.

- [‡] Gruber, A. *et al.* Monitoring of erlotinib in pancreatic cancer patients during long-time administration and comparison to a physiologically based pharmacokinetic model. *Cancer chemotherapy and pharmacology* **81**, 763-71 (2018).
- [†] Li, J., Brahmer, J., Messersmith, W., Hidalgo, M. & Baker, S.D. Binding of gefitinib, an inhibitor of epidermal growth factor receptor-tyrosine kinase, to plasma proteins and blood cells: in vitro and in cancer patients. *Investigational new drugs* **24**, 291-7 (2006).
- [◇] *European Medicines Agency: EMA/CHMP/242419/2013/corr 1 - CHMP assessment report Tafinlar.* <https://www.ema.europa.eu/documents/assessment-report/tafinlar-epar-public-assessment-report_en.pdf> (2013). Accessed May 2017.
- Hoshino-Yoshino, A., Kato, M., Nakano, K., Ishigai, M., Kudo, T. & Ito, K. Bridging from preclinical to clinical studies for tyrosine kinase inhibitors based on pharmacokinetics/pharmacodynamics and toxicokinetics/toxicodynamics. *Drug metabolism and pharmacokinetics*, 1108300227- (2011).
- [£] Kretz, O., Weiss, H.M., Schumacher, M.M. & Gross, G. In vitro blood distribution and plasma protein binding of the tyrosine kinase inhibitor imatinib and its active metabolite, CGP74588, in rat, mouse, dog, monkey, healthy humans and patients with acute lymphatic leukaemia. *British journal of clinical pharmacology* **58**, 212-6 (2004).

Table S 8: Summary of input parameters for the oral bottom-up physiologically based pharmacokinetic simulations using GastroPlus®

	Crizotinib	Dabrafenib	Erlotinib	Gefitinib	Imatinib	Lapatinib	M1	Pazopanib	Trametinib	Vemurafenib
Dose [mg]^a	250	177.7	163.9	250	447.9	2435.6	30	866.7	2.25	960
Dosage form	IR Capsule	IR Capsule	IR Tablet	IR Tablet	IR Tablet	IR Tablet	IR Tablet	IR Tablet	IR Tablet	IR Tablet
Molecular weight ^a	450.34 (72)	615.68 (76)	429.90 (77)	446.9 (78)	589.7 (80)	943.48 (113)	547.1	473.99 (87)	693.5 (90)	489.93 (19)
logP	4.28 (72)	2.9 (76)	3.2 ^b	4.15 (78)	1.99 (80)	6 (113)	3	3.55 ^b	4.99 (90)	3.0 (19)
Basic pKa values	9.4, 5.6 (72)	2.2, 1.5 (76)	5.42 (77)	7.2, 5.4 (78)	8.07, 1.52 (80)	4.6, 6.7 (113)	9.5, 2.8	6.4, 2.1 (87)	n.a.	n.a.
Acidic pKa values	n.a.	6.6 (76)	n.a.	n.a.	n.a.	n.a.	n.a.	10.2 (87)	n.a.	7.9, 11.1 (19)
Unbound fraction in plasma	0.093 (72)	0.003 (76)	0.065 ^c	0.089 (174)	0.05 [*]	0.01 [§]	0.0215	0.001 (87)	0.026 (90)	0.0014 (19)
Blood to Plasma Ratio	1.14 (72)	0.54 (76)	0.71 [‡]	0.76 [†]	1.1 (95)	0.84 (96)	0.8	0.76 ^d	3.2 (90)	0.58 (19)
P_{eff} human [10⁻⁴ cm/s⁻¹]	1.4978	1.7273	3.6387	1.08	1.9237	0.2068		2.0037	1.9215	0.1983
Reference solubility [mg/mL] ^a	0.1894	0.0028	0.0028	0.0011	0.4639	0.0004	0.0654	0.0003	0.0002 (90)	0.0002
pH reference solubility refers to	7.4	6.5 ^e	7.4	7.4	7.4	6.5 ^f	7.4	6.5 ^f	8 (90)	5 ^e
pH dependent solubility a	See Figure 7	See Figure 7	See Figure 7	See Figure 7	See Figure 7	See Figure 7	See Figure 7	See Figure 7	no (90)	See Figure 7
FaSSIF solubility [mg/mL] ^a	0.7430	0.0037	0.0124	0.0887	5	0.0350	0.0728	0.0012	0.0008 (90)	0.0054
FeSSIF solubility [mg/mL] ^a	10	0.0083	0.1125	2.6	5 ^g	0.2844	0.4427	0.0051	0.0039 (90)	0.1302
Precipitation time [s]	900	900	900	900	900	900	900	900	900	900
Dissolution model	Johnson	Johnson	Johnson	Johnson	Johnson	Johnson	Johnson	Johnson	Johnson	Johnson
Particle radius [µm]	25	25	25	25	25	25	6.2	25	25	25
Compartmental model	3 Comp.	2 Comp.	2 Comp.	3 Comp.	3 Comp.	1 Comp.	3 Comp.	3 Comp.	3 Comp.	1 Comp.

^a referring to the clinically relevant salt form

^b sourced from Drug Bank (<https://www.drugbank.ca/>)

^c plasma protein binding 92-95 % (77) → mean value 93.5 % → unbound fraction 0.065

^d blood to plasma concentration ratio 0.59 - 0.93 (87) → mean value 0.76

^e solubility at pH 7.4 higher because of acidic pK_a

^f solubility at pH 7.4 not measurable (too low)

^g interaction with bile salts, biphasic system, using lower solubility than FaSSIF could lead to misfit of bile salt solubilization ratio - however model is not sensitive to bile salt SR at all

Abbreviations: IR - immediate release, logP - decadic logarithm of the partition coefficient, pK_a - acid dissociation constant, P_{eff} - effective permeability converted from measured Caco-2 permeability, Comp. - compartmental model, FaSSIF - fasted state simulated intestinal fluid, FeSSIF - fed state simulated intestinal fluid

References:

The numbers in brackets represent the reference numbers from the main text.

* *US Food and Drug Administration. Imatinib (Gleevec) Clinical Pharmacology and Biopharmaceutics Review - Part 1.* <https://www.accessdata.fda.gov/drugsatfda_docs/nda/2001/21335_Gleevec.cfm> (2001). Accessed July 7 2018.

§ *US Food and Drug Administration. Lapatinib (Tykerb) Medical Review - Part 1.* <https://www.accessdata.fda.gov/drugsatfda_docs/nda/2007/022059s000_MedR_P1.pdf> (2007). Accessed July 27 2017.

‡ Gruber, A. *et al.* Monitoring of erlotinib in pancreatic cancer patients during long-time administration and comparison to a physiologically based pharmacokinetic model. *Cancer chemotherapy and pharmacology* **81**, 763-71 (2018).

† Li, J., Brahmer, J., Messersmith, W., Hidalgo, M. & Baker, S.D. Binding of gefitinib, an inhibitor of epidermal growth factor receptor-tyrosine kinase, to plasma proteins and blood cells: in vitro and in cancer patients. *Investigational new drugs* **24**, 291-7 (2006).

Table S 9: Maximum possible bile salt solubilization ratios, assuming 10-fold different FaSSIF and/or FeSSIF solubility ; FaSSIF (fasted state simulated intestinal fluid) and FeSSIF (fed state intestinal fluid) solubility were independently varied by a factor of 10 to account for potential physiologic variation. The maximum possible bile salt solubilization ratio, that was achieved, by this exercise is shown in Table S 9 and used as upper limit for the parameter bile salt solubilization ration in the parameter sensitivity analysis to optimize the bottom-up predicted PBPK models in GastroPlus®.

Compound	Crizotinib	Dabrafenib	Erlotinib	Gefitinib	Imatinib	Lapatinib	M1	Pazopanib	Trametinib	Vemurafenib
Change in biorelevant solubility	FaSSIF*10 FeSSIF =	FaSSIF*10 FeSSIF/10	FaSSIF = FeSSIF*10	FaSSIF*10 FeSSIF/10	FaSSIF*10 FeSSIF/10	FaSSIF*10 FeSSIF =	FaSSIF = FeSSIF*10	FaSSIF*10 FeSSIF/10	FaSSIF = FeSSIF*10	FaSSIF/10 FeSSIF*10
Maximum value	911,00	226,000	538,000	4,830,000	280,000	9,070,000	1,710,000	722,000	884,000	22,900,000
bile salt solubilization ratio fitted to in vitro data	0	16,200	36,400	473,000	6062	2,040,000	140,000	32,900	71,800	2,860,000

Table S 10: Luminal pH, transit times and bile salt concentrations of the Human-Physiological-Fasted and Human-Physiological-Fed physiologies in GastroPlus®

	<u>Human-Physiological-Fasted</u>			<u>Human-Physiological-Fed</u>		
	pH	Transit time [h]	Bile salt [mM]	pH	Transit time [h]	Bile salt [mM]
Stomach	1.30	0.25	0	4.90	1.00	0
Duodenum	6.00	0.26	2.8	5.40	0.26	14.4
Jejunum 1	6.20	0.95	2.33	5.40	0.95	12.02
Jejunum 2	6.40	0.76	2.03	6.00	0.76	10.46
Ileum 1	6.60	0.59	1.41	6.60	0.59	7.28
Ileum 2	6.90	0.43	1.16	6.90	0.43	5.99
Ileum 3	7.40	0.31	0.14	7.40	0.31	0.73
Caecum	6.40	4.50	0	6.40	4.50	0
Asc Colon	6.80	13.50	0	6.80	13.50	0

Table S 11: pH dependent solubility of vemurafenib, taken from the Zelboraf® FDA Clinical Pharmacology and Biopharmaceutics Review (19)

Table 1. Solubility of crystalline form II in aqueous media across the pH range (pH 1 to 7.5) at 37°C

Medium	pH	pH of supernatant after 24h @ 37°C	RO5185426 (mg/1000 ml)	
			after 2h @ 37°C	after 24h @ 37°C
0.1 N HCl	1.0	1.1	<0.26	<0.26
50 mmol phosphate buffer	3.0	3.0	<0.26	<0.26
50 mmol acetate buffer	4.5	4.5	<0.26	<0.26
50 mmol phosphate buffer	6.8	6.8	<0.26	<0.26
50 mmol phosphate buffer	7.5	7.5	<0.26	<0.26
Water	---	8-9	<0.26	<0.26

Table 2. Solubility of MBP (RO5185426 in non-crystalline form) in aqueous media across the pH range (pH 1 to 7.5) at 37°C

Medium	pH	pH of supernatant after 24h @ 37°C	RO5185426 (mg/1000 ml)	
			after 2h @ 37°C	after 24h @ 37°C
0.1 N HCl	1.0	1.1	<0.26	<0.26
50 mmol phosphate buffer	3.0	3.0	<0.26	<0.26
50 mmol acetate buffer	4.5	4.5	<0.26	<0.26
50 mmol phosphate buffer	6.8	6.8	0.51	0.50
50 mmol phosphate buffer	7.5	7.5	0.38	0.94
Water	---	8-9	<0.26	1.57

Table S 12: pH dependent solubility of trametinib, taken from the Mekinist® FDA Clinical Pharmacology and Biopharmaceutics Review (90)

Table 1. Solubility of trametinib

Solvent	Solubility ¹ (µg/mL)			
	0.5 hour	2 hours	4 hours	24 hours
pH2	ND ²	0.1	0.3	0.4
pH4	ND	0.1	0.3	0.3
pH6	ND	0.1	0.3	0.3
pH8	ND	0.1	0.2	0.2
SGF ³	ND	0.4	0.6	0.4
FaSSIF ^{4,6}	10.8	2.3	1.5	0.8
FeSSIF ^{5,6}	49.1	16.8	8.9	3.9

¹ Determined at 37°C on material typical of commercial drug substance

² ND – not detected, detection limit (DL)=0.025 µg/mL

³ Simulated Gastric Fluid, pH=1.2

⁴ Fasted State Simulated Intestinal Fluid, pH=6.3

⁵ Fed State Simulated Intestinal Fluid, pH=4.9

⁶ The fall in solubility over time is ascribed to precipitation of the less soluble non solvated parent

Source: 3.2.S.1.3. General Properties, p 3.

Table S 13: pH dependent solubility and observed effect of acid-reducing agents on AUC and C_{max} of the model drugs; The C_{max} and AUC without/ with ARA ratios are taken from the clinical ARA studies of the model drugs, referenced in this table. The pH 1.6/ pH 5.0 24 h-solubility ratios were calculated from the measured data presented in Figure 7. The numbers in brackets represent the reference numbers from the main text.

	C_{max} without/ with ARA ratio	AUC without/ with ARA ratio	pH 1.6/ pH 5 24 h-solubility ratio
Crizotinib	1 (104)	0.90 (104)	not available †
Dabrafenib	not available	not available	8
Erlotinib	0.39* (108)	0.54* (108)	36**
Gefitinib	0.29 (109)	0.53 (109)	≥ 20
Imatinib	0.97 (111)	1.07 (111)	≥ 17
Lapatinib	0.76 (113)	0.74 (113)	14
M1	not available	not available	2
Pazopanib	0.58 (115)	0.60 (115)	634
Trametinib	not available	not available	1‡
Vemurafenib	not available	not available	1

† both solubility values are ≥ 10 mg/mL

* In the reference (108), interaction studies with omeprazole and ranitidine are reported. The C_{max} and AUC without/ with omeprazole ratios are shown in this table as the effect of omeprazole on erlotinib exposure was greater than ranitidine's.

** The ratio is also influenced by the different chloride concentrations (59 mM in FaSSGF blank pH 1.6 and 203 mM in FeSSIF blank pH 5.0)

‡ Comparison of pH 2 and pH 4 solubility, see Table S 12 (90)

Table S 14: Performance in the four simulations to evaluate the model performance of the optimized GastroPlus® PBPK models. The success in every simulation exercise to evaluate the performance of the optimized PBPK models is color-coded in green, if the simulation passed the acceptance criteria in Table 28, and in red, if the deviation in PK parameters exceeded the acceptance limit. Moreover, it is indicated, whether the observed PK were over- or underpredicted, when the verification failed.

Model Name	AUC				C _{max}			
	Food effect study dose (fasted)	Lower dose	Higher dose	Acid reduced conditions	Food effect study dose (fasted)	Lower dose	Higher dose	Acid reduced conditions
Crizotinib bottom up		overprediction			overprediction	overprediction	overprediction	
Crizotinib STT ^a		overprediction						
Dabrafenib Opt 1			not available ^c	not available			not available ^c	not available
Gefitinib Opt 1								overprediction ^b
Gefitinib Opt 2								overprediction ^b
Imatinib bottom up		overprediction						
Pazopanib Opt 1				underprediction				underprediction
Pazopanib Opt 2				underprediction				underprediction
Trametinib Opt 1		underprediction	overprediction	not available		underprediction	overprediction	not available
Vemurafenib bottom up		not applicable ^d	not applicable ^d	not available	underprediction	underprediction	not available ^d	not available
Vemurafenib Opt 1			not applicable ^d	not available			not available ^d	not available
Vemurafenib Opt 2		not applicable ^d	not applicable ^d	not available		underprediction	not available ^d	not available

^a Crizotinib bottom-up prediction with prolonged stomach transit time (STT) of 2 h to overcome the C_{max} underprediction and early t_{max}

^b The extent of observed negative ARA effect on C_{max} is not adequately simulated using stomach pH of 4.5, but pH 4.9

^c PK with HPMC capsules at doses higher than in the food effect study (150 mg) is not available, the simulation was substituted by a simulation of a 95 mg oral suspension

^d Only single dose AUC_{0-8h} is available for 240 mg-960 mg. For the simulations with t_{max} is > 8 h, AUC verification based on this data is not appropriate. Moreover, PK at doses higher than the food effect study (960 mg) is not available. To substitute, C_{max} verification performed at the next highest dose available (720 mg).

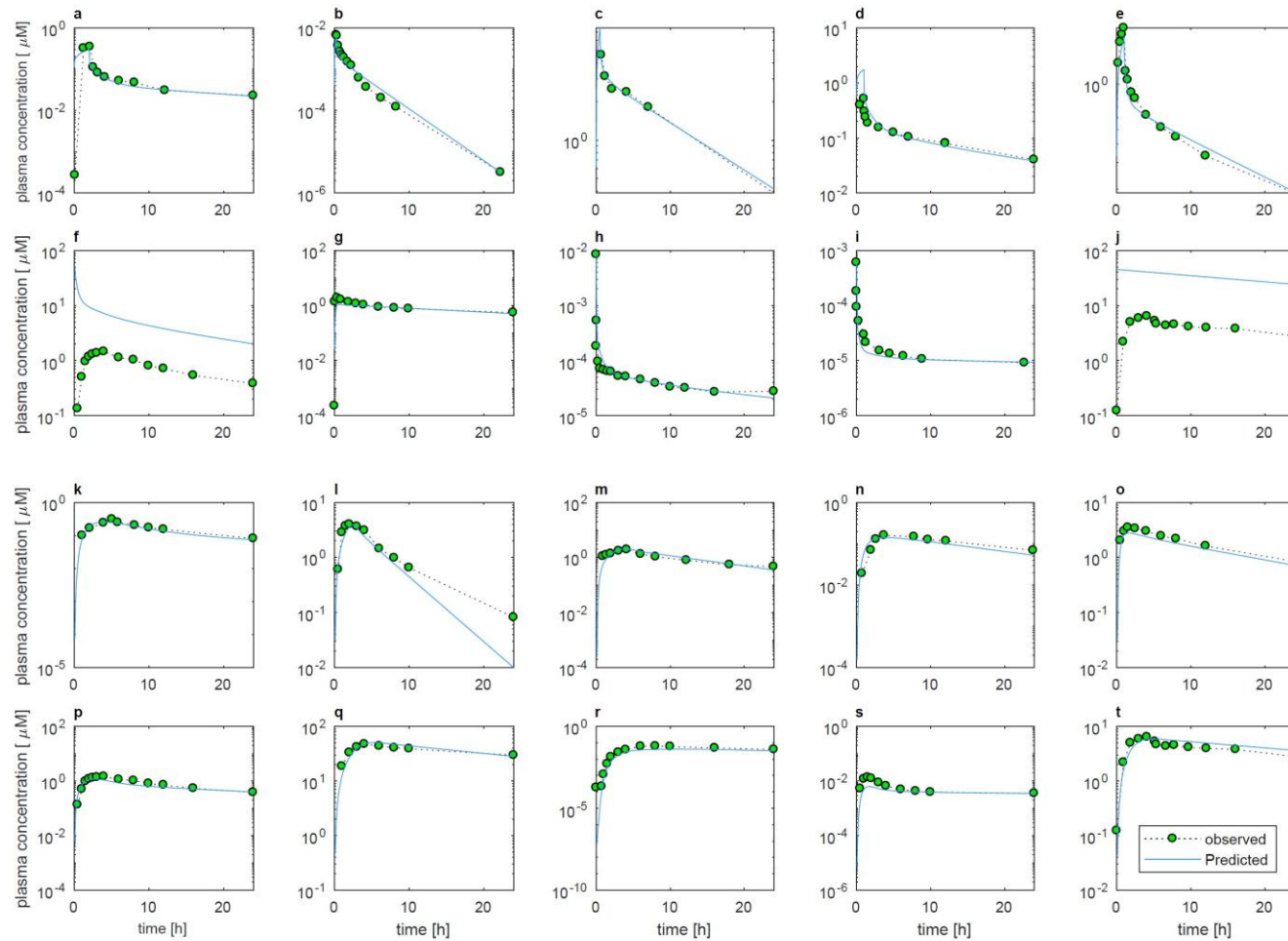


Figure S 1: Observed and predicted intravenous and oral human PK profiles using Caco-2 permeability in the generic PBPK model built in MATLAB® ;(a) 50 mg crizotinib iv; (b) 0.05 mg dabrafenib iv; (c) 75 mg erlotinib iv; (d) 100 mg gefitinib iv; (e) 100 mg imatinib iv; (f) 1,500 mg lapatinib iv simulation with 1,500 mg observed oral profile; (g) 5 mg pazopanib iv; (h) 0.0156 mg M1 iv; (i) 0.005 mg trametinib iv; (j) 96 mg vemurafenib iv simulation with 960 mg observed oral profile; (k) 250 mg crizotinib p.o.; (l) 150 mg dabrafenib p.o.; (m) 150 mg erlotinib p.o.; (n) 250 mg gefitinib p.o.; (o) 400 mg imatinib p.o.; (p) 1,500 mg lapatinib p.o.; (q) 800 mg pazopanib p.o.; (r) 30 mg M1 p.o.; (s) 2 mg trametinib p.o.; (t) 960 mg vemurafenib p.o.

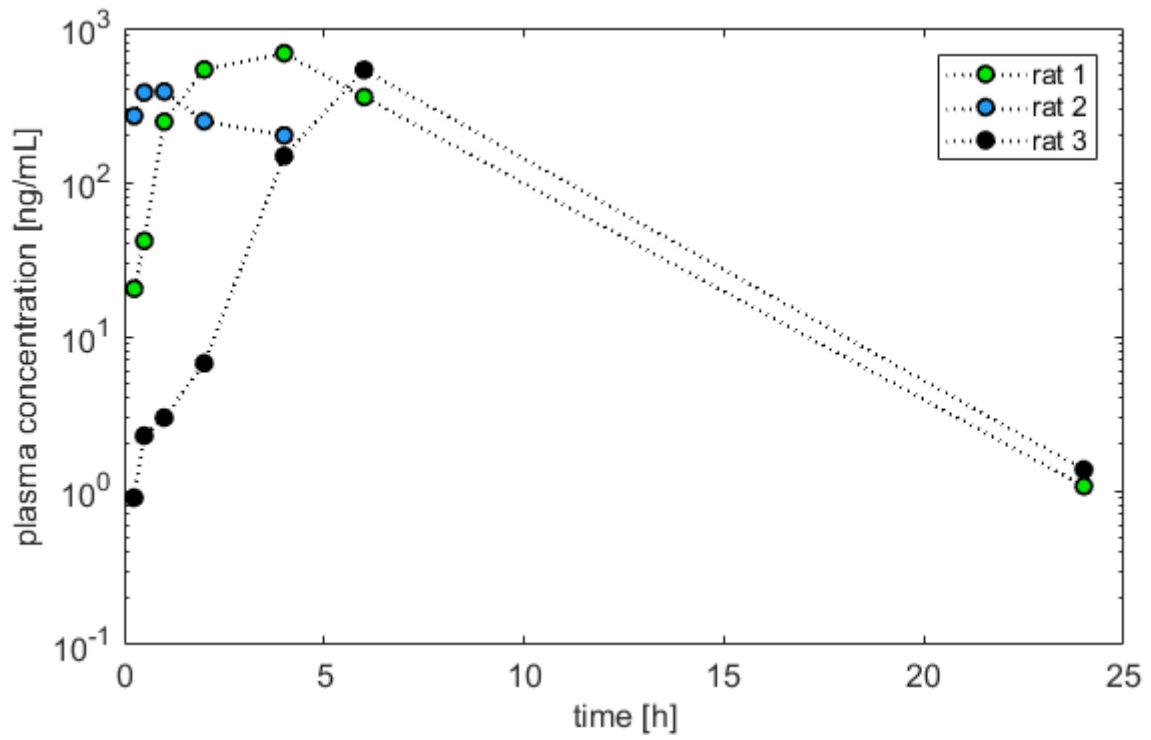


Figure S 2: Individual dabrafenib plasma concentration time profiles in the rat after 3.5 mg/kg p.o. in capsules